PLASMA SURFACE MODIFICATION AND CHARACTERIZATION OF PMMA FILMS

A THESIS SUBMITTED TO
THE GRADUATE SCHOOL OF NATURAL AND APPLIED SCIENCES
OF
MIDDLE EAST TECHNICAL UNIVERSITY

BY

ÖZGE ÖZGEN

IN PARTIAL FULFILLMENT OF THE REQUIREMENTS
FOR
THE DEGREE OF MASTER OF SCIENCE
IN
POLYMER SCIENCE AND TECHNOLOGY

DECEMBER 2011

Approval of the thesis:

PLASMA SURFACE MODIFICATION AND CHARACTERIZATION OF PMMA FILMS

submitted by **ÖZGE ÖZGEN** in partial fulfillment of the requirements for the degree of **Master of Science in Polymer Science and Technology Department, Middle East Technical University** by,

Prof. Dr. Canan Özgen _____
Dean, Graduate School of **Natural and Applied Sciences**

Prof. Dr. Necati Özkan _____
Head of Department, **Polymer Science and Technology**

Prof. Dr. Nesrin Hasırcı _____
Supervisor, **Chemistry Dept., METU**

Prof. Dr. Vasıf Hasırcı _____
Co-Supervisor, **Biology Dept, METU**

Examining Committee Members:

Prof. Dr. Kezban Ulubayram _____
Pharmacy Dept., Hacettepe University

Prof. Dr. Nesrin Hasırcı _____
Chemistry Dept., METU

Prof. Dr. Necati Özkan _____
Polymer Science and Technology, METU

Prof. Dr. Sinan Bilikmen _____
Physics Dept., METU

Assoc. Prof. Burcu Akata Kurç _____
Micro and Nanotechnology, METU

Date: 26.12.2011

I hereby declare that all information in this document has been obtained and presented in accordance with academic rules and ethical conduct. I also declare that, as required by these rules and conduct, I have fully cited and referenced all material and results that are not original to this work.

Name, Last name: Özge Özgen

Signature:

ABSTRACT

PLASMA SURFACE MODIFICATION AND CHARACTERIZATION OF PMMA FILMS

Özgen, Özge

M.Sc., Department of Polymer Science and Technology

Supervisor: Prof. Dr. Nesrin Hasırcı

Co-supervisor: Prof. Dr. Vasıf Hasırcı

December 2011, 114 pages

Surface properties play an essential role for determining the behavior of a material for many applications such as coating, printing, adhesion and prosthesis implanting since the surface is the first part that comes in contact with the environment. Although the bulk properties of some materials are at the desired level, the surface may need to be modified for a better compatibility with its surrounding. Plasma treatment is one generally preferred technique because of its high potential to create various functional groups on the surface of the sample by changing the applied plasma parameters. Some molecules can be successfully immobilized onto these surfaces using these specific chemical functional groups created by plasma. The type of the functional group is important for intended purpose of covalent binding of different molecules on the surface of a material. Present study offers important routes for optimization of the surface functionality of (PMMA) films by changing the plasma parameters. For this purpose, solvent casted polymethylmetacrylate PMMA films were modified by, nitrogen, argon and oxygen plasma by using a radiofrequency (RF) generator; and with various powers (10W, 50W, 100W) for different periods (5min, 15min and 30min). The effects of these plasma parameters (gas type, applied power, plasma time) on hydrophilicity, surface free energy,

surface chemistry, and surface topography were investigated. Also, the types of surface free radicals created with oxygen plasma treatment were analysed and the decay of these radicals were examined by Electron Spin Resonance Spectroscopy (ESR). In general, plasma treatment reduced the contact angle of PMMA films where the most hydrophilic surface was obtained for 100W 30 min argon plasma treated sample showing superhydrophilic character with the water contact angle value of ~10°. Surface free energy measurements were carried out according to Geometric Mean, Harmonic Mean, Acid-Base approach and it was found that oxygen, nitrogen and argon plasma treatments increased the surface free energy for all samples by increasing the polar components and introducing functional groups on the surface. X-Ray Photoelectron Spectroscopy (XPS) analysis results revealed that free carbonyl and carbonate groups were formed by oxygen plasma treatment, whereas carboxylic acid and free carbonyl groups were formed after argon plasma treatment, and imine, primary amine, amide and nitrozo groups were formed by nitrogen plasma. Atomic Force Microscopy (AFM) analysis revealed that the roughness of the surface increased considerably from ~2 nm to ~75 nm for the 100W 30 min oxygen plasma treated samples. ESR analysis indicated the presence of peroxy radicals on the surface of the oxygen plasma treated PMMA and the intensity of these radicals increased with increasing plasma power. Decay study of the newly created radicals demonstrated that after 1 month under the atmospheric conditions there were still peroxy radicals on the surface of PMMA. This functionality is important in leading time for further process for binding of different molecules to the surface of the materials for specific purposes. As a result, RF plasma was found to be an effective tool for modification of surface properties of materials with product diversity for intended purposes.

Keywords: PMMA, surface modification, oxygen plasma, nitrogen plasma, argon plasma , contact angle, SFE, XPS, AFM, ESR.

ÖZ

POLİMETİLMETAKRİLAT'IN PLAZMA İLE YÜZEY MODİFİKASYONU VE KARAKTERİZASYONU

Özgen, Özge

Yüksek Lisans, Polimer Bilimi ve Teknolojisi

Tez Yöneticisi: Prof. Dr. Nesrin Hasırcı

Ortak Tez Yöneticisi: Prof. Dr. Vasıf Hasırcı

Aralık 2011, 114 sayfa

Yüzey bir maddenin çevre ile ilk olarak temas eden parçası olduğu için yüzeyin özellikleri kaplama, baskılama, yapışma, protez yerleştirme gibi birçok uygulamada malzemenin davranışının belirlenmesinde önemli rol oynar. Bazı malzemelerin kütle özellikleri istenilen düzeyde olmasına rağmen, çevre ile daha iyi uyum sağlaması için yüzeylerinin değiştirilmesi gerekebilir. Plasma işlemi, uygulanan plazma parametrelerini değiştirerek aynı örnek yüzeyinde çok farklı fonksiyonel gruplar oluşturmada yüksek olasılığa sahip olduğu için genellikle tercih edilen bir tekniktir. Plasma ile yaratılan özel kimyasal fonksiyonel gruplar kullanılarak bazı moleküller bu yüzeylere başarılı bir biçimde bağlanabilir. Fonksiyonel grubun türü istenilen amaca uygun olarak değişik moleküllerin yüzeye kovalent bağlanması açısından önemlidir. Bu çalışma, polimetilmetakrilat (PMMA) filmlerin yüzey fonksiyonelliğinin plazma parametrelerinin değişimi ile optimize edilmesi konusunda önemli yollar önermektedir. Bu amaç için çözücüden kalıplama yöntemiyle hazırlanmış olan PMMA filmlerin yüzeyleri, radio freakanslı (RF) jeneratörü kullanarak oksijen, azot, ve argon gazları ve plazma ile farklı güçlerde (10W, 50W, 100W) ve değişik zaman periyodlarında (5 dak, 15 dak, 30 dak) plazma uygulaması ile modifiye edilmiştir. Plazma parametrelerinin (gaz türü, plazma uygulama zamanı ve gücü) hidrofilikliğe, yüzey serbest enerjisine, yüzey kimyasına

ve yüzey topografyasına olan etkileri incelenmiştir. Ayrıca oksijen plazma uygulaması ile yüzeyde yaratılan serbest radikaller ve yeni oluşturulan serbest radikallerin atmosfer ortamında zamanla sönümlenmesi Elektron Spin Rezonans spektrometresi (ESR) ile analiz edilmiştir. Genelde, plazma uygulaması PMMA filmlerin temas açısını azaltmıştır ve en hidrofilik yüzey ~10° su temas açısı ile süperhidrofilik özellik gösteren, 100W 30 dakika argon plazma uygulaması yapılan örnek için elde edilmiştir. Yüzey serbest enerjisi, Geometrik ortalama, Harmonik ortalama, Asit-Baz yaklaşımlarına göre hesaplanmış ve oksijen, azot, argon plazma uygulamaları bütün örneklerde yüzeyde yeni fonksiyonel grupların eklenmesi ve polar bileşenini arttırması ile, yüzey serbest enerjisinin değerini arttırmıştır. X Işını Fotoelektron Spektroskopisi (XPS) analiz sonuçları, oksijen plazma uygulaması sonrasında serbest karbonil ve karbonat gruplarının, argon plazma uygulaması sonrasında karboksilik asit ve serbest karbonil gruplarının, azot plazma uygulaması sonrasında imin, birincil amin, amid, nitrozo gruplarının oluştuğunu göstermiştir. Atomik Kuvvet Mikroskopisi (AFM) analizi yüzey pürüzlülüğünün, 100W 30 dakika oksijen plazma uygulaması ile ~2 nm den ~75 nm' ye dikkat çekecek derecede arttığını göstermiştir. Elektron Spin Rezonans Spektroskopisi (ESR) analizi oksijen plazma uygulanmış PMMA yüzeyi üzerinde peroksi radikalleri varlığını tesbit etmiştir ve bu radikallerin yoğunluğu plazma uygulama gücü arttırıldıkça artmıştır. Yeni oluşturulan serbest radikallerin sönümlenmesi çalışması, PMMA yüzeyi üzerinde atmosfer ortamında 1 ay sonra hala peroksi radikalleri olduğunu göstermiştir. Bu fonksiyonellik, özel amaçlar için yüzeye farklı moleküllerin bağlanabilmesi için gerekli işlemler için zaman tanınması açısından önemlidir. Sonuç olarak, RF plazma, malzemelerin yüzey özelliklerini istenilen amaca uygun ürün çeşitliliği verecek şekilde değiştiren etkili bir araçtır.

Anahtar Kelimeler: PMMA, yüzey modifikasyonu, oksijen plazma, azot plazma, argon plazma, SFE, XPS, AFM, ESR.

To my dearest grandfather...

ACKNOWLEDGEMENTS

First of all, I would like to thank my supervisor Prof. Dr. Nesrin Hasırcı for giving me a chance to join her overqualified and well organised laboratory. The opportunity she gave me by introducing this interesting research topic and also the working discipline opened up a unique route in my life. Her perpetual encouragement and invaluable advice are greatly appreciated.

I would like to express my special thanks to Prof. Dr. Vasıf Hasırcı, my co-supervisor, for enlightening my professional and academic vision with his support. I am also thankful for making me a member of BIOMAT group that gave me the possibility of joining the academic organizations.

I especially wish to thank Dr. Eda Ayşe Aksoy for her endless guidance and support with her valuable comments and helps preparing my posters and articles. Also thanks for performing my ESR analysis.

I would like to thank my friends Aysel Kızıltay, Tuğba Endoğan, Gülçin Çiçek, Ümran Aydemir, Şeniz Uçar, Filiz Kara, Shahla Bagherifam and the rest of my friends sharing with the same great atmosphere in the Lab-D148 for their friendship and help. I am also thankful to my dearest lab partner Aysun Güney for her valuable friendship and moral support all through any time in my life.

I wish to thank to all BIOMAT group members and Biotechnology Research Unit for helping me with goniometer in contact angle measurements.

TUBITAK is gratefully acknowledged for the financial support throughout my graduate studies.

I am grateful to the lovely people in METU Central Laboratory for their kindly support and endless understanding during the XPS, AFM and ESR analysis.

Special thanks to the my dear friends İlke Şimşek and Duygu Aksakal for their everday support and wonderful friendship. Especially I want to thank Türker Ertikaysın and Tufan Turan for helping me to solve many of software problems.

Last but not least, I would like to give my special thanks to my mother Dilek Özgen, my father Ali Özgen, my dear sister Berke Özgen and the rest of the members of my precious family for their encouragement, never ending supports, strenght to work on my thesis.

TABLE OF CONTENTS

LIST OF FIGURES

FIGURES

LIST OF TABLES

TABLES

ABBREVIATIONS

γ	Surface Tension
γ_c	Critical Surface Tension
θ	Contact Angle
AC	Alternative Current
BSA	Bovine Serum Albumin
DBD	Dielectric Barrier Discharge
DC	Direct Current
DIM	Diiodomethane
DLC	Diamond Like Carbon
DMSO	Dimethyl Sulfoxide
DW	Distilled Water
ECR	Electron Cyclotron Resonance
ESR	Electron Spin Resonance Spectroscopy
FA	Formamide
IOL	Intra Ocular Lens
MMA	Methyl Metacrylate
PC	Polycarbonate
PEG	Poly Ethylene Glycol
POE	Post Operative Endophthalmitis
PU	Polyurethane
RF	Radio Frequency
RF-PECVD	Radio Frequency Plasma Enhanced Chemical Vapor Deposition
SFE	Surface Free Energy
XPS	X Ray Photoelectron Spectroscopy

CHAPTER 1

INTRODUCTION

1.1 Surface

Surface is known as two dimensional outer boundary of a three dimensional objects. Without exception, every material just as polymers, ceramics, metals, biomaterials, metals, semiconductors have a surface and also an interface at the touching points to the air or contacting points with another material. The chemical or physical properties of the interface region may totally differ from bulk properties. It is an unquestionable fact that surface is the most important part of an object since it controls the interactions between the material and the environment. Surface characteristics of a material determine how well the product performs in its interactions.

1.2 Surface Properties

The Society of Polymer Science carried on an opinion research in 1982, and 29% respondents of the 405 companies in Japan found ‘surface interactions of polymers’ the most compelling topic among the three categories that the others related with ‘surface morphology’, ‘chemical compositions’ and ‘reactions at the surface of the polymers’. According to the participants surface properties are crucial for operating performance, at the same time control of the surface properties is very complex and problematic [Castner et al., 2002]. Surface properties can be changed with different surface modification methods which will be mentioned later and Figure 1 gives a summary of the surface properties that can be altered by different techniques.

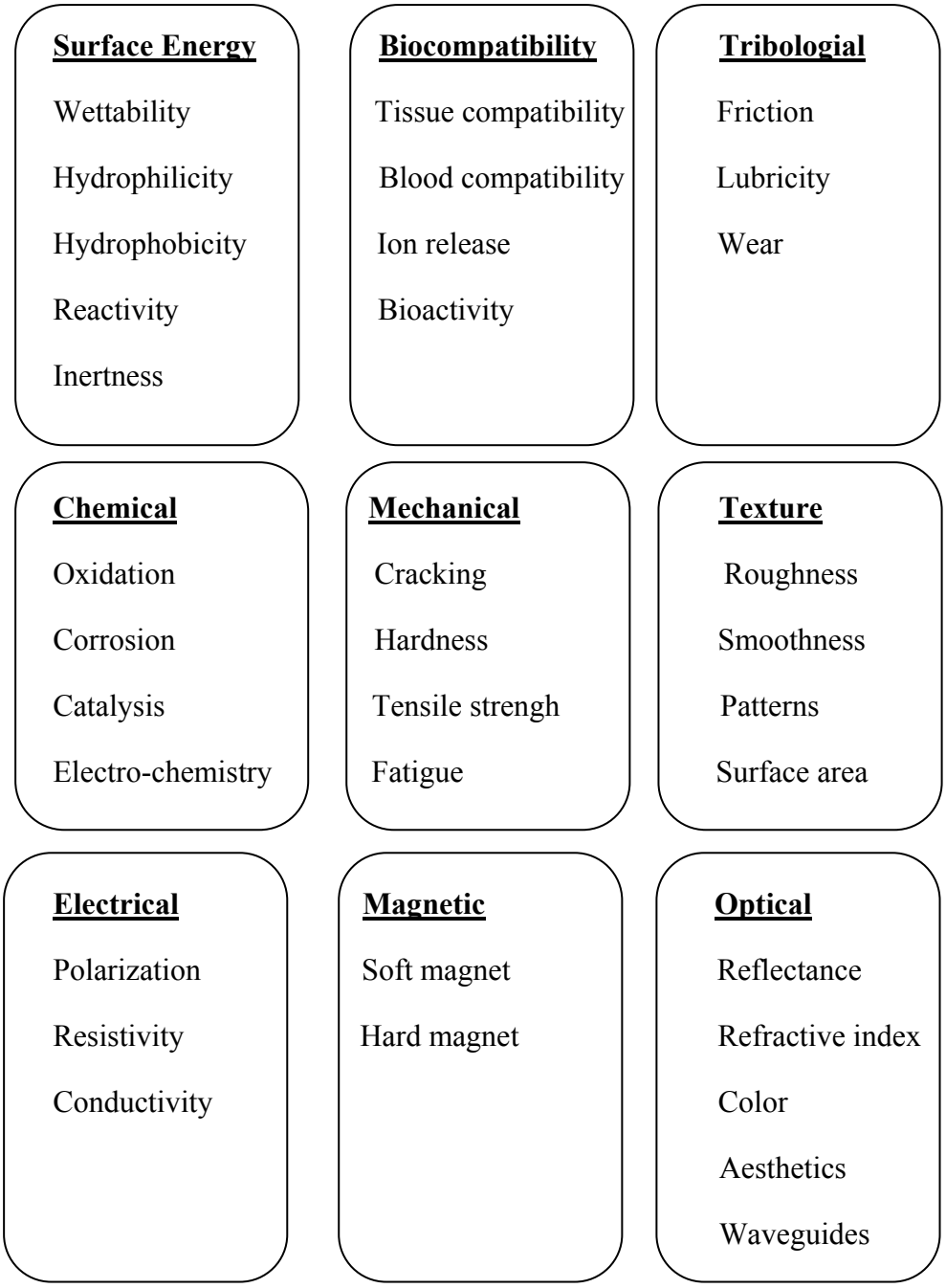

Figure 1: Surface properties that can be modified by different techniques [Chu et al., 2002]

1.2.1 Wettability

Wettability is one of the fundamental surface properties of a solid which plays vital role in industry, agriculture, as well as daily life. If innumerable applications of wetting are put into an endless list, some of the contents can be summarized as cleaning, lubrication, soldering, jet printing, painting, dying, coating, spray quenching, pesticide applications, etc. Controlled wettability of functional surfaces attracts great attention because of large scaled application areas, and some of them can be given as body implants, contact lenses, biomaterials, biofilm growth, offset printing, packaging, non sticky surfaces, self cleaning, superhydrophobic surfaces, semiconductor wafers, electronic products, cosmetic products, hot melt adhesives and so on [Sun et al., 2005].

The concept of "wetting phenomenon" was first proposed by Galileo in 1612. When a liquid drops and spreads on a solid, wetting is the resultant process. Wetting is the degree to how much a solid substrate is wetted by a liquid and it is closely related with the surface properties of the solid, also the nature of the liquid [Roucoules et al., 2002]. Wettability can be determined by calculating the spreading coefficient or measuring the contact angle of the liquid formed on the solid surface.

1.2.2 Contact Angle

Contact angle is the angle between the touching point of the two interfaces at the three phase line of contact. A cross sectional representation of a liquid resting on a solid surface is shown in Figure 2. The contact angle is a result of the surface tension relationship between the solid-liquid-vapor phases.

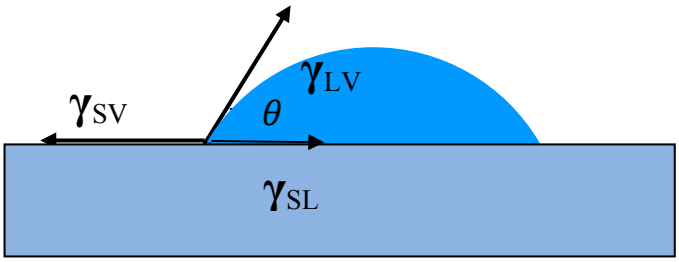

Figure 2: Balance of three interfacial energy parameters result in a contact angle

Contact Angle, θ, comes up from the equilibrium between the surface interface tensions of three phases, which are; γ_{SV} (the interfacial tension between solid and vapor interface) γ_{LV} is the interfacial tension between the liquid and vapor interface, and γ_{SL} (the interfacial tension between the solid and liquid interface). The relationship between the three interfacial tension is stated by Young Equation as given below;

$$\gamma_{SV} = \gamma_{LV} . \cos\theta + \gamma_{SL}$$

The mathematical equation of contact angle was first inspired by the idea of Thomas Young who is accepted as the father of scientific research on contact angle. Young (1805) put forward the following idea of the contact angle.

"*But it is necessary to premise one observation, which appears to be new, and which is equally consistent with theory and experiment; that is, that for each combination of a solid and a fluid, there is an appropriate angle of contact between the surfaces of the fluid, exposed to the air, and to the solid.*" [Gao et al., 2009].

Since all the approaches rely on the validity of Young's above comment and equation, it is considered as a master equation for all surface free energy approaches (will be discussed later) as well as the concept of work of adhesion which are the fundamentals of surface science.

The parameters that strongly affect the contact angle can be listed as: temperature, static electricity, surface contamination, preparation manner of the surface, surface roughness and the environmental conditions like air current, humidity.

Actually, contact angle of a liquid formed on a surface is between 0 and 180 degrees. If the measured contact angle of is 0°, this means the surface is perfectly wetted by the liquid and the solid-liquid interactions are overmuch higher than liquid-liquid interactions. 0° or close to 0° contact angle points that the liquid can easily spread over the surface. Between the 0° and 90° of any angle means 'wetting'. The situation that contact angle is greater than 90° indicates 'non wetting' process in which the liquid is prone to run off the surface. For water, there is a special term which is called 'hydrophilic' for wettable surface and 'hydrophobic' for a non wettable surface. If contact angle of a surface is greater than 150°, this case indicates 'superhydrophobicity'. In the case of superhydrophobicity there is nearly no contact point between the surface and the liquid drop. This event is mostly called 'Lotus Effect' with the similarity of the results when considered the interaction of lotus leaf with water. The leaf surface of lotus is covered with many wax crystals leading protrusions which increase roughness meaningfully. These protrusions lead to water drop to form 162° contact angle on lotus leaf surface. So lotus leaf is one of the typical example of natural superhydrophobic surfaces. Considerable efforts have been made to mimic natural superhydrophobic surfaces such as Nelumbo Nucifera (Lotus) and Colocasia Esculenta since superhydrophobic surfaces have widespread application areas including anti snow sticking surfaces, restraining the contaminants, coatings for buildings, antioxidation coatings, microfluidic devices and so on [Burton et al., 2005 and Li et al., 2007].

There are many ways to obtain superhydrophobic surfaces including photolithography-based microfabrication which arises from biomimetic inspiration of lotus leaves, rice leaves and legs of insects, solidification of melted alkylketene dimmer, microwave plasma enhanced chemical vapor deposition of trimethoxylmethoxysilane, mixing of a sublimation of material with silica or boehmite, domain selective oxygen plasma treatment, phase separation, sol-gel method, molding and fluorination of surfaces [He et al., 2003 and Onda et al., 1996].

1.2.3 Hydrophilicity

The term ‘hydrophilicity’ coming from the combination of hydros which means water in Greek and philia stands for love. So it can be understood from the name hydrophilic material is water loving substance such molecules have a propensity for interacting with or to be dissolved by water or another polar solvents. Since a hydrophilic molecule tends to form hydrogen bonding, a hydrophilic surface easily can form bond with the water molecules. Weaker bonds of hydrogen atoms which belong to different water molecules are readily broken and able to form new bondings with the molecules of the hydrophilic surface. Therefore maximize the water surface interaction on hydrophilic surface.

The contact angle demonstrates inverse relationship with the degree of wettability in that hydrophilic surfaces possess lower water contact angle than hydrophobic surfaces as can be seen from the Figure 3. In Figure 3, the surface shown in the Figure 3-c has the lower water contact angle which means higher attractive forces between water and the solid surface compared to the sample given in Figure 3-b and water.

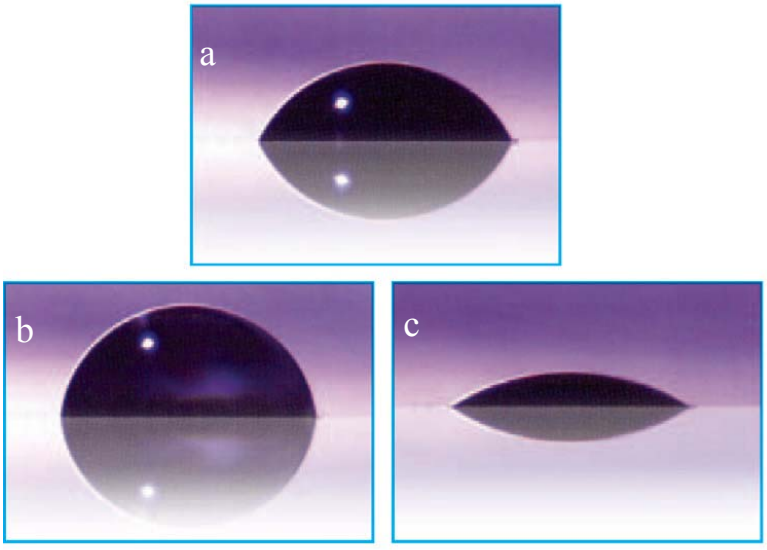

Figure 3:Wetting behavior of surfaces with different degree of wettability a) Wetting of conventional wettable surface. b) Low wettability of hydrophobic surface. c) High wettability of hydrophilic surface

Hydrophilicity is also quite important in biological applications such as implant and prosthesis surfaces where initial effective factor to control the protein adsorption is a desired hydrophilicity/hydrophobicity ratio of a surface. Also it should be taken into account that the protein adsorption is the initial parameter understanding the response of the surface for cell attachment in tissue engineering applications since specific interaction of cell surface is determined by the amount of adsorbed proteins on the surface [Lin et al., 2006]. According to molecular self-association theory, proteins are repulsed by hydrophilic surfaces because of the closed hydrogen bonding arrangement. Based on this consideration it can be concluded that hydrophobic surfaces are more preferable than hydrophilic ones for protein adsorption [Horbett et al., 2006 and Tziampazis et al., 2000]. Although there are publications showing contradictory results.

There is impressive amount of studies carried out in order to elucidate the relationship between the surface wettability and adsorptivity of the proteins and some of these are given below.

Kayırhan N. et al. investigated the adsorption behavior of bovine serum albumin (BSA) and fibrinogen on polyurethane (PU) membranes having the surface of various degree of wettability. Authors reported that the adsorptivity of the BSA was reduced to one fifth value of the control after argon and oxygen plasma treatments which demonstrated water contact angle values of 52.5° and 45.7° after argon respectively [Kayırhan et al., 2001].

Ozdemir Y. et al. modified the PU membranes by RF oxygen plasma with different power values such as 10W and 100W for 15 minutes and investigated the changes in hydrophilicity and adhesion of vero cells on the considered surfaces. The results revealed that for the same plasma application time, increasing power values reduced the vero cell attachment on the PU membranes which means increasing hydrophlicity caused lower cell attachment [Ozdemir et al., 2002].

Yıldırım M. S. et al. studied the correlation between surface hydrophilicity and adsoption amounts of salivary high molecular weight mucins on the surface of acrylic resins modified with oxygen plasma treatment, as well as polymerization of 2-hydroxyethylmethacrylate or hexamethyldisiloxane monomers with glow

discharge plasma at 50W and 100W for 15 min. Among the all modification conditions the highest adsorption amount of mucins detected for the surfaces modified by using 2-hydroxyethylmetacrylate with 100W 15min oxygen glow discharge which showed moderate hydrophilicity by the contact angle of 46° [Yıldırım et al., 2006].

It is noteworthy that the way to obtain hydrophilic surface as well as more wettable surface, additional surface modification should be performed. The surface modification is necessary for the creation of chemical polar groups on the surface. The introduction of polar functional groups such as carbonyl, carbonate, carboxyl, hydroxyl, amine, and amide increase the hydrophilicity of the surface as well as the surface free energy of the surface [Moroni et al., 2008].

Introducing the oxygen containing functional groups on the surface of poly (3-hydroxybutyrate-co-3-hydroxyvalerate) films were achieved by application of RF oxygen plasma at various conditions such as 100W or 50W applied for 10 min and 20 min. Among the various plasma treated samples, the most hydrophilic surface was obtained for the samples treated at 100W for 20 min and these samples had the highest amount of oxygen containing functional groups [Hasirci et al., 2003].

1.2.4 Surface Free Energy (SFE)

The surface properties of a material are different from the bulk properties. The inner molecules are attracted by the neighbouring molecules in all directions so it can be said that there is no net force operating on these molecules. Therefore the molecules inside the bulk of a liquid have balanced forces. On the contrary, molecules at the surface are attracted only by the side and inward molecules so existing net force prevents balancing of the surface molecules as can be seen in Figure 4. Unbalancing forces of the surface molecules induce a tension or free energy. This thermodynamic quantity is called ‘Surface Tension’ or ‘Surface Free Energy’ (SFE). Also surface free energy is defined as ‘the work required to increase the area of a substance by unit amount’. The units for surface free energy are mN/m, mJ/m^2 or dynes/cm. The reactivity of the surface is determined by surface free energy as well as the type and result of the interaction between the surface and environment [Combe et al., 2004].

The general methods used for the calculation of SFE are Zisman plot, Girifalco and Good model, Fowkes approach, Geometric Mean approach, Harmonic Mean approach, and Acid-Base approach. The methods are explained below.

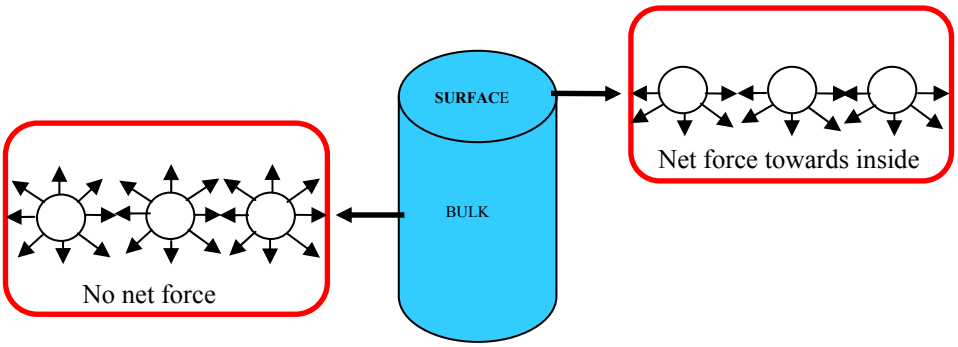

Figure 4: Interactive forces between the molecules at the surface and bulk of a material.

1.2.4.1. Zisman Plot and Critical Surface Tension

Fox and Zisman were the earliest surface scientists who first offered the ‘‘*critical surface tension*’’ with the empirical relationship between the contact angles and liquid surface tensions in 1950’s. This mentioned relationship is demonstrated as a Zisman plot which consists of y axis showing the cosine values of contact angle (cos θ) and x axis corresponding to the surface tension values of various liquids [Fox et al., 1952].

The test liquids should be chosen as a homologous series of organic compounds like n-alkanes in order to obtain a straight line plot. Zisman defines a critical surface tension which is the maximum value of surface tension of a liquid that can completely spreads and wets the solid. Based on this consideration Zisman proposes;

$$\gamma_C = \lim_{\theta \to 0} \gamma_{LV} \qquad (1)$$

where critical surface tension (γ_C) equals to γ_{LV} at the point where θ=0. This result can be found with the extrapolation of the straight line to the value where cos θ=1. The straight line of Zisman plot can be seen from the Figure 5 implying Zisman plot of contact angle as a function of liquid surface tension for 1, 3, 5, 15 min plasma

treated polyethylene (PE). Each plot point reflects the contact angle of a specified liquid and the general trend moving to the right for more hydrophilic surfaces compare to the untreated or relatively less hydrophilic PE surfaces. Zero contact angle indicates the complete wetting.

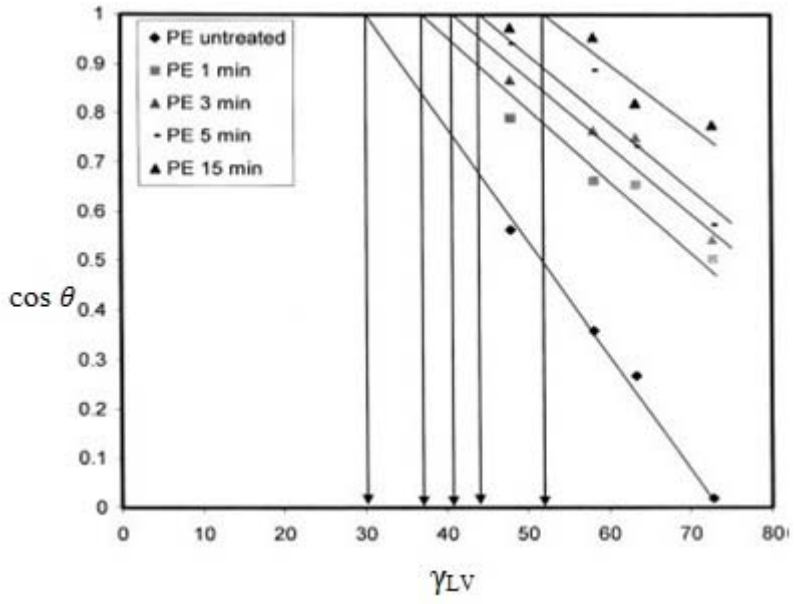

Figure 5: Zisman plot of contact angle as a function of liquid surface tension for polyethylene [Deshmukh et al., 2008]

The linearity of Zisman plot is not universal. For the selection of water or any other liquid having hydrogen bonding deteriate the straight line. Also being devoid of the explanation of polar and dispersive component of SFE makes Zisman approach less rigorous model [Deshmukh et al., 2008].

1.2.4.2 Girifalco and Good Model

In the second half of the 1950's Girifalco and Good attempted to formulate the equation as shown below;

$$\gamma_{SL} = \gamma_S + \gamma_L - 2\Phi(\gamma_S . \gamma_L)^{1/2} \quad (2)$$

where $\Phi = (\rho_1\rho_2)^{1/2}$ defines the interaction parameter of the solid-liquid system and its value usually is between 0.5 and 1.0. ρ_1 and ρ_2 gives the fractions of intermolecular interactions attributed to London type forces among molecules of pure material (1) and liquid (2), respectively. Also Φ is the characteristic of the solid-liquid system and it is determined by the molecular properties of the solid and liquid phases [Zenkiewicz et al., 2007]. The insertation of the Girifalco-Good equation (equation 2) into Young equation, gives the relationship between solid surface tension and contact angle as below:

$$\gamma_S = \gamma_L (1+\cos\theta)^2 / 4\Phi^2 \quad (3)$$

From the result it can be concluded that it is possible to reach the solid surface tensions by measuring the contact angle at once and also for only liquid. Girifalco and Good equation is viable when the solid-liquid interactions are mostly dispersive.

1.2.4.3 The Fowkes Approach

Fowkes introduced the dispersion component of the SFE. According to Fowkes dispersion component of SFE related with the London interactions resulted from the electron dipole fluctuations due to the attraction between the atoms and molecules of the matter [Fowkes et al., 1964]. Fowkes approach is valid for dispersive forces of nonpolar solid ($\gamma_S = \gamma_S^d$) and the liquid, ($\gamma_L = \gamma_L^d$). Under these conditions, SFE of a solid-liquid interface can be written

$$\gamma_{SL} = \gamma_S + \gamma_L - 2\left(\gamma_S^d . \gamma_L^d\right)^{1/2} \quad (4)$$

Combining the equation with Young equation, the following equation can be obtained;

$$\gamma_S^d = \gamma_L (1+\cos\theta)^2 / 4 \quad (5)$$

This formula can be used to calculate SFE of a solid.

1.2.4.4 Geometric Mean Approach

Geometric mean approach of SFE, which is also called OWRK coming from the first letters of Owens-Wendt-Rabel-Kalble, exhibits similarities with Fowkes method in the aspect of dispersive contribution of SFE. According to geometric mean approach beside the dispersive contribution of SFE, polar contribution should also be taken into account. The following equation is attained in order to calculate the polar and dispersive components of SFE, and the total SFE value of the solid surface.

$$\gamma_{SL} = \gamma_S + \gamma_L - 2\left(\gamma_S^d . \gamma_L^d\right)^{1/2} - 2\left(\gamma_S^p . \gamma_L^p\right)^{1/2} \quad (6)$$

Combination of the above equation with the Young equation gives the following equation which expresses the relationship between the contact angle and surface free energy values of solid, liquid and also their polar and dispersive components.

$$\gamma_L (1+\cos\theta) = 2\left(\gamma_S^d . \gamma_L^d\right)^{1/2} + 2\left(\gamma_S^p . \gamma_L^p\right)^{1/2} \quad (7)$$

Where superscript ‘d’ refers to dispersive component and ‘p’ refers to polar components. In the above equation there are two unknowns: γ_S^d and γ_S^p which are dispersive and polar components of free energy for solid surface, respectively. So at least two contact angle measurements are required to calculate the surface free energy components of the solid surface free energy. This means at least two test liquids have to be chosen for the calculation. While calculating the SFE, one of the chosen liquids should demonstrate dominantly polar character whereas the other should be relatively dispersive. As a test liquid, water and diiodomethane are the most preferred ones for the aim of calculating the SFE with geometric mean approach [Mangipudi et al., 1995].

1.2.4.5 Harmonic Mean Approach

Wu follows the same approximation with geometric mean approach splitting the surface free energy in two components which are polar and dispersive, but Wu uses harmonic mean equation to obtain the addition of the polar and dispersive components of SFE. Harmonic mean equation can be written as:

$$\gamma_{SL} = \gamma_S + \gamma_L - 4\left(\frac{\gamma_L^{d} \cdot \gamma_S^{d}}{\gamma_L^{d} + \gamma_S^{d}} + \frac{\gamma_L^{p} \cdot \gamma_S^{p}}{\gamma_L^{p} + \gamma_S^{p}}\right) \quad (8)$$

Combination of the above equation with the Young equation gives the equation of harmonic mean approach **[**Zenkiewicz et al., 2007**]**

$$\gamma_L (1+\cos\theta) = 4\left(\frac{\gamma_L^{d} \cdot \gamma_S^{d}}{\gamma_L^{d} + \gamma_S^{d}} + \frac{\gamma_L^{p} \cdot \gamma_S^{p}}{\gamma_L^{p} + \gamma_S^{p}}\right) \quad (9)$$

1.2.4.6 Acid-Base Approach

Van Oss, Chaudhury, and Good introduced the components of the surface free energy of solid (γ_S) such like γ_S^{LW} and γ_S^{AB}. Where γ_S^{LW} refers to Lifshitz- Van der Waals component which is concerning long range interactions dominated by dispersion forces, and γ_S^{AB} refers to acid-base component related with short range interactions because of the polar attraction forces. According to Acid-Base approach, γ_S^{AB} component is divided into two subcomponents as γ_S^{+} which refers acidic and γ_S^{-} which refers basic interactions. The following equation represents the relationship between the acid-base component and it's including parameters;

$$\gamma_S^{AB} = 2\left(\gamma_S^{+} \cdot \gamma_S^{-}\right)^{1/2} \quad (10)$$

Where γ_S^{+} is the Lewis acid parameter and γ_S^{-} is the Lewis base parameter. Lewis acid parameter is also called electron acceptor parameter in the literature because of the assumption that the acidic sites act as electron acceptors. Following the same idea but this time for basic site, the terms electron donor parameter is used for Lewis base parameter. According to Good, Chaudhury and Van Oss, if a sample shows interaction with only γ^{LW} component, then Lewis acid and base parameters should be zero such as;

$\gamma^{+} = \gamma^{-} = 0$

They selected α- bromonaphathalene, methylene iodide and alkanes as liquids which have Lewis acid parameter and Lewis base parameter are equal to zero. In order to calculate the SFE value of a solid and its components (dispersive and acid-base) by

using Acid-Base approach, at least three liquids should be used because of the three unknowns of the material, which are γ_S^{LW}, γ_S , γ_S^+ in the following equation;

$$\gamma_L (1+\cos\theta) = 2\left(\sqrt{\gamma_L^{LW}\cdot\gamma_S^{LW}} + \sqrt{\gamma_L^{+}\cdot\gamma_S^{-}} + \sqrt{\gamma_S^{+}\cdot\gamma_L^{-}}\right) \quad (11)$$

where + and – superscripts stand for Lewis acidic and Lewis basic parameters, respectively. Also as mentioned before γ^{LW} refers to Lifshitz Van der Waals component of SFE. The equation states that measuring the contact angle of the system with inserting the polar and dispersive components of the test liquids, SFE value of the solid surface can be calculated as well as acid and base components. It is worth mentioning that the equation also points out that acidic component of liquid surface free energy interacts with the basic component of the solid surface free energy and vice versa. [Oss et al., 1986]

The basic idea of Acid-Base approach can explain the hydrogen bonding of water molecules by accepting $\gamma^+ = \gamma^- = 25.5$ mJ/m^2. In this equation, Lewis acid and Lewis base parameters are given for water. The equalence of acidic and basic site leads to interact water molecules with neighboring molecules. The basic site will interact with the acidic site of the neighbour molecule. This special Lewis acid base interaction result in hydrogen bonding. Moreover Acid-Base approach is a good merit for the calculation of solid surface free energy being consistent with the concept of 'work of adhesion' which will be defined in the following section [Deshmukh et al., 2008].

1.2.4.7 Work of Adhesion

Adhesion of a liquid on a solid surface is one of the most commonly used and at the same time such important process that many industrial and biomedical applications are concerning. Obtaining information about the adhesion properties between the solid and liquid surface is crucial not only for printing, gluing, varnishing but also for blood-biomaterial interaction, cell-biomaterial interaction. So in these mentioned cases it is useful to know the optimum work of adhesion. The formula of the work of adhesion can be written as follows;

$$W_{SL} = \gamma_S + \gamma_L - \gamma_{SL} \quad (12)$$

Where W_{SL} is the work of adhesion of the liquid drop to the solid surface at the solid-liquid-vapor equilibrium, as mentioned before γ_S is the solid surface free energy, γ_L is the liquid surface free energy, γ_{SL} is the free energy of the solid-liquid interface which formed reversibly. Insertation of the Young equation to the above equation leads to;

$$W_{SL} = \gamma_L (1+\cos \theta) \quad (13)$$

The work of adhesion of the liquid to the adlayer covered solid surface can be interpreted as if one can know the contact angle value at equilibrium and also the liquid surface free energy then the work of adhesion can be calculated. Work of adhesion depends on the temperature, type of the liquid and the properties of the solid surface [Oss et al., 1988].

1.2.4.8 Importance of SFE

Interaction of the surface of a material with other fluids or materials is determined by the reactivity of the surface which is dominantly designated by the surface free energy. Having knowledge about the surface free energy of the surface and also chemical and physical forms of the material which will interact with surface offers a unique route for estimating the results of the material-surface interaction [Ozcan et al., 2008 (a)].

In order to obtain information about the wetting behavior of a surface, work of adhesion is the key requirement as well as the surface free energy. For instance in the wetting process of a foil with different color pigmented inks, the aspect of which ink will demonstrate good adhesive property on the mentioned surface will be determined by the surface free energy values of the ink and the foil.

In the field of medical treatments especially dental applications which are the most commonly carried out treatments on the human bodies, the importance of surface free energy comes into prominence. Dental restorative materials such as cavity lining, cavity filling, luting, orthodontic and periodontal applicants should exhibit

good resistance to water absorpsion, besides these materials should prevent discoloration. Since it was reported that hydrophobic materials show better color stability, surface free energy value should be taken into account when performing treatments with dental restorative materials [Ramakrishna et al., 2001].

Saliva and bacteria adhesion on the dental surfaces is one of the biggest problems has to be solved. Beside surface roughness, surface free energy is the most critical parameter governing the adhesion process of bacteria on the surface of the dental prostheses and implants. It was hypothesized that low surface free energy surfaces show better resistance to bacteria plaque formation [Mandracci et al., 2008].

Also the absorption mechanism of proteins on the surfaces is closely affected by the surface free energy of the substrate surface as well as protein molecules. In addition water molecules act dominant role as being moderating and mediating matter in surface-protein interaction process where the substituting ability of protein molecules with hydrating water determines adsorption behavior [Messina et al., 2009].

Getting information about surface free energy elicits quick and cost effective way instead of performing painstaking, long biocompatibility tests in order to fulfill successful surface-biomaterial interaction. Cell attachment and also proliferation is one of the most preferred demand for dental and bone implants. For instance periodontal ligaments cells proliferation around the dental implant plays important role for mimicking the natural teeth [Kokubu et al., 2008].

For cell-material interactions there are many factors affecting the process such as roughness, surface chemistry, surface topography, surface polarity, surface charge, and surface free energy, and optimum value of surface free energy is essential in order to obtain maximum cell attachment. Ozcan et al. reported that 61 mJ/m^2 is the optimum value of surface free energy calculated by Harmonic Mean approach for maximum attachment of 3T3 cells on PMMA surface [Ozcan et al., 2008 (b)].

More recently Hasirci N. et al. claimed that there should be an optimum value of surface free energy for fulfilling maximum cell attachment and this value is found about 60 mJ/m^2 for the attachment process of 3T3 fibroblast cells on PLGA films [Hasirci et al., 2010].

1.3 Why There is a Need To Modify Polymer Surfaces?

There is growing interest for common usage of polymers in modern industry such as automotive, aerospace, railway, also chemical and food industries, civil construction works, microelectronics, and biomedical field [Bhowmik et al., 2004 and Papakonstantinou et al., 2007].

Having high strength-to-weight ratio, resistance to corrosion, good electrical and thermal insulation, lower rigidity to some extent, also low cost and weight make polymers attractive for various industrial and engineering applications. However being chemically inert, possessing low surface free energy and hydrophobic characteristics restricts their endless demand [Wen at al., 2006 and Lai et al., 2006].

Polymeric materials play an essential role in biomedical field serving as artificial heart valves, sutures, vascular grafts, scaffolds, implants [Junkar et al., 2010]. But it is difficult to find such a biomaterial with excellent bulk properties and also has the desired surface properties like good biocompatibility, bioactivity, and adhesion at the same time. Therefore there is a great need to improve the surface properties in the desired direction by using various surface modification techniques. Also it should be taken into account that when a biomaterial is placed into the body, the surface is the first contacting point; therefore the initial comeback of the living tissue to the biomaterial is strongly related with its surface properties. For example, modifying the surface of an implant makes it more biocompatible and improves its biointegration in the enclosing tissue [Thevenot et al., 2008].

It is worth thinking of a biosensor with ideal mechanical properties but it is unacceptable if it corrodes instantly after contacting the body fluid. In order to enhance the corrosion resistance it is mandatory to modify the surface of that biosensor. On the other hand, when foreign surface of the hemodialysis catheter disposed to the blood, remaining slippery with low surface friction is important for patient [Chu et al., 2002].

To alter the surface for intended purpose there are numerous surface modification techniques which are mainly divided into four categories such as physical, chemical, biological and radiation. Table 1 is given as a summary of these modification categories

Table 1: Surface Modification Techniques

PHYSICAL	CHEMICAL	BIOLOGICAL	RADIATION
Physical Adsorption Langmuir-Blodgett Film	Ozone treatment Incorporation of functional groups Oxidation by strong acids Chemisorption Hydrogel grafts Flame treatment	Heparinization Protein-enzyme immobilization Lipid immobilization Hyaluronic acid coating	Plasma treatment Corona discharge Photo activation (UV) Gamma irradiation Electron beam Ion beam Laser

Among these techniques, plasma treatment is one generally preferred because of being fast, dry, and results uniformity. Besides, plasma treatment provide modification only on the surface (a few nanometer range) remaining the original bulk properties unchanged.

1.4 Plasma Surface Modification

1.4.1 Plasma State

State of matter can be divided into solid, liquid and gas states. Besides, as it is widely accepted now, the fourth state of matter is plasma. Plasma can be thought as a partially ionized gas having equal number of positive and negative charged particles. The major differences between plasma and gas state are, plasma comprises of free moving electrons, ions, excited atoms and molecules, UV photons and radicals, and plasma is at high energy level since energy is needed to break off electrons from atoms to make plasma [Wu et al., 2002].

1.4.2 Plasma Types

Plasmas can be classified into two categories such as cold (non equilibrium) plasmas and hot (near equilibrium) plasmas. Figure 6 represents the subcategories of cold and hot plasmas [Denes et al., 2004]. Hot plasmas having extremely high temperatures of heavy particles and electrons so they give rise to atomization of molecules which is unsuitable for heat sensitive materials like polymers. Hot plasma treatment can be one of the appropriate modification techniques for metals and metal oxides rather than polymers. On the contrary, cold plasmas involving relatively cold heavy particles such as charged and neutral atoms and molecules and high temperature electrons. Surface modification with cold plasmas is very appropriate technique for polymers and other heat sensitive materials minimizing the deformation effect of heat damage because of the heavy particles staying cold [Morent et al., 2011].

Atmospheric pressure plasmas including DBD (Dielectric Barrier Discharge) and corona discharges are actuated in a wide range of pressure and temperature confining electrical discharges. DBD, the most illustrative atmospheric pressure plasma type is generated in the presence of individual filamentary breakdown channels that are formed due to the solid dielectric layer between the metal electrodes. Individual filamentary discharges, generally called micro discharges, permeate on the dielectric layer forming charge zones on the insulator surface. Dielectric barrier manifolds the individual filamentary discharges spreading through the electrode. Micro discharges acting as ionized plasma channels. DBD give rise to numerous inelastic collisions reaching equilibrium in 10 ps at atmospheric pressure condition [Denes et al., 2004].

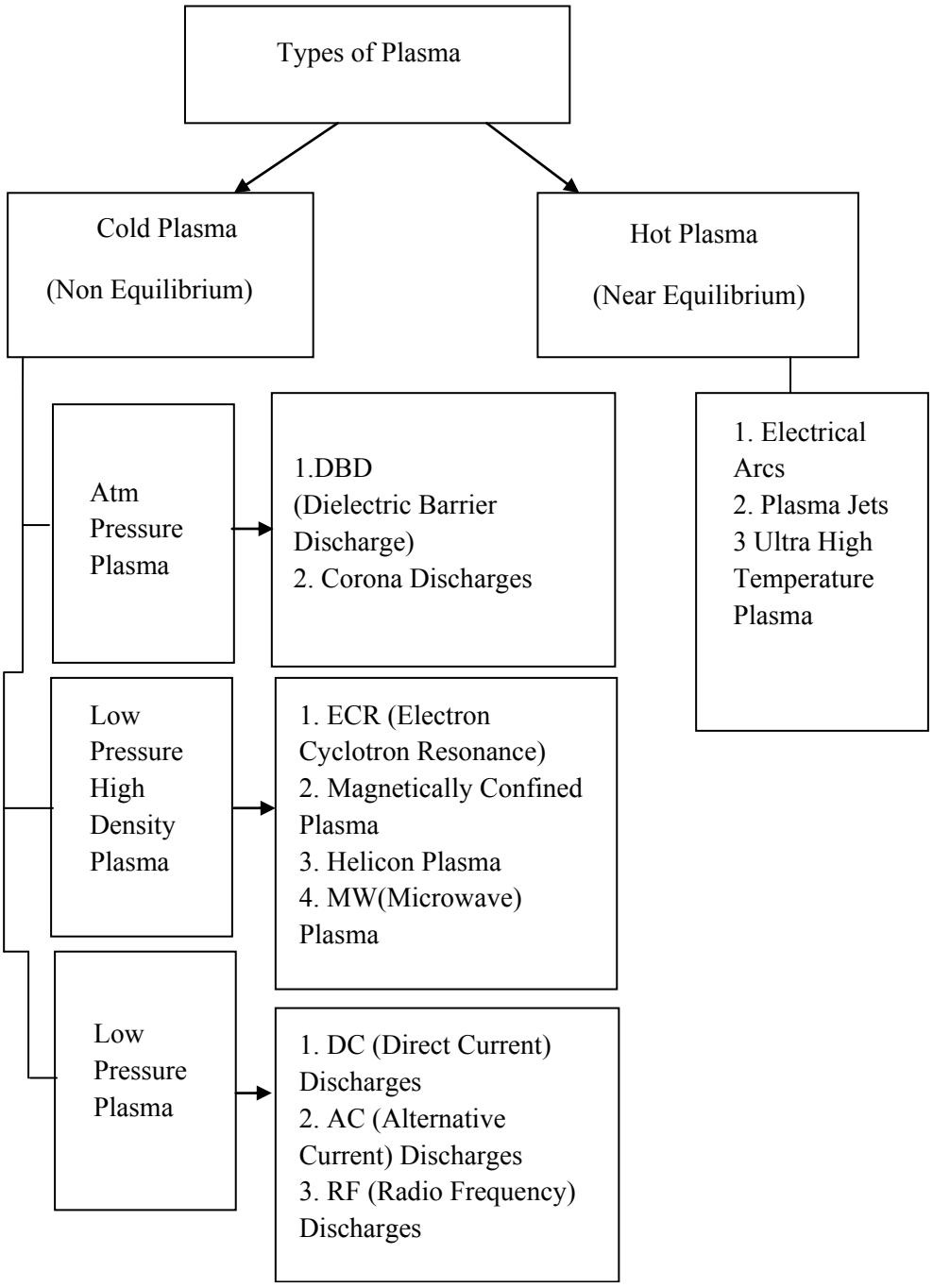

Figure 6: Types of plasmas

Corona discharges are the gas discharges operated when there is extinction of insulating surfaces or dielectric surfaces are far away from the discharge zone. In corona discharges drift region positioned between the ionization zone and electrode. Excitation, recombination, neutralization (will be discussed later) reactions take place in the drift region. If ionization zone is very near to the stressed electrode, this type of coronas identified as unipolar conduction coronas which leading to the formation of positive ions as a result of the electron bombardment of point anode. Under the effect of inelastic collisions of positive ions and gas molecules, approximately 95% of the electric energy transferred to gas molecules in the drift region. In the presence of highly non uniform electric field, corona discharge emerges as a glow placed around a point tip which acting as anode. Very small size of anode leads to intensified voltage near it. Ionization process of gas depends on the geometry of the electrodes. Concerning with the configuration of electrodes corona discharges can be categorized into three groups such as point to plane, wire-cylinder, wire to plane corona discharges [Denes et al., 2004].

Low pressure high density plasmas involving ECR (Electron Cyclotron Resonance), magnetically confined plasma, helicon plasma and MW (Microwave) plasma are operated at high degree of ionization compared with RF discharges. ECR (Electron Cyclotron Resonance) source can be obtained at applying microwave power to the plasma chamber through a quartz window around which solenoidal electromagnets arranged in order to create magnetic field of 850 Gauss giving rise to the rotation of the electrons in helical orbit with the angular frequency of 2.45 GHz under the resonance condition which can be defined as the equivalence of the applied microwave frequency and cyclotron frequency of electrons (angular frequency of the electron). Energy transfer can expeditiously achieved when resonance condition is fulfilled but the generated plasma does not show uniform distribution. [Denes et al., 2004].

In the case of magnetically confined plasma electrons enclosed in plasma by magnetic field in order to increase the efficiency of ionization. The system of magnetically confined plasma consists of two electromagnetic fields having the frequency of 13.56 MHz and 100 kHz. The field of 13.56 MHz frequency triggers

and maintains the discharge, the other one is responsible for the bias and flux of the charged particles [Boozer et al., 2004].

Helicon plasma is another kind of low pressure high density plasma which composed of rolled helicon antenna around quartz or glass cylinder. Two source type suggested for helicon plasma; one is helicon wave coupling in which the antenna circulating current generated magnetic field, the other is RF inductive or capacitive coupling with combination of magnetic field. Higher ion density can be obtained with helicon wave coupling with no need for internal electrodes. Helicon plasmas are used for etching of metals, semiconductors and deposition of hard coatings of thin films [Charles et al., 1993].

Discharge of microwave (MW) plasmas are initiated and pursued by microwave energy for electron acceleration. Generally 2.45 GHz typical microwave frequency is used through the microwave frequency range of 300 MHz to 300 GHz. MW discharges are used for ensuring a lasing environment for CO_2 gas lasers which have extensive application area at optical lithography and marking [Denes et al., 2004].

As for low pressure low frenquency plasmas, direct current (DC) plasma is generated by electrical discharge between two conducting electrodes and high voltage is applied them giving rise to a constant current. Under the effect of high voltage free electrons accelerated toward the anode. Inelastic collisions between energetic, hot electrons and heavy, slow moving, cold gas molecules resulted in ionization and excitation processes, while the elastic collisions dominate at low voltages. Discharge is emerged due to ionization process at high voltages in the range of 100-1000 V. Glow discharge appears at high voltages (a few hundred Volts) between anode and cathode and at low currents which are less than 1 ampere, but arc discharge occurs at low voltage (nearly 10 Volts) and at high current (1-100.000 amperes). Discharge characteristics depend on the applied voltage such that at low voltages free electrons form a negligible current, while at high voltages the current increases because of the effective ionization. The breakdown voltage of the DC plasma, which can be defined as the process in which newly produced electrons are accelerated toward the anode, relating with the geometrical configuration of the electrodes, pressure, and the type of process gas. Need for conductive electrodes, dependence of discharge

characteristics on the geometry of the discharge tube are disadvantages of DC discharges [Eliezer S and Eliezer Y.].

As the name suggests, alternative current (AC) discharges are generated by the alternative current of high voltage transformer at the frequency level of lower than 100 Hz. AC discharges can be considered as a sequence of short discharges, in which the two electrodes alternatingly play the role of cathode and anode. In this case discharge can not be sustained continuously since the half period of the AC field is higher than the charging up time of the insulator. So high frequency plasmas like RF glow discharges are more uniform and efficient when compare with the AC discharges.

Among the cold plasma types, radio frequency (RF) glow discharges are widely preferred for altering the material surfaces for industrial and medical applications.

1.4.3 RF Glow Discharges

The name of the RF (Radio Frequency) glow discharges comes from the frequency range which participates in generating plasma. However the entire RF band is between 1kHz-1GHz, most of the RF plasmas set having the standard 13.56 MHz industrial frequency or its harmonies, in order to keep clear of the interference with communication networks. Three requirements should be ensured in order to generate plasma: 1) a vacuum system for sustaining the plasma state, 2) chamber for reactions, 3) an energy origin for ionization. As an energy source, mostly electrical energy is preferred.

At low pressure, by applying potential difference between anode and cathode the glow discharge can be generated. Due to the potential difference, electrons that are ejected from the cathode by the omnipresent cosmic radiation, are accelerated away from the cathode, and give rise to collisions with the gas atoms or molecules (excitation, ionization, dissociation). On account of the potential difference, ionization of the process gas atoms occurs forming positively charged ions and free electrons. Electron- ion collisions are predominant at higher levels of ionization. In the plasma chamber, positive ions accelerate toward the cathode and electrons absorb the power from RF field transferring it throughout elastic and inelastic collisions. Due to the enormous mass difference between electrons and molecules, elastic collisions reduce

very little part of the electrons' energy but they change their direction. When this direction change synchronizes with the change in the electric field, electrons acquire extra energy resulted in formation of ionization process even at low electric fields in the case of RF discharge, differently from the rest of discharge plasma types. As a result of the collisions between accelerated electrons and other particles, depending on the energy gained, excitation, ionization and molecular dissipation occurs which induces active species. If the atom or molecule gain energy more than the ionization potential of the atom or molecule itself, ionization takes place but the excitation of the atom or molecule occurs when the ionization potential is higher than the energy gained from the interactions. The excitation collisions causes the formation of excited species producing light as a result of emission to lower levels. This process is account for the the typical name of the 'glow' discharge [Bogaerts et al., 1999 and Denes et al., 2004].

Schematic illustration of RF glow discharge plasma is given in Figure 7. RF glow discharge system composes of a vacuum system, plasma reaction chamber, matching network, and RF generator. Rotary pump and oil diffusion pump compose the vacuum system which is essential for maintaining the plasma state. As it can be clearly seen from the figure, RF power supplies coupled the plasma reaction chamber through a matching network which decreases the loss of power because of the undesired reflections.

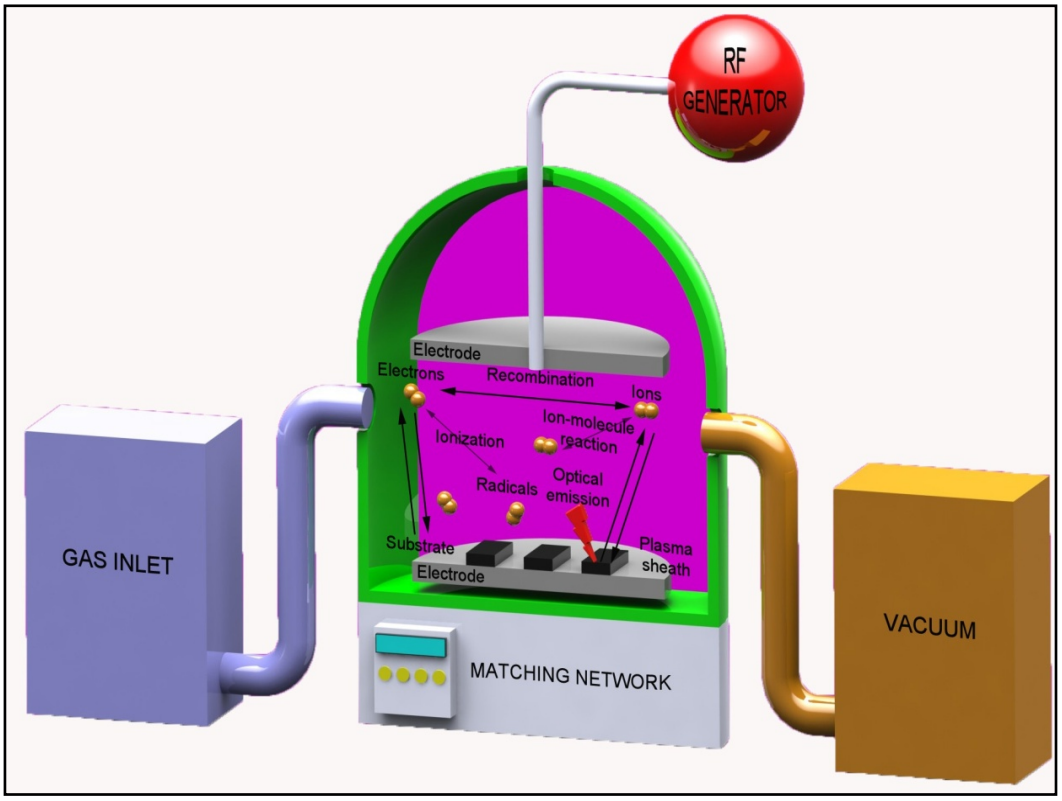

Figure 7: Schematic illustration of RF glow discharge plasma

1.5 Interactions Between Plasma and Materials

As mentioned before plasma can be considered as a mixture of highly exited and energetic species, since ionized and excited molecules are chemically reactive, energy is transmitted to the plasma treated surface from these energetic species. Energy transfer leads to the activation of surface molecular layers of the material having the following synergetic results: 1) Eradication of low molecular contaminants and simultaneous removal of weakly bound polymer overlays, specifically called ‘etching’ [Panditaraj et al., 2009]. 2) Formation of desired chemical functional groups and chains such as alcohol, hydroperoxide, acid, ester, aldehyde, carbonate, carbonyl, primary, secondary and tertiary amines, much the same amides and so on. 3) Activation of surface resulting in rendering of some surface functional groups to other chemical functional groups by radical reactions can be said ‘grafting’ [Landgraf et al., 2009].

Favia and d'Agostino classify the plasma treatment into three categories: 1) Plasma enhanced chemical vapor deposition (PECVD) 2) Plasma treatment 3) Plasma etching [Favia et al., 1998]. More recently Gomathi et al. proposes plasma treatment of a material can be resulted in two ways, one is 'non polymer-forming' plasma which also involving removal of surface contaminants, etching, substitution of chemical groups, plasma induced grafting. In the second way, if the implemented gas is organic gas such as hydrocarbons and alkylsilanes, the treatment is resulted in 'polymer forming' reaction specifically called plasma polymerization [Gomathi et al., 2008]. Formation of free radicals, UV radiation in the reaction chamber, the effects of the ions present on the surface are the answer of the responsible factors of the effects of plasma surface modification [Johansson et al., 2002].

The result of implementation of plasma treatment is based on the type of the exposing gas, chemical properties of the polymeric material and the energy level of the plasma.

1.6 Poly (methyl methacrylate) (PMMA)

Poly (methyl methacrylate) (PMMA) is a linear thermoplastic polymer which mainly composed of methyl ester groups. Repeating unit of PMMA is given in Figure 8. If surface ester side chains modified physically or chemically, biomolecules can be easily adsorbed on PMMA gaining high binding affinity. Its bulky side groups and being lack of complete stereoregularity make PMMA amorphous polymer.

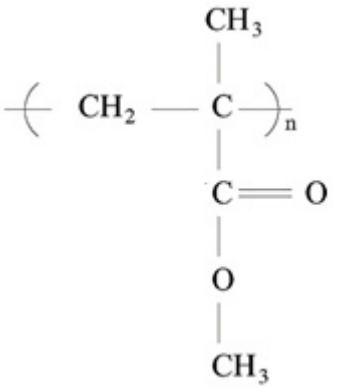

Figure 8: Repeating unit of Polymethylmetacrylate (PMMA)

PMMA can be considered as having excellent optical properties on account of being transparent, transmitting visible light up to 92% giving about 4% reflection from its surface, and similarly filtering process of UV light with ordinary glass. Besides lightweight and shatter resistant properties make it to be an alternative to glass. Also its low cost induces being used as an economical alternative to PC (polycarbonate) even lower impact strength. The environmental stability of PMMA makes it one of the most preferred materials for outdoor applications. For example advertising boards, aircraft windows, windshields of the cars, exterior light lenses of automobiles, helmet visors and police bucklers are made of PMMA. The usage of PMMA in medical field can be listed in the intraocular lens, bone cement, skull defect filler, denture, cosmetic surgery, bio implant and microfluidic applications. Despite there are many promising plastics emerge, reliability and versatility characteristics of PMMA make it to remain its popularity. Furthermore PMMA is one of the extensively used organic material in the usage of medical technologies due to its low toxicity, biocompatibility, bio-inertness, biologically non degradability and easy manipulation.

The usage of PMMA for medical applications began in 1950's. PMMA was the first substance to be used in the production of intraocular lenses (IOLs) [Gozum et al., 2003]. Permanence of epithelioid cells on IOL surface indicates the foreign body reaction and it is a fact that foreign body reaction and disruption of blood-aqueous barrier cause postoperative inflammatory after cataract surgery operations. So candidate IOL should not induce any inflammatory or immunological reaction. As

complement system's reaction is considered as poor biocompatibility, based on this consideration it was reported that PMMA IOL is more biocompatible than prolene and silicon IOL [Chehade et al., 1997].

The biocompatible characteristic of PMMA lies on the surface properties which are able to be upgraded with surface modification techniques. Surface modification of PMMA such as plasma treatment, ion implantation, heparinization, polyethyleneglycol (PEG) grafting decrease the risk of postoperative inflammation and cell adhesion after cataract surgery. On the other hand, acute postoperative endophthalmitis (POE) is still one of the commonly faced crucial problems of cataract surgery. Bacterial adherance to IOL is thought to be the reason of bacteria induces POE. It was reported that bacterial adhesion on any IOL is directly related with surface roughness, hydrophilicity, surface electric charge and surface chemistry [Kodjikian et al., 2008].

In dentistry, PMMA based composite brideges and removable dentures are alternatively used as inexpensive and easy preparation method instead of current gold bridges [Miettinen et al., 1997]. Although PMMA denture resin is mostly selected material for denture bases, the surface of the substratum is a candidate for Candida Albicans adhesion inducing 'Denture Induced Stomatitis' which is one of the serious problems after the application of denture prostheses. Surface modification of PMMA denture with chemical treatments or plasma treatment or pretreatment with plasma then antimicrobial agent coating reduces the biofilm formation as well as the adhesion of Candida Albicans. For this purpose, Miura et al, treated PMMA samples with O_2 plasma (200W-10 min) then coated the surface with protamine, microbial peptide; reduction of fungal growth was detected on the protamine coated surface [Miura et al., 2010]. Besides its other excellent qualities, the esthetic appearance of PMMA makes it favored material being used for anterior teeth instead of gold and amalgam in the dental restorative applications [Kennedy et al., 1998]. In orthopedic surgery operations, PMMA bone cement is being used the most acceptable for infixing implants and transforming lost bone. Sometimes PMMA bone cement and bone particles or glass powders are mixed for the aim of mechanical fixation of PMMA.

Another utilization area of PMMA is microfluidic systems which are used not only in the molecular biology, robotics for genomics, proteomics, and cellular research but also in diagnostics for medical applications. Biocompatibility, high transparency, low cost and very low autofluorescence over a wide spectral range of PMMA forced biotechnologies to migrate from silicon technologies to thermoplastic polymers [Becker et al., 2002 and Tsao et al., 2007].

Surface properties are also critical issue for microfluidic research field where surface interactions between small amount of liquid and comparatively large surface area channels are dominant. So in these kinds of micro systems surface properties should be controlled carefully. Surface modification of microfluidic devices enhances device performance improving flux and selectivity, at the same time reducing fouling [Kim et al., 2007].

1.7 Plasma Surface Modification of PMMA

There are quite a number of studies about plasma surface modification of PMMA, and some of them are mentioned below.

Johansson et al. investigated the effect of plasma parameters on the cell attachment using RF air plasma treatment of PMMA by means of XPS and contact angle measurements and the results indicated that 500W 5 min plasma treated PMMA surface had the highest amount of HeLa cervix carcinoma cells among the 300W-5 min and 500W-5 min RF air plasma treatment conditions [Johansson et al., 2002].

Liu et al. produced atomic transfer radical polymerized PEG grafted PMMA microcapillary electrophoresis chips by oxygen plasma to activate the surface of PMMA substrates in order to immobilize 2-Bromoisobutyryl bromide. Surface modification of chips decreased the electroosmic flow and adherence of bovine serum albumin on the channel surfaces. The results suggested that surface modified PMMA capillary electrophoresis microchips can be used for protein analysis [Liu et al., 2004].

Chai et al. summarized the oxidation process of PMMA by DC pulsed oxygen plasma treatment and the increase in the hydrophilicity on account of the increasing amount of oxygen functional groups were observed [Chai et al., 2004].

Yoshinari et al. modified the surface of PMMA denture base with RF oxygen plasma (200W-10min) in order to ease the immobilization of Peptide Histatin 5 which induces inhibition of biofilm formation. The results indicated that oxygen plasma treatment increased the amount of adsorbed Peptide Histatin 5 on the PMMA surface six times with respect to unmodified one [Yoshinari et al., 2005].

Tang et al. compared the influences of argon plasma at different levels of plasma pressures such as RF atmospheric pressure plasma and RF low pressure plasma, on the surface free energy of PMMA plates. 120W atmospheric pressure argon plasma treated PMMA plates at various treatment times like 10-30-60-90-120 seconds demonstrated higher surface free energy values than that of low pressure argon plasma treated PMMA plates at the same power and treatment time parameters. According to the results atmospheric pressure plasma increased surface free energy higher and faster than that of low pressure plasma [Tang et al., 2008].

Ozcan et al. investigated the effects of plasma conditions on the surface free energy and cell attachment and reported that the highest amount of 3T3 cell attachment was attained on PMMA modified at 100W- 15 min oxygen plasma treatment having the total surface free energy value of 61.77 mJ/m^2 according to Geometric Mean approach. [Ozcan et al., 2008 (b)].

Zhang et al. compared the antithrombogenicity activity of the pristine PMMA, 40W-5 min RF argon plasma treated PMMA, plasma pretreated Heparin (Hp) coated PMMA, plasma pretreated polyethyleneglycol (PEG) coated PMMA, plasma pretreated and both Hp and PEG coated PMMA for the usage of medical grade intraocular lenses. Lowest numbers of blood platelets were obtained on the surface of plasma pretreated and Hp coated PMMA in comparison to the other modified surfaces and unmodified PMMA surface [Zhang et al., 2009].

Barhai et al. studied the power effect on the surface morphology of diamond like carbon (DLC) deposited PMMA substrate changing the process power from 10W to 90W by succesively increasing 10W each time for 60 min treatment of radio frequency plasma enhanced chemical vapor deposition (RF-PECVD). The results revealed that 40W- 60 min deposition of DLC film led ultra smooth surface of PMMA substrate with increased hydrophilicity [Barhai et al., 2009].

Chen et al. carried out the surface modification of PMMA with RF atmospheric pressure spin plasma jets selecting the plasma power values as 50W, 100W, 150W and 5-10-15 mm processing gap values at various number of process cycles (from number 1 to 5) in order to investigate the plasma parameters on the surface properties of PMMA samples. The results showed that plasma power and processing gap play key roles in improving the hydrophilicity whereas number of process cycles play secondary role [Chen et al., 2009].

Tsougeni et al. nanotextured the PMMA surface by using helicon type plasma with RF power source, where oxygen plasma treatment followed deposition of C_4F_8 gas as Teflon precursor for the purpose of obtaining superhydrophobic surfaces. The results showed that there was a direct proportion between the plasma treatment time and pillar height. There was an increase in the pillar height about 300 nm in a minute of plasma application [Tsougeni et al., 2009].

Baytekin et al. investigated the wettability of the microwave low pressure oxygen plasma treated interior side of PMMA microchannels to be used as microfluidic devices. The results elicited that plasma treatment decreased the contact angle up to 45°, but aging effect showed itself at the ratio of 10-25 % after treatment. In order to investigate aging effect, plasma treated samples were dipped into 70% v/v EtOH/water solution for 3 min after plasma treatment and rinsed with bi distilled water [Baytekin et al., 2010].

D'Sa et al. focused on the albumin adhesion, cell attachment and cell spreading on PMMA surfaces modified with atmospheric pressure dielectric barrier discharge (DBD). Results showed that surface modified PMMA having more viscoelastic layer of albumin whereas unmodified surface induced flattened protein adsorption. Attachments of the human lens epithelial cells were nearly same for the untreated and treated PMMA surfaces but DBD modified surface of PMMA showed better cell spreading with formation of actin stress fibres. The findings of the study suggested that low DBD energy doses were useful for enhanced cell adhesion [D'Sa et al., 2010].

Tennico et al. improved a technique for bonding polymer microchips in order to use in microfluidic devices. For this purpose PMMA substrate surface pretreated with

20W-90 s RF oxygen plasma then the surface was silanized using 10% tetraethyl ortho silicate (TEOS) solution in 60:40 (v/v) isopropyl alcohol:water. After then again oxygen plasma activation was carried out, and activated surfaces bonded and pressed. No bonding ability was observed for pristine PMMA so the results showed that plasma surface activation and TEOS modification can be used as an effective method for bonding polymer microchips [Tennico et al., 2010].

Wei et al. tried to find the optimum RF argon plasma conditions for surface activation and graft polymerization of PEG on PMMA in order to attain a surface having antistatic property. The results indicated that 40W 3 min argon plasma treated and PEG grafted PMMA surface showing the lowest resistivity property, so argon plasma activated PEG grafted PMMA surface can gain antistatic property [Wei et al., 2010].

Mukhopadhyay et al. created various surfaces of PMMA such as dielectric barrier discharge (DBD) treated PMMA, nitrogen plasma treated PMMA and undoped DLC (diamond like carbon) coated PMMA in order to investigate the influences of surface free energy, water contact angle, surface roughness on the fluid flow and filling time of these created surfaces to be used for microfluidic devices. Results demonstrated that fluid flow time decreased significantly for DBD treated PMMA microchannels which having the lowest water contact angle equaling 44.35° [Mukhopadhyay et al., 2011].

Although there are many studies in literature, there is no detailed report making the comparison of effects of different plasma powers, application times and gas type on the properties of PMMA surfaces, which will be considered in this study.

1.8 Aim of the Study

The aim of the present study is to investigate the influence of RF plasma parameters such as power, application time and process gas type on the surface properties of PMMA films, to confirm the fact that starting from single material, various surfaces can be attained by only changing the applied plasma parameters. This study can set light to choose an appropriate plasma condition for surface modification of PMMA as a candidate to be used in several applications especially for the immobilization of

the some specific molecules for biosensors, such as bioactive molecules like DNA, protein A, hyaluronic acid, heparin, immunoglobulin G, glucose isomerase, carboxyl methyl-dextrans. The choice of the plasma parameters used for the modification is important factor for controlling the surface properties in order to obtain the surface having desired chemical functional groups.

The effect of plasma input power (10W, 50W, 100W), application time (5 min, 15 min, 30 min), and process gas type (nitrogen, argon and oxygen) on the surface free energy as well as surface free energy components were examined. The change in surface free energy depending on the plasma parameters were calculated according to Geometric mean, Harmonic mean and Acid-base approaches and the results were compared. Additionally the relationship between the plasma parameters and contact angle, surface free energy, surface chemistry, surface topography, surface radicals and the radicals stability were investigated. Surface chemistry of untreated and plasma treated PMMA films in terms of newly formed chemical functional groups were investigated by X-Ray Photoelectron Spectroscopy (XPS). The changes in the surface morphology and surface roughness with respect to plasma treatment were investigated by Atomic Force Microscopy (AFM) analysis. Electron Spin Resonance Spectroscopy (ESR) analysis were done to detect radicals created on the surface of PMMA by oxygen plasma treatment.

CHAPTER 2

EXPERIMENTAL

2.1 Materials

Poly (methyl methacrylate) (PMMA), $[-CH_2C(CH_3)(CO_2CH_3)-]_n$, with a molecular weight of 120000, was purchased from Aldrich, Germany. Chloroform ($CHCl_3$) was purchased from Lab-Scan, Ireland. All liquids used in contact angle measurements were reagent grade. Formamide ($HCONH_2$) was a product of Merck (Darmstadt, Germany), Diodomethane (CH_2I_2) was a product of Sigma Aldrich (Steinheim, Germany), and Dimethyl sulfoxide (C_2H_6OS) was a product of Acros (New Jersey, USA). In all experiments, double distilled water was used.

2.2 Methods

2.2.1 Preparation of PMMA Films

PMMA films were prepared by solvent casting method. Solutions containing PMMA (20% w/w in chloroform) were prepared at room temperature and dropped on microscope slides placed in petri dishes. The petri dishes were covered with stretch films to keep the surface clean where the stretch films were pierced in order to let the solvent evaporate (Figure 9). Solvent evaporation was achieved at room temperature for 7 days and then in vacuum oven for 24 h. The thickness of the films were measured by a micrometer at least from 5 different places of the slides and found to be 1.5 ± 0.3 μm.

Figure 9: PMMA film preparation on microscope slides

2.2.2 Plasma Modification of PMMA Films

Plasma treatment of PMMA films were performed with (Advanced Plasma Systems Inc, USA) as shown in Figure 10-a. System consists of RF generator, a reaction chamber, vacuum pump, manifold unit, matching network box, and RF power supply. Manifold unit, joining the three gas tubes, has two gas flow channels where one is for vacuum pump and the other is for creating the gas atmosphere in the reaction chamber. Vacuum pump works at two stages. First step removes the gas from the chamber, second step insures continuos flow. After placing the samples into the reaction chamber which is like a cylindrical shaped container, the system was evacuated to about 20 mTorr. Then reactive gas was allowed to flow into the chamber. The RF power at 13.56 MHz frequency was applied to the system with internal aluminum electrodes by capacitive coupling. Matching network box was used for keeping the reflected power at minimum by adjusting the impedance manually.

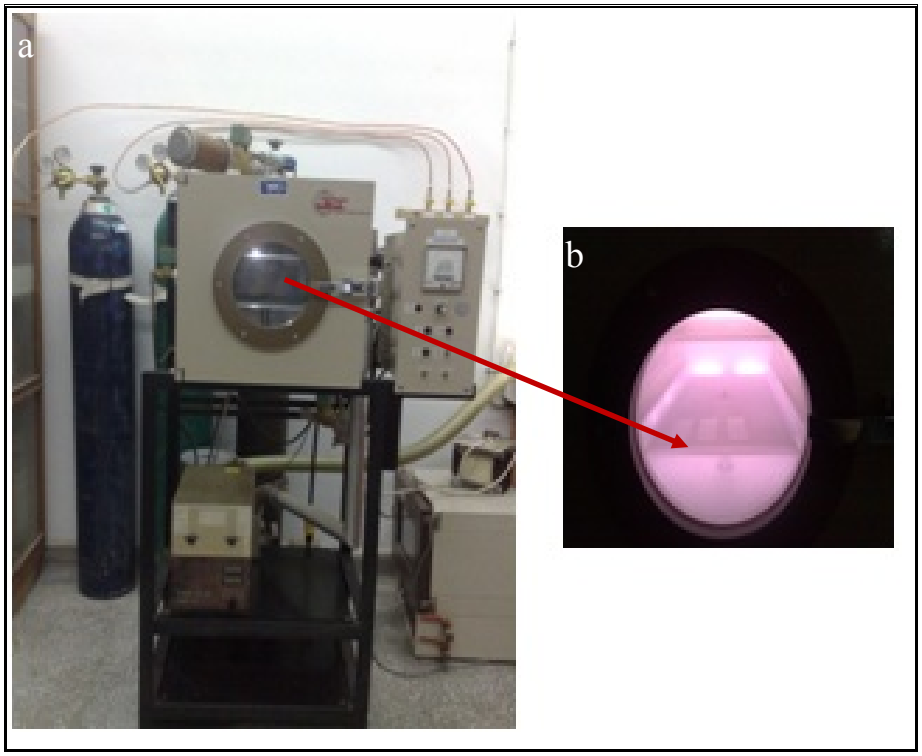

Figure 10: Photographs of RF Plasma treatment. a. The instrument b. PMMA films during oxygen plasma application.

The system was runned by using different discharge powers (10W, 50W, 100W), different durations (5min, 15min, 30min) and different gases (O_2, N_2, Ar) at 600mTorr. After plasma discharge, power was turned off, the system was extra subjected to 30 min gas flowing to stabilize the created surface radicals and active species. Table 2 gives samples codes and conditions applied to the PMMA samples. For sample coding the first capital letter indicates the type of gas used (O for oxygen, N for nitrogen, and A for argon). After capital letter the first number showes the applied power value and second number gives the the plasma treatment time. For instance, the PMMA sample treated with oxygen plasma for 10 watt power and for 5 min duration is coded as O-10/5.

Table 2: PMMA samples and plasma treatment conditions

Sample Name	Process Gas	Plasma Power (Watt)	Treatment Time (Min)	Total Energy (Watt x Min)
C-0/0	No gas	0	0	0
O-10/5	Oxygen	10	5	50
O-10/15	Oxygen	10	15	150
O-10/30	Oxygen	10	30	300
O-50/5	Oxygen	50	5	250
O-50/15	Oxygen	50	15	750
O-50/30	Oxygen	50	30	1500
O-100/5	Oxygen	100	5	500
O-100/15	Oxygen	100	15	1500
O-100/30	Oxygen	100	30	3000
N-10/5	Nitrogen	10	5	50
N-10/15	Nitrogen	10	15	150
N-10/30	Nitrogen	10	30	300
N-50/5	Nitrogen	50	5	250
N-50/15	Nitrogen	50	15	750
N-50/30	Nitrogen	50	30	1500
N-100/5	Nitrogen	100	5	500
N-100/15	Nitrogen	100	15	1500
N-100/30	Nitrogen	100	30	3000
A-10/5	Argon	10	5	50
A-10/15	Argon	10	15	150
A-10/30	Argon	10	30	300
A-50/5	Argon	50	5	250
A-50/15	Argon	50	15	750
A-50/30	Argon	50	30	1500
A-100/5	Argon	100	5	500
A-100/15	Argon	100	15	1500
A-100/30	Argon	100	30	3000

2.2.3 Contact Angle Measurements

Goniometer (KSV CAM 200, Finland) was used for the measurement of contact angle values of N_2, Ar and O_2 plasma treated and untreated PMMA films. The system consists of a CCD camera connected to a computer and with an automatic liquid dispenser. Static contact angles were determined by placing 5 μL drop of distilled water (DW), diiodomethane (DIM), formamide (FA), and dimethyl sulfoxide (DMSO) on the samples and the contact angles of at least five drops were measured at 25°C.

2.2.4 Surface Free Energy (SFE) Determination

SFE determination of PMMA films were performed by goniometer using different approaches, namely Geometric Mean, Harmonic mean and Acid–Base approaches. The values of surface tension and its components for the liquids used in SFE calculations were obtained from the literature and are given in Table 3 [Cantin et al., 2006].

Table 3: Surface free energy parameters of test liquids according to acid-base approach

Liquid	Total SFE γ_L (mJ/m^2)	Lifshitz-Van Der Waals Component γ_L^{LW} (mJ/m^2)	Acid Base Interaction γ_L^{AB} (mJ/m^2)	Acidic Component γ_L^{+} (mJ/m^2)	Basic Component γ_L^{-} (mJ/m^2)
DW	72.8	21.8	51.0	25.5	25.5
DIM	50.8	50.8	0	0	0
FA	58.0	39.0	19.0	2.3	39.6
DMSO	44.0	36.0	8.0	0.5	32.0

2.2.5 X-Ray Photoelectron Spectroscopy (XPS) Analysis

Characterization of surface functional groups for untreated and plasma treated PMMA films were investigated by XPS at PHI 5000 VersaProbe, Japan, equipping with an argon ion gun and employing Al monocromatic X-Ray source. The electron take off angle was 45° and the pass energy was 187.850 eV for survey spectra. Peak fitting was performed with v4.12 Seasolve computer program.

2.2.6 Atomic Force Microscopy (AFM) Analysis

Surface morphology of plasma treated and untreated PMMA films were characterized by Atomic Force Microscopy (AFM) by using Vecoo MultiMode V AFM, USA. The surface topography images of plasma treated and untreated samples were captured at tapping mode with silicon tip. Scan size was (5 μm x 5 μm).

2.2.7 Electron Spin Resonance (ESR) Analysis

ESR analysis were carried out only for the oxygen plasma treated PMMA surfaces for characterization of radicals created on the samples. For ESR analysis a special technique was developed like that the prepared PMMA pieces were cut into small pieces (1 mm x 1 mm) as can be seen from Figure 11-a, 500 mg of PMMA films was placed into a pyrex petri dish which has a special inlet (Figure 11-b). RF oxygen plasma treated samples were immediately transferred into the quartz ESR tubes with the help of special neck without touching the samples by hands. ESR tube was placed into liquid nitrogen, placed into the ESR spectrometer cavity (Figure 11-c) and then ESR analysis was implemented at Bruker; E580 Elexsys ESR device (Germany) using X Band cavity with center field of 3517 G and 0.5 mW power values for each scan. Resonance frequency value was fixed to 9.85 Hz.

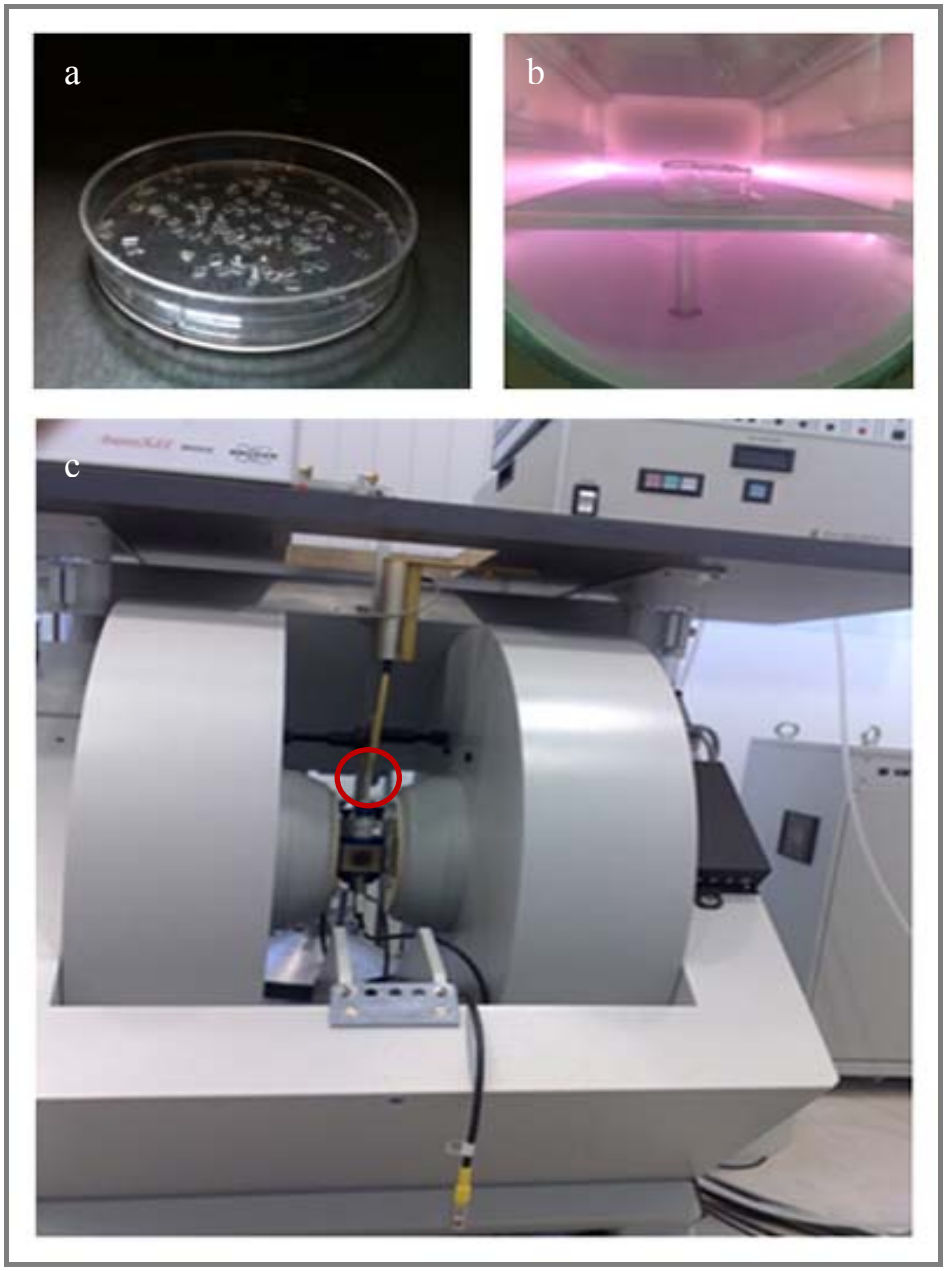

Figure 11: Preparation of PMMA samples for ESR analysis. a) PMMA film pieces, b) Plasma application to PMMA film pieces, c) ESR device and its cavity pointed by the red circle

CHAPTER 3

NITROGEN PLASMA APPLICATION

In the plasma surface modification experiments, nitrogen, argon and oxygen gases were used by application of three different powers for three different durations. The results obtained for each gas are discussed in different chapters. This chapter deals with nitrogen plasma modification results, where chapter 4 and 5 deal with argon and oxygen plasma modifications, respectively.

3.1 Contact Angle Results of Nitrogen Plasma Treated PMMA Films

Contact angle measurements values of distilled water (DW), diiodomethane (DIM), formamide (FA) and dimethyl sulfoxide (DMSO) on the surface of nitrogen plasma treated and untreated PMMA films are given in Table 4.

Table 4: Contact angle values of nitrogen plasma treated PMMA films

Liquid / Sample	DW	DIM	FA	DMSO
C-0/0	71.3 ±0.3	32.4 ±0.8	54.8 ±1.3	31.1 ±1.1
N-10/5	35.8 ±0.8	23.2 ±0.6	13.6 ±0.6	7.6 ±0.7
N-10/15	28.2 ±0.9	25.3 ±0.6	11.6 ±0.4	7.5 ±0.4
N-10/30	32.9 ±0.8	13.7 ±1.3	10.4 ±0.6	7.8 ±0.7
N-50/5	33.2 ±0.8	22.6 ±0.8	15.7 ±0.6	10.4 ±1.8
N-50/15	21.5 ±1.3	8.9 ±0.3	7.3 ±0.3	6.8 ±0.2
N-50/30	28.5 ±1.3	7.9 ±0.3	7.3 ±0.5	6.7 ±0.2
N-100/5	30.3 ±1.2	19.6 ±0.8	11.4 ±0.9	8.3 ±0.7
N-100/15	20.3 ±2.2	7.2 ±0.5	6.0 ±0.9	5.9 ±0.8
N-100/30	16.3 ±2.2	6.7 ±0.8	5.8 ±0.9	5.3 ±0.4

For the untreated control group; water contact angle was 71.3° having low hydrophilicity. There was significant water contact angle reduction down to 35.8° for the sample N-10/5, and to 28.2° for the sample N-10/15. There was an increase to 32.9° for sample N-10/30 (Figures 12 and 13). The results agreed well with the literature where the researchers applied 25W RF nitrogen plasma for 2, 4, 6, 8, 10 minutes, the results showed that up to 8 min plasma treatment, water contact angle decreased gradually with increasing plasma treatment time but then rised up to 55° for 10 min treatment [Dorranian et al., 2009]. For 50W plasma treatment, the same trend was observed for fluctuation of water contact angle for 10W nitrogen plasma application while treatment time changes from 5 min to 30 min (Figures 12 and 13). This might be because of rearrangement of the surface chemical groups due to the longer exposure of the sample to the plasma or because of the cleaning away of the adsorbed contaminants and polar organic molecules leading hydrophobicity after 15 min plasma application duration.

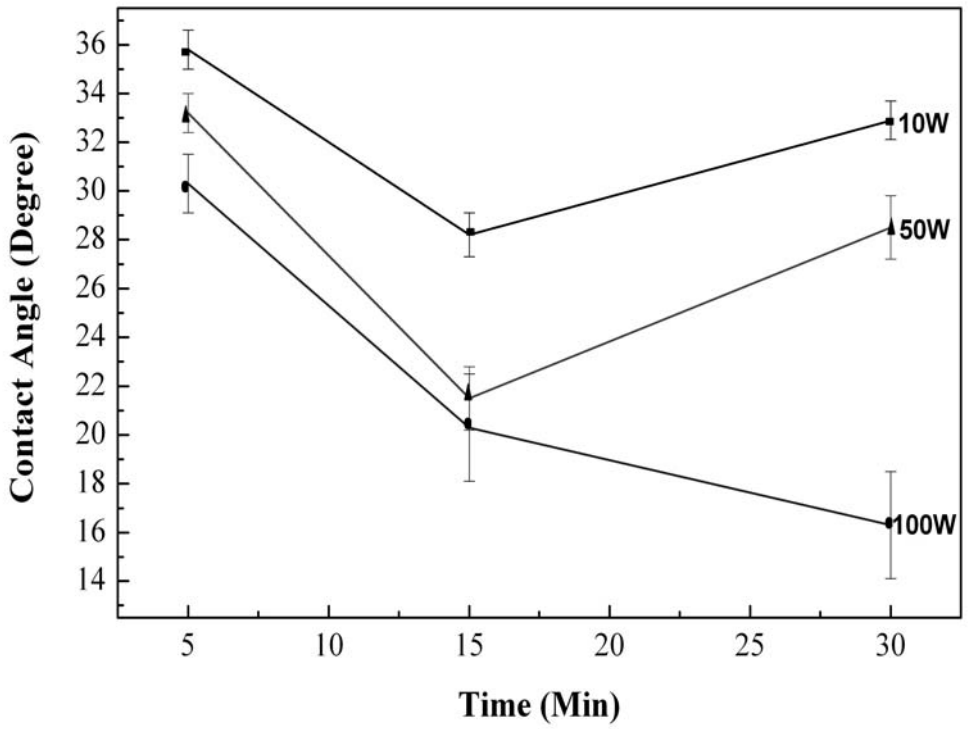

Figure 12: Water contact angle versus time graph for nitrogen plasma treated PMMA films

For samples, N-50/5, N-50/15, N-50/30 static water contact angles were obtained as 33.2°, 21.5°, 28.5°, respectively. The same fluctuation trend was detected by Tang et al after increasing the plasma treatment time from 10s to 20s and 60s for atmospheric pressure RF plasma treatment where water contact angle values increased from 32.1° to 29.3° and 39.7° for PMMA plates [Tang et al., 2008].

100W nitrogen plasma treated PMMA surfaces exhibited more regular changes in the static water contact angle as well as the contact angle of diiodomethane, formamide, and dimethylsulfoxide. Increase in the plasma treatment time caused gradual decrease in the contact angles of all the test liquids. This result indicated that the nitrogen plasma treatment at higher RF power was more effective in reducing the contact angle uniformly. If the same treatment time taken into consideration, the water contact angle decreased with increasing plasma input power. This is most probably resulted by the application of higher energy able to break various bonds of PMMA and forming different polarity and functionality. Whereas this result was not valid for the other test liquids.

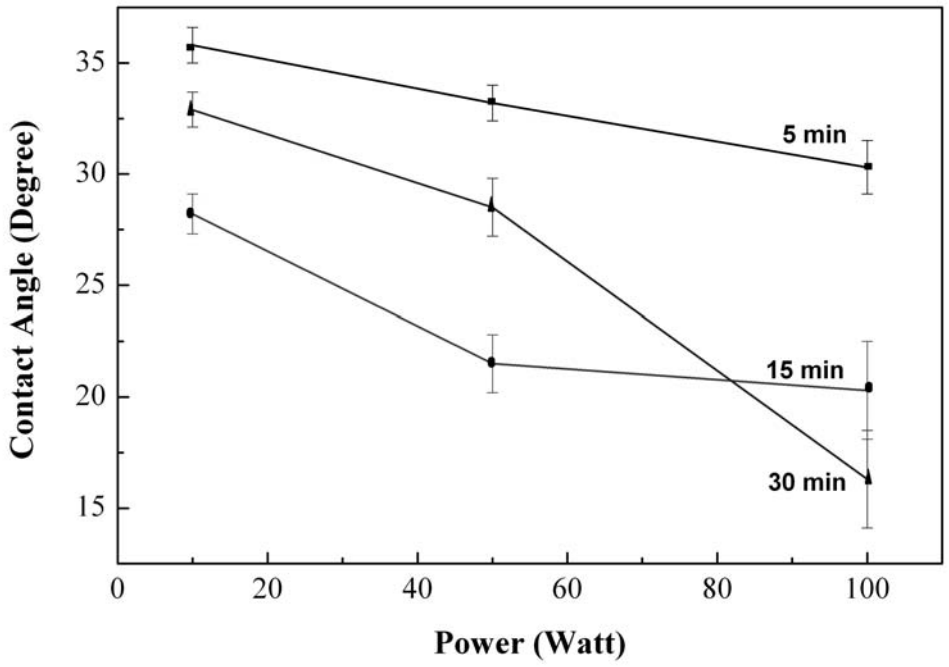

Figure 13: Water contact angle versus power graph for nitrogen plasma treated PMMA films

On the other hand, N-100/30 sample demonstrated the lowest water contact angle as 16.3° under the effect of nitrogen plasma treatment for the maximum total input energy (3000 Watt x Min). This result reveals that the maximum energy leads to minimum water contact angle as can be seen from Figure 14. Also maximum input energy- minimum contact angle trend was valid for diiodomethane, formamide, and dimethylsulfoxide. 100W 30min nitrogen plasma treatment resulted in very low contact angles about 5° for diiodomethane, formamide, dimethylsulfoxide.

By looking at Figure 14, it can be understood that power effect manifesting itself for total energy of 1500 Watt x Min. The samples N-100/15 and N-50/30 having the same total energy but having different responses of water contact angle. It was appreciably observed that 100W 15 min nitrogen plasma treatment was more effective reducing the water contact angle which equals 20.3° and it equals 28.5° for 50W 30 min plasma treatment. So it can be concluded that power effect dominated the time effect for the nitrogen plasma treatment.

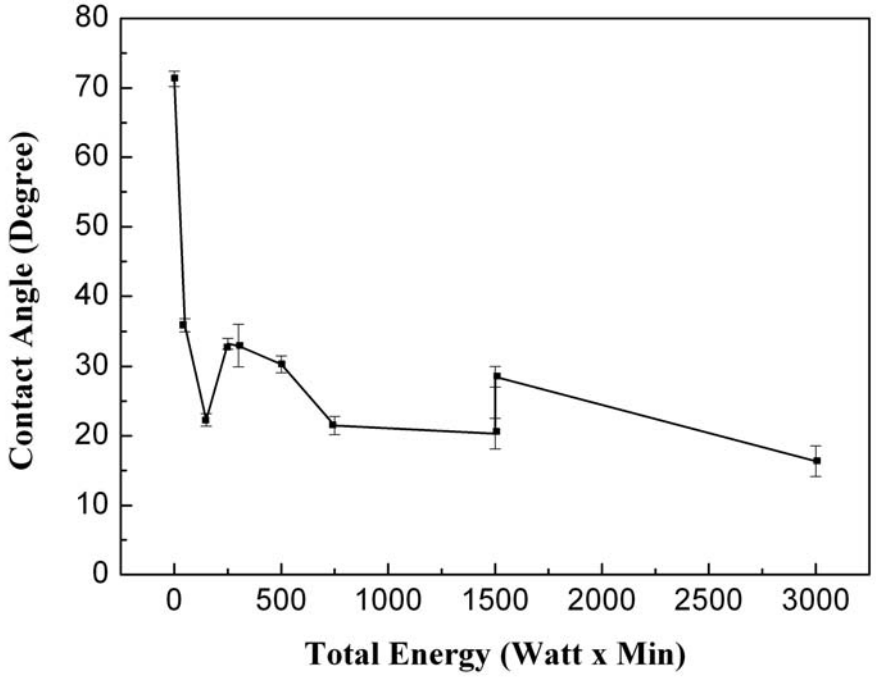

Figure 14: Water contact angle versus. total energy graph for nitrogen plasma treated PMMA films

One important point is; even a very low power applied for a short time cause a significant change in surface hydrophilicity by dropping water contact angle about 36° from 71°. Further energy lower it ~19° from 35° for N-10/5 to 16° for N-100/30.

3.2 Surface Free Energy (SFE) Results of Nitrogen Plasma Treated PMMA Films

SFE results calculated according to Harmonic Mean, Geometric Mean, and Acid-Base approaches of nitrogen plasma treated PMMA films are given in the Table 5. As can be seen from Table 5, according to Harmonic Mean approach, total SFE of untreated PMMA was 45.8 mJ/m^2 with the polar component of 10.2 mJ/m^2. These values increased to 72.3 mJ/m^2 and 33.6 mJ/m^2 respectively in the case of 100W 15min nitrogen plasma treatment. The total SFE value obtained for the sample N-100/15 was the highest among the other nitrogen plasma treated samples. After all nitrogen plasma treatments, total SFE values increased apparently as well as polar components of SFE but dispersive component of SFE remained about the same.

The sample N-10/5 having 65.4 mJ/m^2 total SFE value for Harmonic Mean approach demonstrated a slight increase to 68.1 $mJ/m^2$for the sample N-10/15. Interestingly, if the plasma application time increased to 30 min, total SFE value decreased to 50.3 mJ/m^2. Parallel changes were observed in the total SFE when according to the Geometric Mean and Acid-Base approaches. The results were consistent with the literature [Dorranian et al., 2009]. Dorranian et al. found a decrease in polar component of total SFE even with increasing RF plasma treatment time for 25W. According to Harmonic Mean approach the researchers found 31.26 mJ/m^2 , 16.34 mJ/m^2 , as the polar components of total SFE for 8 min and 10 min plasma treatment time, respectively. Namely, the polar component of SFE demonstrated parallel decreasing when there was a passing from the sample N-10/15 to the sample N-10/30. When Acid-Base approach is taken into account, the basic component increased dramatically with increasing plasma treatment time up to 15 min treatment, and then, for 30 min plasma application there was a rapid decreasing in the basic component.

Table 5: Results of total SFE and its components for nitrogen plasma treatment

Method	γ^p (mJ/m^2)	γ^d (mJ/m^2)	γ^+ (mJ/m^2)	γ^- (mJ/m^2)	γ^{tot} (mJ/m^2)
Sample C-0/0					
Harmonic	10.2	35.5			45.8
Geometric	6.5	36.2			42.7
Acid Base	1.16	43.1	0.6	3.6	44.3
Sample N-10/5					
Harmonic	28.2	37.1			65.4
Geometric	25.3	35.4			60.8
Acid Base	3.0	46.4	0.2	6.6	49.4
Sample N-50/5					
Harmonic	29.4	36.8			66.2
Geometric	26.6	34.8			61.5
Acid Base	1.6	46.7	0.1	6.8	48.3
Sample N-100/5					
Harmonic	28.8	38.1			66.9
Geometric	22.7	39.6			62.3
Acid Base	2.2	49.0	0.3	7.2	51.2
Sample N-10/15					
Harmonic	31.9	36.1			68.1
Geometric	29.8	33.6			63.4
Acid Base	2.9	45.5	0.2	7.2	48.5
Sample N-50/15					
Harmonic	33.2	37.8			71.1
Geometric	30.7	35.2			65.9
Acid Base	2.6	50.0	0.1	7.6	52.6
Sample N-100/15					
Harmonic	33.6	38.7			72.3
Geometric	29.7	37.1			66.8
Acid Base	3.8	51.0	0.3	8.1	54.8
Sample N-10/30					
Harmonic	13.4	36.9			50.3
Geometric	8.5	38.5			47.1
Acid Base	4.9	41.3	0.7	3.3	46.3
Sample N-50/30					
Harmonic	28.6	38.7			67.3
Geometric	27.8	37.3			65.1
Acid Base	1.3	51.8			53.1
Sample N-100/30					
Harmonic	29.5	39.2			68.7
Geometric	33.6	41.5			75.1
Acid Base	4.9	58.3	0.3	7.1	63.2

The sample N-50/5 had 66.2 mJ/m^2 total SFE value according to Harmonic Mean approach. This value increased to 71.1 mJ/m^2 for the sample N-50/15 then decreased to 67.3 mJ/m^2 for the sample N-50/30. Dispersive component of SFE stayed constant according to each approach. The same trend which was comparatively lower total SFE and polar component with increasing plasma treatment time after 15 min nitrogen plasma application was catched for 100W nitrogen treatment. For the sample N-100/5 the total SFE was 66.9 mJ/m^2, this value increased to 72.3 mJ/m^2 for 100W 15min application then decreased to 68.7 mJ/m^2 when the application time was extended to 30 min. Due to the fluctuation in the variation of the imine groups with increasing plasma duration may cause the decrease and then increase in the total surface free energy values for 100W treatment.

Consequently, total SFE value of nitrogen plasma modified PMMA films increased gradually with increasing plasma power when Harmonic mean, Geometric mean and Acid-Base approaches are taken into account because of the increase in the polarity of the nitrogen plasma treated surfaces due to the addition of newly formed nitrogen containing polar groups such as imine, primary amine, amide and nitrozo.

3.3 X-Ray Photoelectron Spectroscopy (XPS) Results of Nitrogen Plasma Treated PMMA Films

The chemical structure of the monomer unit of PMMA addressing the C1s peaks is given in Figure 15. Representation of components of C1s envelope as a result of peak fitted XPS analysis for the untreated PMMA is given in Table 6.

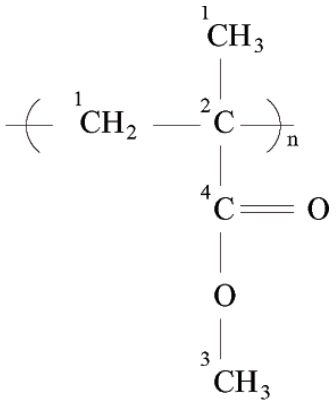

Figure 15: Chemical structure of monomer unit of PMMA

Table 6: The result of C1s peaks for untreated PMMA

Peak No	**B.E (eV)**	**Relative Peak Areas (%)**	**Bond Type**	**Chemical Structure**
1	284.6 ±0.2	47	Hydrocarbon	
2	285.6 ±0.2	22	**C** atom in α position	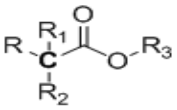
3	286.7 ±0.1	17	Methoxy group **C**	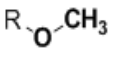
4	289.0 ±0.3	14	**C** in the ester group	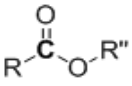

XPS analysis detected that untreated PMMA consisting of four different types of C atom because of the different chemical environment. However in the previous

literature Fakes et al elucidated the C1s peaks of untreated PMMA as three main component giving the intensity ratio of 1:1:3 [Fakes et al, 1987]. According to our XPS results, C1s (1) peak located at 284.6 eV was attributed to C-C, C-H bonds (hydrocarbon) having a good agreement with literature results [Brinen et al., 1999, Chai et al., 2004 and Liu et al., 2010]. 285.6 eV positioning C1s (2) peak is assigned to quaternary carbon atom in α position to ester group and C1s (3) at 286.7 eV corresponded to methoxy group carbon which are similar to obtained by Tsougeni et al. [Tsougeni et al., 2009]. C1s (4) locating at 289.0 eV is assigned to the carbon in the ester group.

XPS analysis of RF nitrogen plasma treatment was carried out only for 100W plasma applied PMMA films and the results were interpreted in terms of C1s, O1s and N1s core shell spectrum. XPS analysis results revealed that Nitrogen plasma treatment created nitrogen containing chemical functional groups on the surface of PMMA at the same time changed the relative area ratios of C1s and O1s peaks. (Figures 16, 17, 18). The binding energy values of created nitrogen containing functional groups and the relative peak area ratios of the N1s peaks for the samples of N-100/5, N-100/15, N-100/30 are displayed in Table 7.

Table 7: The result of N1s peaks for nitrogen plasma treated PMMA

Peak No	**B.E (eV)**	**Bond Type**	**Relative Peak Area (%) N-100/5**	**Relative Peak Area (%) N-100/15**	**Relative Peak Area (%) N-100/30**
1	395.0 ±0.2	-C=NH	3	7	2
2	398.0 ±0.1	-C-NH_2	9	20	17
3	399.5 ±0.1	-CO-NH_2	83	63	51
4	401.1 ±0.1	-R-N=O	5	10	30

N1s spectrum components of this present study agrees well with the literature. Tang et al reported the four components of N1s envelope for the air pressure plasma treatment of PMMA such as 1) -C=NH (389.9 eV) 2) -C-NH_2 (399.9 eV) 3) -CO-NH_2(401.1 eV) 4) -R-N=O (402 eV) that were quite close to the results obtained at

this current study [Tang et al., 2008]. Newly generated nitrogen containing groups which were imine, primary amine, amide, nitrozo, respectively were the products of surface radicals and reactive nitrogen species in the plasma environment. Active nitrogen containing groups were generated breaking the delocalized bonds on the O-C=O. This was confirmed by the C1s results such that nitrogen plasma treatment decomposed the ester groups on the surface of PMMA or newly generation of nitrogen containing groups might be due to the abstraction of hydrogen in CH_2 groups. Nitrogen plasma created reactive nitrogen species causing hydrocarbon bond breaking resulted in hydrogen abstraction from the surface of PMMA. Newly formed imine functionalities converted to primary amines because of the hydrogen transfer in the nitrogen plasma environment. This convertion rate increased with increasing plasma treatment time. The result of the N1s spectrum for the sample N-100/30 indicating the lowest amount of imine functional groups.

Amide functional groups formed may be due to the vulnerability of nitrogen plasma treated PMMA films to air before XPS analysis. Increasing plasma treatment time resulted in a overall trend toward increasing relative peak area ratio of –R-N=O functional group from 5% to 30% where the maximum amount of –R-N=O obtained for 100W 30min nitrogen plasma treated samples. The relative peak ratio of the –$CO\text{-}NH_2$ group dwindled away with increasing plasma duration time. Most probably, conversion of –$CO\text{-}NH_2$ groups to –R-N=O had took place as the plasma application time was extended.

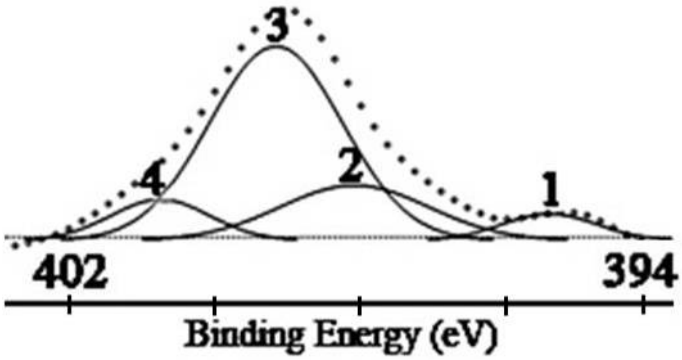

Figure 16: XPS N1s spectrum of N-100/5 sample

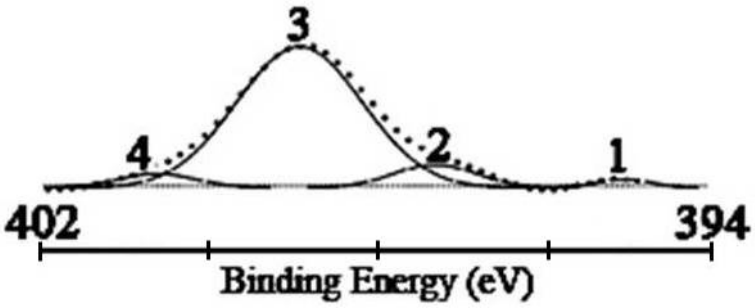

Figure 17: XPS N1s spectrum of N-100/15 sample

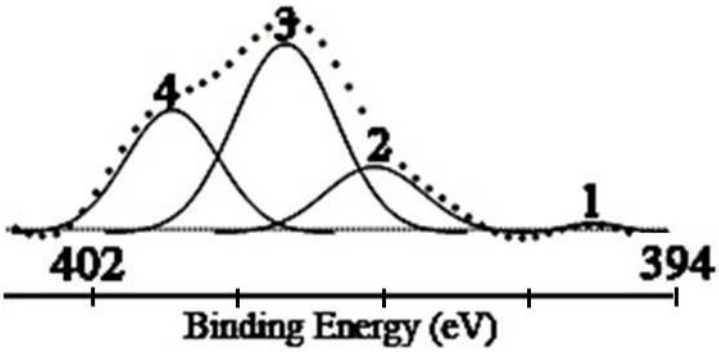

Figure 18: XPS N1s spectrum of N-100/30 sample

XPS results of C1s spectrums of nitrogen plasma applied samples of N-100/5, N-100/15, N-100/30 are given in Figures 20, 21, 22; and the binding energy values of C1s spectrum and the relative peak area ratios of the C1s peaks can be seen in Table 8**.**

Table 8: The result of C1s peaks for nitrogen plasma treated PMMA

Peak No	**B.E (eV)**	**Bond Type**	**Relative Peak Area (%) N-100/5**	**Relative Peak Area (%) N-100/15**	**Relative Peak Area (%) N-100/30**
1	284.0 ±0.1	Hydrocarbon	45	43	36
2	284.4 ±0.2	C atom in α position	10	16	16
3	285.8 ±0.1	Methoxy group C	24	21	26
4	287.8 ±0.1	Free Carbonyl group	21	20	22

The results indicated that the nitrogen plasma treatment reduced the relative peak area ratio of the hydrocarbon peaks from 45% to 36%. The reduction in the hydrocarbon peak compensated for the newly formation of free carbonyl group and the increase in the amount of methoxy group carbon. The main difference between the untreated and nitrogen plasma treated PMMA was the disappearance of ester groups. Nitrogen plasma treatment decomposed the ester groups on the surface of PMMA. Decomposition of ester groups resulted in the formation of free carbonyl groups which were formed most probably after opening the reactor chamber to the atmospheric pressure so that the samples come in contact with the atmospheric oxygen.

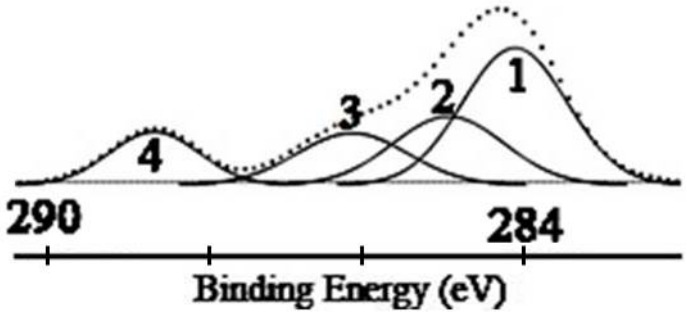

Figure 19: XPS C1s spectrum of C-0/0 sample

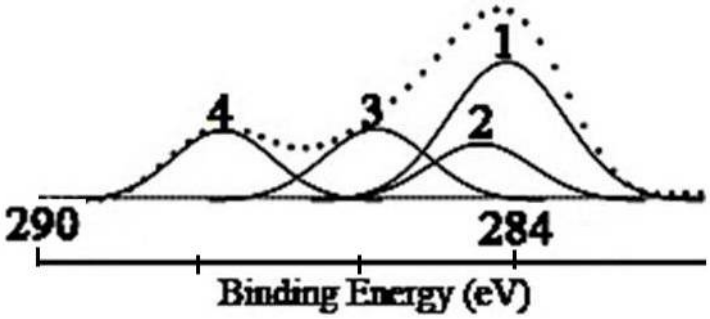

Figure 20: XPS C1s spectrum of N-100/5 sample

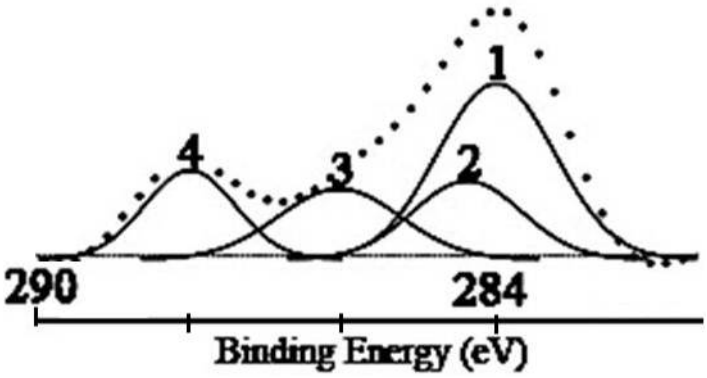

Figure 21: XPS C1s spectrum of N-100/15 sample

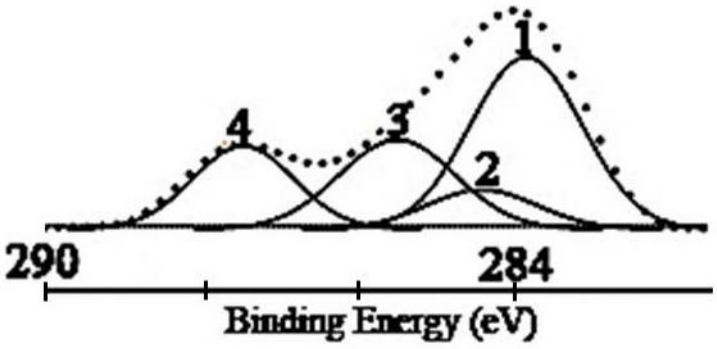

Figure 22: XPS C1s spectrum of N-100/30 sample

The O1s spectrum of untreated PMMA consisted of two main components. One was O=C group at a binding energy of 532.3 eV with the 49% relative peak area and the other was O-C group at a binding energy of 533.8 eV with the 51% relative peak area. O1s spectrum of nitrogen plasma treated PMMA samples consisted of two main components as can be seen from the Figures 24, 25, and 26.

Table 9: The result of O1s peaks for nitrogen plasma treated PMMA

Peak No	**B.E (eV)**	**Bond Type**	**Relative Peak Area (%) N-100/5**	**Relative Peak Area (%) N-100/15**	**Relative Peak Area (%) N-100/30**
1	531.2 ±0.1	O=C	71	63	57
2	532.4 ±0.3	O-C	29	37	43

One peak was belong to O=C group (number 1) at a binding energy of 531.2 ± 0.1 eV and the other was O-C group (number 2) at a binding energy of 532.4 ± 0.3 eV. The relative peak area ratio of the O=C group increased and in consequence the relative peak area ratio of the O-C group decreased on account of the nitrogen plasma treatment. The maximum relative area ratio of the O=C group which equals 71 % obtained after 100W 5 min plasma treatment. There was a decreasing trend of the relative peak area ratio of the O=C group with increasing plasma treatment time at 100W power value. This is most probably because of opening of –C=O bonds and

formation of either hydroxyl (C-OH) or ether (C-O-C) bonds as the amount of total energy increase in nitrogen plasma application.

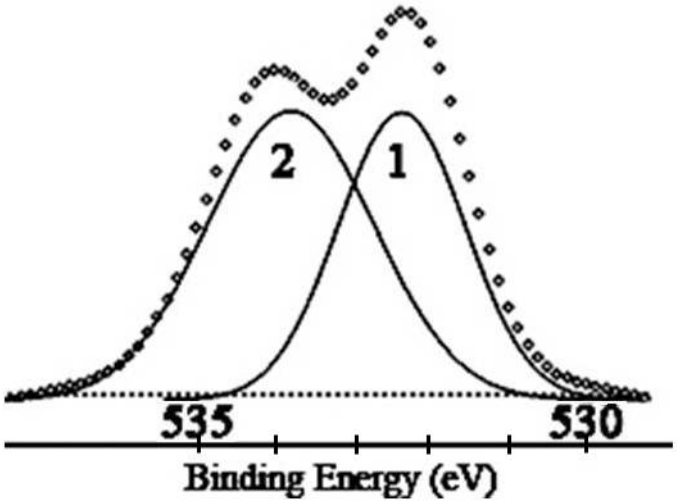

Figure 23: XPS O1s spectrum of C-0/0 sample

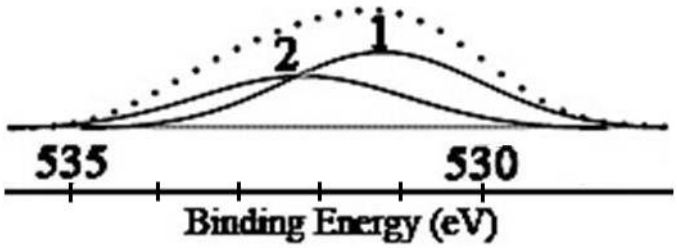

Figure 24: XPS O1s spectrum of N-100/5 sample

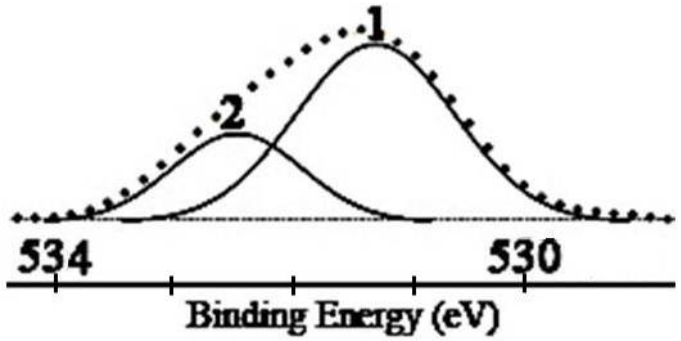

Figure 25: XPS O1s spectrum of N-100/15 sample

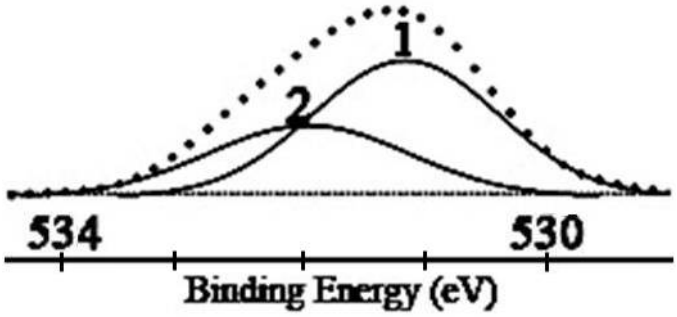

Figure 26: XPS O1s spectrum of N-100/30 sample

CHAPTER 4

ARGON PLASMA APPLICATION

Argon known as an inert gas. Crosslinking, cleaning and etching of a surface is expected with application of argon plasma. Therefore PMMA films were modified with argon plasma with application of three different power for three different duration. The obtained results are discussed in this chapter.

4.1 Contact Angle Results of Argon Plasma Treated PMMA Films

Contact angle measurement values of distilled water (DW), diiodomethane (DIM), formamide (FA) and dimethyl sulfoxide (DMSO) on the surface of argon plasma treated and untreated PMMA films are given in Table 10.

Table 10**:** Contact angle values of argon plasma treated PMMA films

Liquid / Sample	DW	DIM	FA	DMSO
C-0/0	71.3 ±0.3	32.4 ±0.8	54.8 ±1.3	31.1 ±1.1
A-10/5	36.5 ±0.4	24.2 ±0.4	13.1 ±0.2	11.9 ±0.5
A-10/15	37.1 ±0.5	14.8 ±0.7	11.5 ±0.1	12.2 ±0.3
A-10/30	47.1 ±1.4	13.7 ±0.5	8.0 ±0.4	6.5 ±0.6
A-50/5	33.2 ±0.4	18.5 ±0.3	11.0 ±0.2	9.8 ±1.5
A-50/15	39.9 ±1.2	9.8 ±0.1	10.6 ±0.1	12.8 ±0.3
A-50/30	34.1 ±0.5	9.2 ±0.3	9.4 ±0.1	8.9 ±0.4
A-100/5	35.1 ±0.5	16.5 ±0.2	8.4 ±0.5	8.8 ±0.5
A-100/15	14.7 ±0.1	4.7 ±0.3	7.2 ±1.0	8.6 ±0.2
A-100/30	11.8 ±1.6	5.2 ±0.2	7.2 ±0.5	8.8 ±0.1

For pure PMMA samples, the water contact angle was found as 71.3° and this value decreased to 36.5° after argon plasma treatment of 10W 5 min, to 37.1° after 10W 15 min, and to 47.1° after 10W 30 min. Increasing plasma exposure time from 5 min to 30 min, did not cause substantial change in the static water contact angle.

For these samples treated with 10W, the increase in the water contact angle as the application time is extended, could be the result of crosslinking effect of the inert gas. It is well known that inert gas plasma treatment is privileging a “casing” process (as the name suggests cross linking by activated species in inert gases) at the polymer surface [Guruvenket et al., 2008]. Further extension of application time to 30 min, surface activation of the PMMA occurred leading to the formation of surface radicals and because of these functionalities water contact angle increased with increasing time duration for 10W plasma treatment.

The cross linking effect was closely related to the input power. Namely, different power applications (10W-50W-100W) caused changes in the water contact angles as can be clearly seen from Figure 27. As for 50W treatment, water contact angle of argon plasma treated PMMA surface decreased to 33.2° after 5 min plasma application, and increased to 39.9° after 15 min treatment. Further application caused a further reduction down to 34.1°.

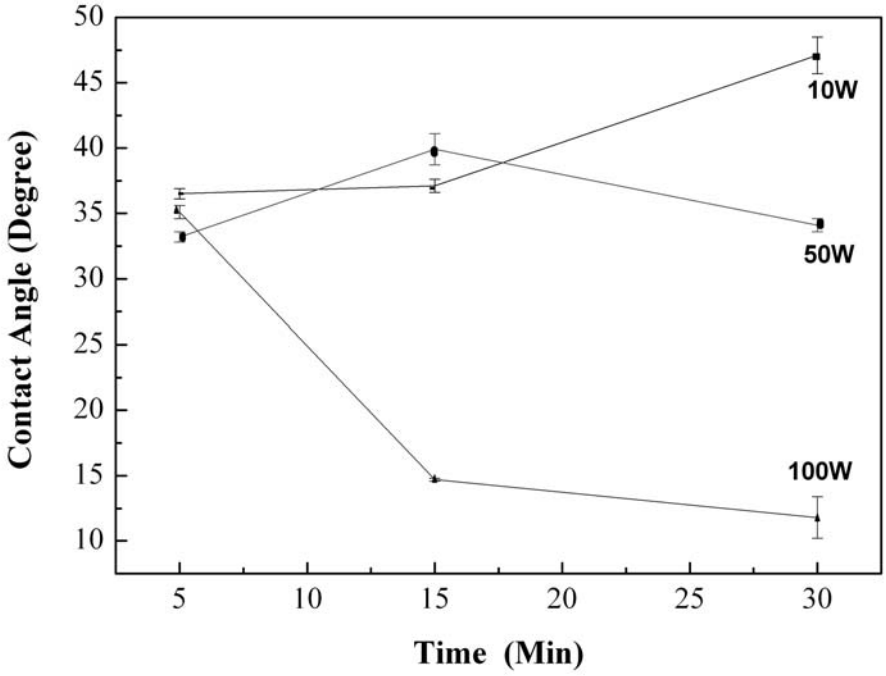

Figure 27: Water contact angle versus time graph for argon plasma treated PMMA films

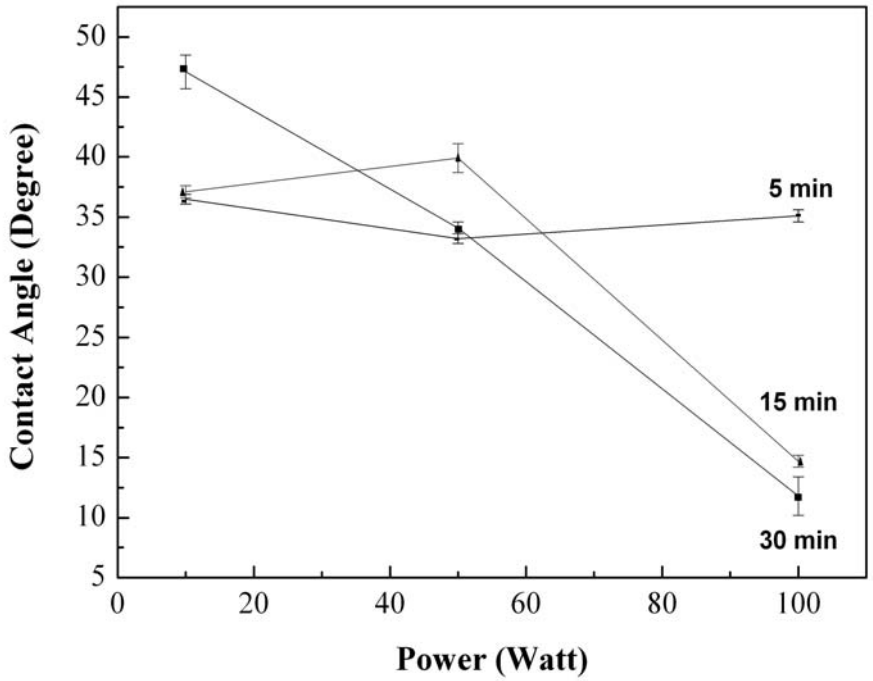

Figure 28: Water contact angle versus power graph for argon plasma treated PMMA films

The most important observation was observed for 100W power applied samples and almost superhydrophilic surfaces with water contact angles lower than 15° were obtained for A-100/15 and A-100/30 samples. Longer time durations did not always lead to the formation of cross linking at higher rate especially at higher RF power values. This was confirmed by 100W plasma application. In contrast to lower plasma power application (10W and 50W), there was a gradual decrease in water contact angle with increasing plasma treatment time (Figure 28). Surface of the sample A-100/30 having water contact angle value of 11.8°, was very near to superhydrophilicity. Also the sample of A-100/30 possessing the highest amount of total input energy as can be seen from Figure 28. Most probably, capturing of oxygen entities from atmosphere by highly activated surface sides created by the plasma was the reason of the improvement of the hydrophilicity for A-100/30 samples. At 100W power treatment there may be so dynamic surface equilibrium that tended to capture oxygen entities from atmosphere when the samples are opened up to the atmosphere after the argon plasma treatment.

Chemical functionalization of PMMA surface was strongly influenced by argon plasma treatment and highly activated radicals are created so that there were dramatic changes in the contact angle values. These changes in the water contact angle versus total input energy demonstrated in Figure 29 and in general, a decreasing trend for water contact angles with increasing total energy was observed.

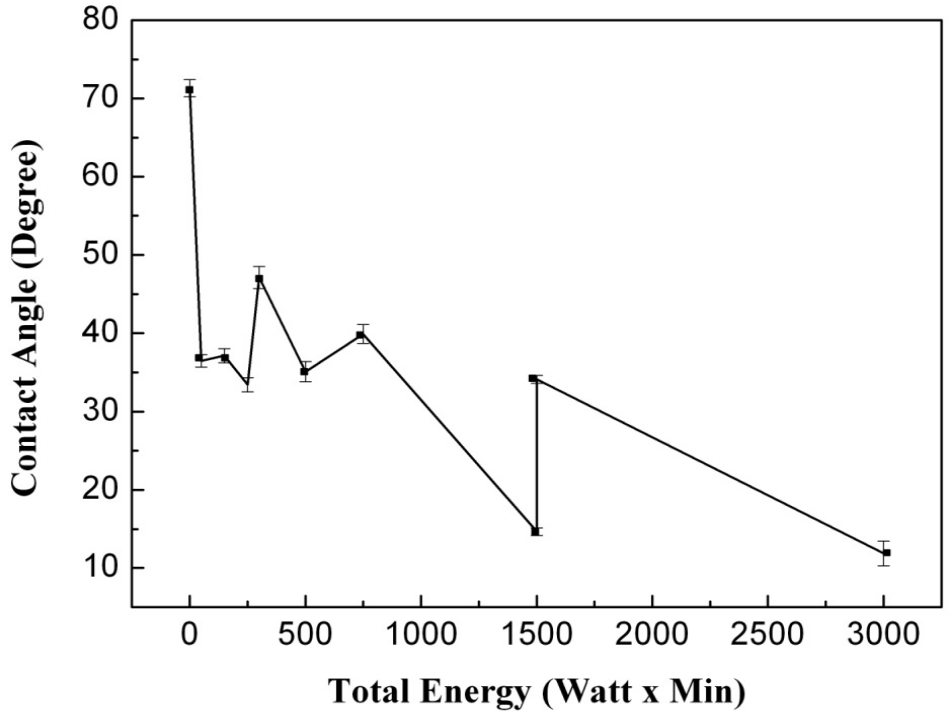

Figure 29: Water contact angle versus total energy graph for argon plasma treated PMMA films

4.2 SFE Results of Argon Plasma Treated PMMA Films

SFE results calculated according to Harmonic Mean, Geometric Mean, Acid-Base approaches of argon plasma treated PMMA films are given in the Table 11.

Table 11: Results of total SFE and its components for argon plasma treatment

Method	γ^{p} (mJ/m^2)	γ^{d} (mJ/m^2)	γ^{+} (mJ/m^2)	γ^{-} (mJ/m^2)	γ^{tot} (mJ/m^2)
Sample C-0/0					
Harmonic	10.2	35.5			45.8
Geometric	6.5	36.2			42.7
Acid Base	1.16	43.1	0.6	3.6	44.3
Sample A-10/5					
Harmonic	28.2	36.9			65.2
Geometric	25.2	35.2			60.5
Acid Base	3.2	46.1	0.2	6.6	49.3
Sample A-50/5					
Harmonic	29.2	36.3			65.6
Geometric	26.6	34.9			61.0
Acid Base	4.4	44.9	0.3	6.7	49.4
Sample A-100/5					
Harmonic	28.2	38.2			66.4
Geometric	24.9	36.6			61.6
Acid Base	1.5	48.4	0.1	6.7	49.9
Sample A-10/15					
Harmonic	27.1	38.3			65.2
Geometric	23.7	36.9			60.7
Acid Base	0.7	48.9	0.05	6.5	49.6
Sample A-50/15					
Harmonic	25.6	39.1			64.7
Geometric	21.9	37.9			59.9
Acid Base	0.5	49.7	0.04	6.8	50.2
Sample A-100/15					
Harmonic	35.6	37.5			73.1
Geometric	33.4	34.4			67.8
Acid Base	4.6	50.4	0.3	8.1	55.0
Sample A-10/30					
Harmonic	22.3	40.1			62.4
Geometric	17.8	39.9			57.8
Acid Base	3.2	49.0	0.3	5.5	52.3
Sample A-50/30					
Harmonic	38.7	33.8			72.6
Geometric	38.1	29.8			67.9
Acid Base	5.1	42.2	0.3	8.1	47.3
Sample A-100/30					
Harmonic	35.7	37.4			73.2
Geometric	33.6	34.2			67.8
Acid Base	4.7	50.3	0.3	8.0	55.0

Argon plasma treatment caused significant changes in total SFE as well as polar component of SFE in the modified PMMA surfaces depending on the plasma process parameters. Generally total SFE increased with increasing input power according to Harmonic Mean approach. The samples of A-10/5, A-10/15, A-10/30 showed around 65 mJ/m^2 total SFE values about 20 mJ/m^2 higher than the control group which has SFE value of 45.8 mJ/m^2. Extension of application time from 5 min to 30 min, did not significantly altered the dispersive (~36-38 mJ/m^2) and polar (~28-29 mJ/m^2) components of SFE. According to Hegemann et al, this may be because of high energy surface is vulnerable to adsorb contaminants from the atmosphere to reduce its surface free energy [Hegemann et al., 2003].

Harmonic Mean approach showed that the plasma treatment of the samples A-50/5, A-50/15 and A-50/30 resulted in 65.6 mJ/m^2 , 64.7 mJ/m^2 , 72.6 mJ/m^2 total SFE values respectively. For 50W and 100W plasma treatments the same trend which was the increase of total SFE with increasing plasma treatment time (5-15-30 min) was obtained. So it can be concluded that various plasma power applications (10-50-100W) resulted in different responses in terms of total SFE and its components. On the other hand, mainly increasing plasma power increased the total SFE values of modified PMMA surfaces when the application duration was fixed at any value. This may be because of the breaking and rearranging of the cross linking at the higher levels of total input power values. Maximum total surface free energy value which was 73.2 mJ/m^2, obtained for the surface of the sample A-100/30 according to Harmonic Mean approach. This may be because of the introduction of newly formed hydroxyl groups at the surface which was revealed by XPS analysis. Also the high amount of free carbonyl groups may cause this high value of SFE. Again, that case agreed well with the hydrophilicity of the surface having the minimum water contact angle value for A-100/30 among samples all the 30 min plasma treated PMMA samples.

According to Acid-Base approach, A-100/15 samples demonstrated showing the maximum total SFE with basic component of 8.1 mJ/m^2. It was also noteworthy that the surface which possessing the maximum SFE had the highest basic component (8.1 mJ/m^2). So it can be deduced that there is a close relationship between the basic component and total SFE when Acid-Base approach is taken into account. The

results pointed out that argon plasma treatment modifies surface of PMMA films causing enhancement of the total SFE especially when the total energy is higher.

4.3 X-Ray Photoelectron Spectroscopy (XPS) Results of Argon Plasma Treated PMMA Films

The chemical structure of the monomer unit of PMMA addressing the C1s peaks is given in Figure 30. Representation of components of C1s envelope as a result of peak fitted XPS analysis for untreated PMMA was given in Table 12.

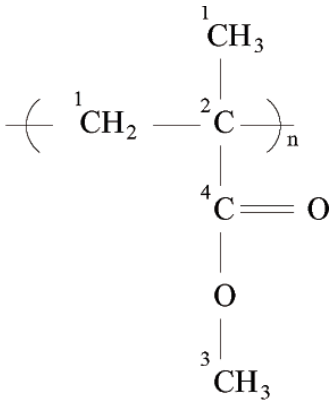

Figure 30: Chemical structure of monomer unit of PMMA

XPS analysis detected that untreated PMMA consisting of four different types of C atom because of the different chemical environment. However in the previous literature Fakes et al elucidated the C1s peaks of untreated PMMA as three main component giving the intensity ratio of 1:1:3 [Fakes et al, 1987]. According to our XPS results, C1s (1) peak located at 284.6 eV was attributed to C-C, C-H bonds (hydrocarbon) having a good agreement with literature results [Brinen et al., 1999, Chai et al., 2004 and Liu et al., 2010]. 285.6 eV positioning C1s (2) peak is assigned to quaternary carbon atom in α position to ester group and C1s (3) at 286.7 eV corresponded to methoxy group carbon which are similar to obtained by Tsougeni et

al. [Tsougeni et al., 2009]. C1s (4) locating at 289.0 eV is assigned to the carbon in the ester group.

Table 12: The result of C1s peaks for untreated PMMA

Peak No	B.E (eV)	Relative Peak Areas (%)	Bond Type	Chemical Structure
1	284.6 ±0.2	47	Hydrocarbon	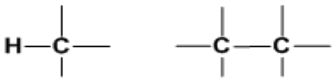
2	285.6 ±0.2	22	**C** atom in α position	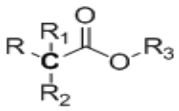
3	286.7 ±0.1	17	Methoxy group **C**	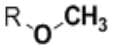
4	289.0 ±0.3	14	**C** in the ester group	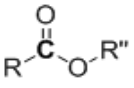

XPS analysis of RF argon plasma treatment was carried out only for 100W plasma applied PMMA films and the results were interpreted in terms of C1s and O1s core shell spectrum. After 100W 5min argon plasma treatment, two new functional groups are created. One of these was located at 287.8 eV which was assigned to the free carbonyl groups, and the other was positioned at 290.1 eV corresponding to carboxylic acid groups (Figure 32, 33, 34) These results are fitting well with the data given by Amor et al. [Amor et al., 2000]. Table 13 represented the binding energy values and the relative area ratios of C1s peaks argon plasma treated samples. C1s envelope of the sample A-100/5 consisted of five components differently from the samples of A-100/15 and A-100/30. As can be seen from Table 13 there was an

increase in the hydrocarbon relative peak area ratio from 47% (for unmodified PMMA) to 68% after 100W 5min argon plasma exposure. This result agrees well with the results found by Dabhade et al. which reported an increase in the hydrocarbon peak area from 63% to 77% after 5W- 5 min DC argon plasma treatment [Dabhade et al., 2004] 'Casing' effect of the argon plasma treatment leaded to the new formation of hydrocarbon bonds. There is a significant reduction of the relative peak area of quaternary carbon atom in α position to ester group which is found 17% for control group and 6% for A-100/5 with argon plasma treatment. The decrease in the amount of methoxy group C with respect to untreated PMMA, as can be seen from Table 13, there was side chain degradation combining with crosslinking because of argon plasma application [Schulz et al, 2001]. Gröning et al suggested the reducing effect of argon plasma on the number of ester groups because of partial degradation leading the intermediate new oxygen functionalities which was confirmed by the current study [Gröning et al., 1995].

Table 13: The result of C1s peaks for argon plasma treated PMMA

Peak No	**B.E (eV)**	**Bond Type**	**Relative Peak Area (%) A-100/5**	**Relative Peak Area (%) A-100/15**	**Relative Peak Area (%) A-100/30**
1	283.8 ±0.1	Hydrocarbon	68	45	42
2	284.3 ±0.2	C atom in α position	6	18	12
3	285.6 ±0.4	Methoxy group C	12	19	24
4	287.8 ±0.1	Free Carbonyl group	11	18	22
5	290.2 ±0.2	Carboxylic Acid	3	0	0

The results obtained from C1s spectrum of argon plasma treated PMMA confirmed this result by detecting the enormous decrease from 14% to 0% in the relative peak area of ester groups. It was also reported by Gröning et al, Ar^+ ions decompose the ester groups on the PMMA surface because of the partial degradation leading to the generation of new oxygen containing groups [Gröning et al., 1995]. According to C1s spectrum, also can be seen from Table 13, new oxygen containing groups such as free carbonyl and carboxylic acid were formed. Amor et al. suggested that these newly formed oxygen functionalities were formed due to splitting up of ester groups or direct being captured of oxygen entities by surface radicals present in plasma [Amor et al., 2000]. Surface of the sample A-100/15 exhibited reduction of the relative peak area of hydrocarbon from 47% (control group) to 45% and methoxy group C from 17% (control) to 12% whereas there was an increase from 11% to 18% in the peak area of free carbonyl group. The maximum amount of newly created free carbonyl group detected at 100W 30 min argon plasma treatment and at this condition the minimum value for of hydrocarbon peak was observed. The trend of decreasing hydrocarbon relative peak area with increasing plasma treatment time was observed. Conversely the amount of free carbonyl group increases gradually with increasing plasma application time.

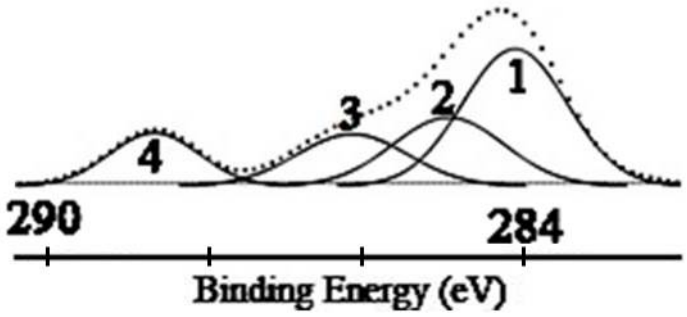

Figure 31: XPS C1s spectrum of C-0/0 sample

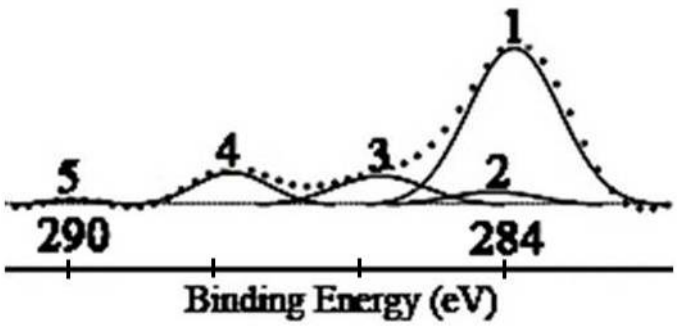

Figure 32: XPS C1s spectrum of A-100/5 sample

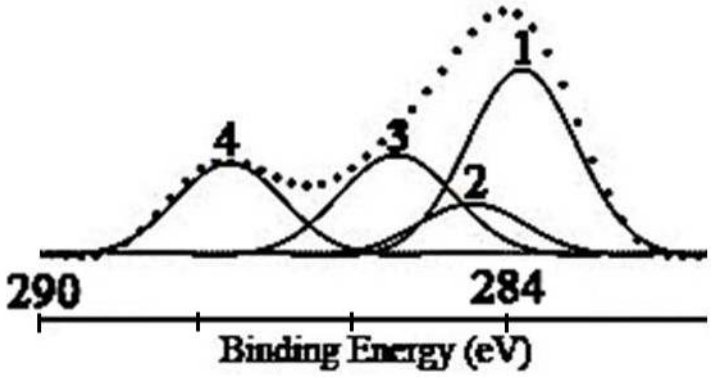

Figure 33: XPS C1s spectrum of A-100/15 sample

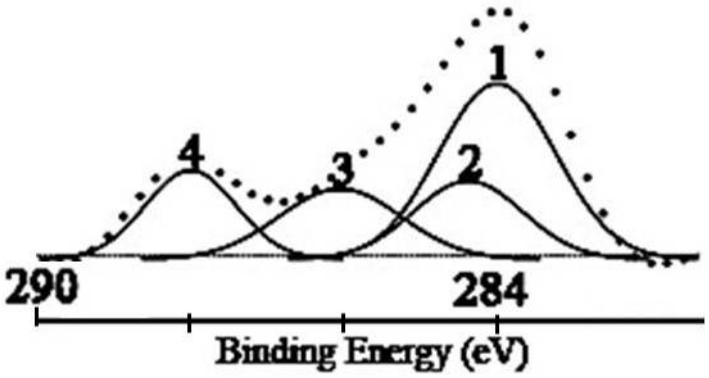

Figure 34: XPS C1s spectrum of A-100/30 sample

The O1s spectrum of untreated PMMA consisted of two main components. One was O=C group at a binding energy of 532.3 eV with the 49% relative peak area and the other was O-C group at a binding energy of 533.8 eV with the 51% relative peak area. The effect of plasma treatment time on O1s spectrum shown in Table 14.

Table 14: The result of O1s peaks for argon plasma treated PMMA

Peak No	**B.E (eV)**	**Bond Type**	**Relative Peak Area (%) A-100/5**	**Relative Peak Area (%) A-100/15**	**Relative Peak Area (%) A-100/30**
1	531.1 ±0.1	O=C	49	58	57
2	532.5 ±0.3	O-C	42	26	27
3	533.4 ±0.3	-COH	9	14	16

For argon plasma treated samples, an extra peak was detected at 533.4 eV differently from untreated PMMA. This extra peak was assigned to hydroxyl groups bonded to C atom (-COH) by Ozden et al and Schulz et al. [Ozden et al., 1999 and Schulz et al., 2001]. Our results revealed that the amount of hydroxyl group increased with plasma treatment time. The maximum relative peak area of hydroxyl group obtained for 100W 30min argon plasma treated samples. Also decrease in the relative peak area of O-C detected when argon plasma treatment was carried out. The relative peak area of O-C reduced to 26% from 51% (control) as a result of 100W 15min argon plasma treatment. The decrease in the O-C functionality may be due to the side chain degradation under the effect of argon plasma treatment.

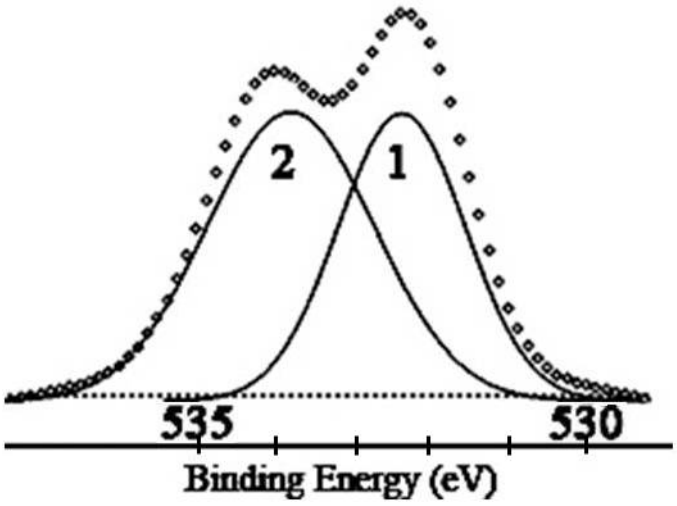

Figure 35: XPS O1s spectrum of C-0/0 sample

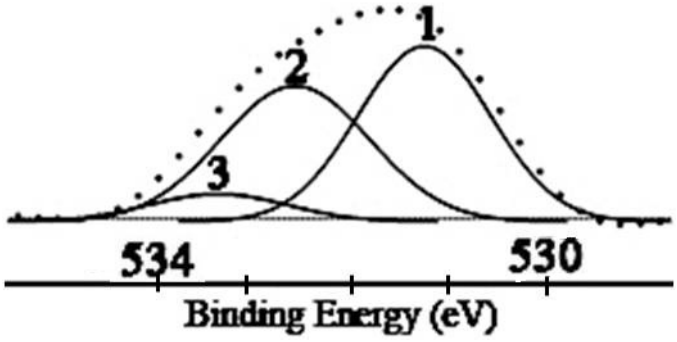

Figure 36: XPS O1s spectrum of A-100/5 sample

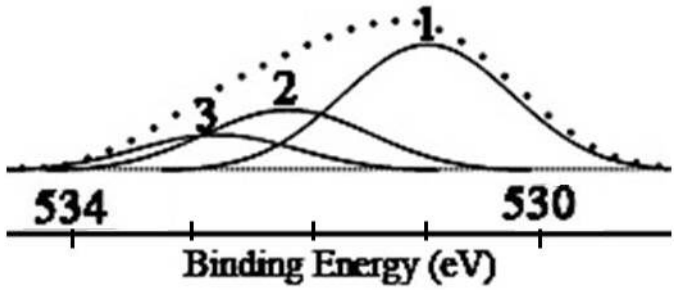

Figure 37: XPS O1s spectrum of A-100/15 sample

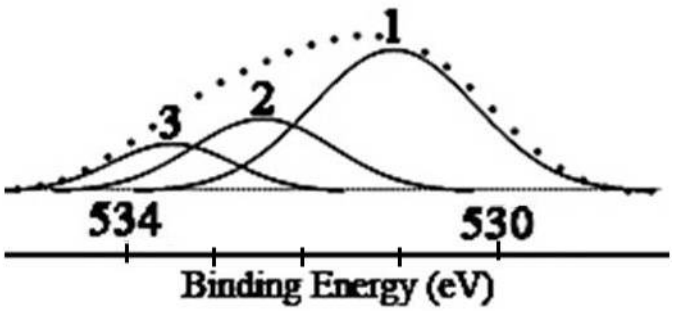

Figure 38: XPS O1s spectrum of A-100/30 sample

CHAPTER 5

OXYGEN PLASMA APPLICATION

Oxygen known as a reactive gas. Sterilization and etching of a surface is expected with application of oxygen plasma. Therefore PMMA films were modified with oxygen plasma with application of three different power for three different duration. The obtained results are discussed in this chapter.

5.1 Contact Angle Results of Oxygen Plasma Treated PMMA Films

Contact angle measurement values of distilled water (DW), diiodomethane (DIM), formamide (FA) and dimethyl sulfoxide (DMSO) on the surface of oxygen plasma treated and untreated PMMA films are given in Table 15.

Table 15: Contact angle values of oxygen plasma treated PMMA films

Liquid / Sample	DW	DIM	FA	DMSO
C-0/0	71.3 ±0.3	32.4 ±0.8	54.8 ±1.3	31.1 ±1.1
O-10/5	40.8 ±0.8	29.6 ±0.6	18.3 ±0.3	13.7 ±0.5
O-10/15	34.8 ±0.8	15.1 ±1.4	12.5 ±0.6	12.6 ±1.4
O-10/30	36.1 ±0.7	9.2 ±0.6	9.6 ±0.4	5.8 ±0.8
O-50/5	34.7 ±0.9	28.6 ±0.6	13.2 ±0.4	9.8 ±0.7
O-50/15	27.7 ±2.7	13.6 ±0.4	10.2 ±0.5	11.7 ±0.9
O-50/30	25.3 ±0.5	7.0 ±1.1	8.6 ±0.7	5.9 ±0.5
O-100/5	30.1 ±1.5	27.9 ±0.7	13.0 ±1.0	10.9 ±0.3
O-100/15	30.3 ±0.8	7.1 ±0.4	14.0 ±0.5	7.4 ±1.4
O-100/30	26.3 ±2.2	6.9 ±0.8	6.2 ±0.9	5.3 ±0.7

Water contact angles are important in determining hydrophilicity of the materials. A decrease of contact angle of water from 71.3° was detected for all samples indicating the enhancement of hydrophilicity. Specifically, increasing high powers applied for longer periods increased the hydrophilicity (Figures 39 and 40).

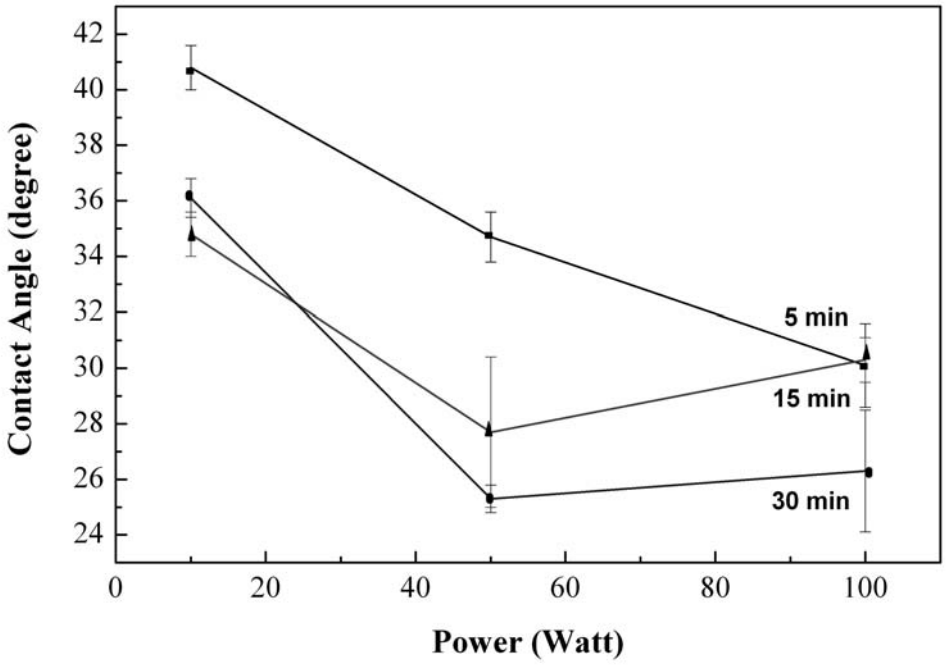

Figure 39: Water contact angle versus time graph for oxygen plasma treated PMMA films

The most hydrophilic surfaces were obtained for the samples treated for 30 min with application of 50W or 100W. The decrease in the water contact angle manifested itself at the first instants of oxygen plasma application as can be seen in Figure 39. Water contact angle sharply decreased from 71.3° to 40.8° for the sample O-10/5, to 34.7° for O-50/5, and to 30.1° for O-100/5. Increasing plasma exposure time decreased the static water contact angle. Moreover increasing plasma exposure time led reducing effect on contact angle to some extent especially for low power applications like 10W. Figure 40 displayed water contact angle versus time graph for oxygen plasma treated PMMA films from which it can be deduced that after 15 min

treatment, increasing treatment time did not cause significant effect for 10W plasma application contact angle decreased from 40.8° to 36.1°. This was not valid for higher power applications such as 50W and 100W. This may be due to the cross linking formation when longer plasma treatment was applied. For 50W and 100W oxygen plasma application, increasing plasma treatment time induced higher degree of reduction in water contact angle. 100W power application caused a sharp decrease from 71.3 (for control group) to 30.1° (for O-100/5). Further increase in time from 5 min to 15 min and 30 min did not bring significant change in the water contact angle which is consistent with the literature. (Figure 39) Chai et al, 2004, modified PMMA surface with DC pulsed plasma and found that after some time (2s) water contact angle remained same around 51° even if they increased the plasma treatment time to 5s and 10s then decreased with increasing plasma treatment time (50s) [Chai et al., 2004].

If the contact angle results were interpreted in terms of fixed power with changing application time as can be followed from Figure 40, in general there was a trend of decrease in contact angles indicating an increase in hydrophilicity of the surfaces This result was in a good agreement with the results were found by Ozcan et al. for 1 min RF oxygen plasma treated PMMA films that showing the water contact angle values 43°, 38.3°, 39.5° for 20W, 100W and 300W respectively. [Ozcan et al., 2008 (a)]

The variation of the water contact angle with respect to total input energy is given in Figure 41. By means of total input energy the lowest water contact angles were obtained at the input energy of 1500 and 3000 (Watt x Min) which correspond to oxygen plasma treatments of 50W 30 min and 100W 30 min having water contact angle values as 25.3° and 26.3°, respectively. On the other hand, water contact angle obtained for 50W 15 min oxygen plasma treatment demonstrated a very close value to these having 27.7°. This result revealed that surface hydrophilicity stays almost constant after a certain watt x min value. It was worth to mention that the same amount of input energy produced very close results where 50W-30min and 100W-15 min plasma application have the same total energy (1500 Watt x Min) and had 25.3° and 30.3°, respectively indicating high hydrophilicity for both samples.

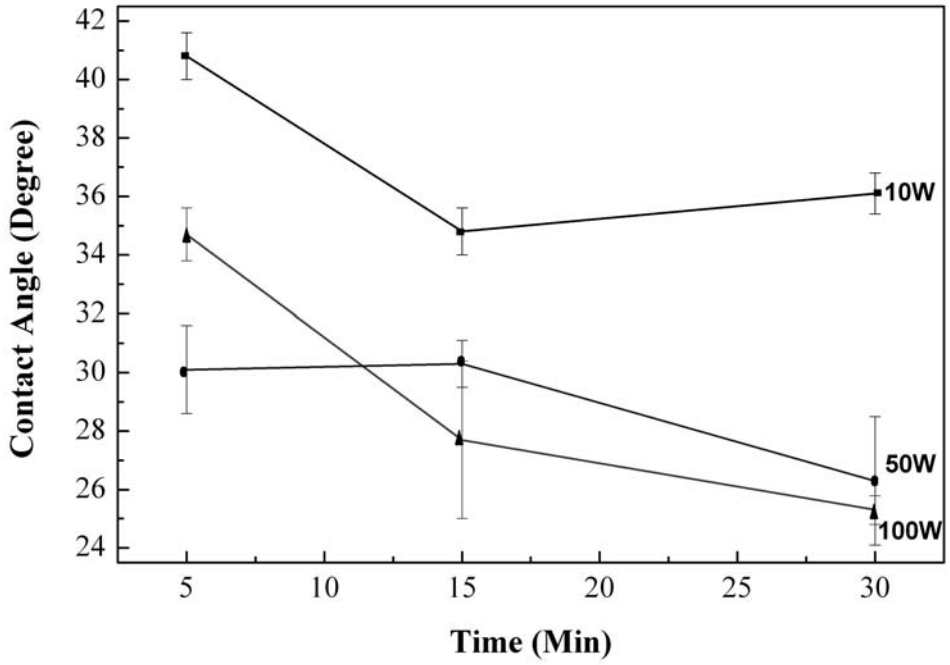

Figure 40: Water contact angle versus time graph for oxygen plasma treated PMMA films

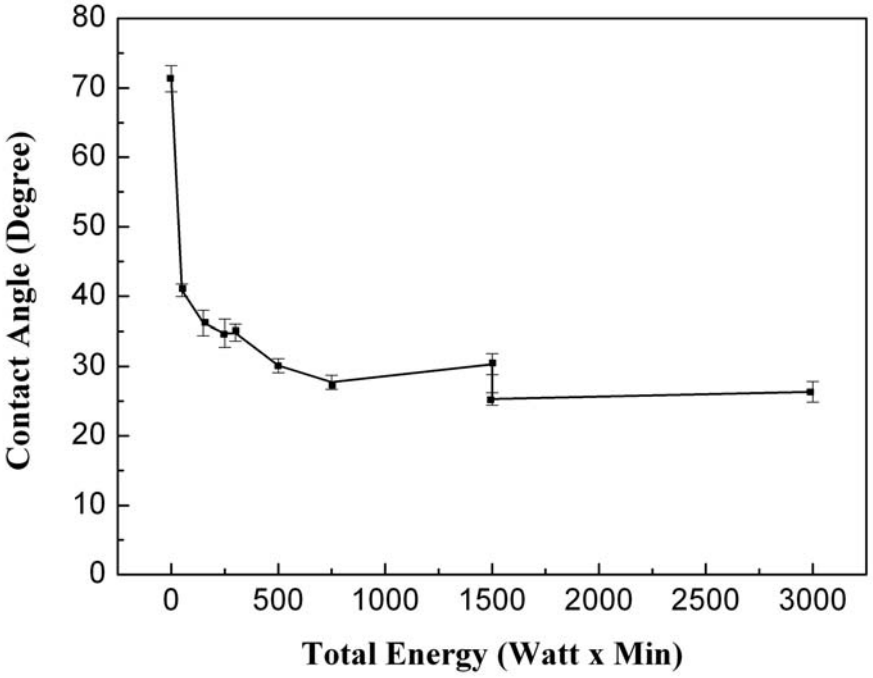

Figure 41: Water contact angle versus. total energy graph for oxygen plasma treated PMMA films

The change in the amount of surface functional groups detected by XPS analysis brought about the differences in water contact angle. Since various application time created not only different amount of functional groups but also different kind of chemical functional groups. According to XPS results for 10W plasma treatment, polar carbonate groups emerged only at 10W 30min oxygen plasma application.

5.2 SFE Results of Oxygen Plasma Treated PMMA Films

SFE measurements were performed by using various liquid couples and triplets to calculate, polar, dispersive, acidic and basic components of the SFE. These values were applied to obtain total SFE values by using different approaches, namely Geometric Mean, Harmonic Mean and Acid-Base approaches. SFE and components of SFE values obtained according to different approaches such as Geometric Mean, Harmonic Mean and Acid Base are given in Table 16. As can be seen, variences in SFE values were detected when the applied aproximation was changed.

Table 16: Results of total SFE and its components for oxygen plasma treatment

Method	γ^p (mJ/m^2)	γ^d (mJ/m^2)	γ^+ (mJ/m^2)	γ^- (mJ/m^2)	γ^{tot} (mJ/m^2)
Sample C-0/0					
Harmonic	10.2	35.5			45.8
Geometric	6.5	36.2			42.7
Acid Base	1.16	43.1	0.6	3.6	44.3
Sample O-10/5					
Harmonic	26.8	35.9			62.8
Geometric	23.8	34.5			58.3
Acid Base	5.1	43.9	0.4	6.2	48.9
Sample O-50/5					
Harmonic	29.2	36.3			65.6
Geometric	26.6	34.9			61.0
Acid Base	4.4	44.9	0.3	6.7	49.4
Sample O-100/5					
Harmonic	31.1	35.8			66.9
Geometric	28.8	33.4			62.3
Acid Base	3.8	44.7	0.3	7.0	48.5
Sample O-10/15					
Harmonic	26.8	35.9			62.8
Geometric	23.8	34.5			58.3
Acid Base	5.0	43.9	0.4	6.2	48.9
Sample O-50/15					
Harmonic	28.7	38.1			66.8
Geometric	25.5	36.3			61.9
Acid Base	0.06	49.0	0.1	6.8	49.1
Sample O-100/15					
Harmonic	30.3	37.1			67.5
Geometric	27.8	34.9			62.8
Acid Base	5.6	50.2	0.4	7.4	55.8
Sample O-10/30					
Harmonic	31.2	35.5			66.7
Geometric	29.1	33.1			62.2
Acid Base	6.2	43.2	0.4	6.9	49.5
Sample O-50/30					
Harmonic	27.0	39.1			66.1
Geometric	23.4	37.8			61.3
Acid Base	0.2	50.1	0.01	6.5	50.3
Sample O-100/30					
Harmonic	31.4	38.1			69.6
Geometric	28.6	35.9			64.5
Acid Base	2.9	50.1	0.1	7.3	52.2

According to Harmonic Mean approach, total SFE was found as 45.8 mJ/m^2 while the polar and dispersive components of SFE were measured as 10.2 mJ/m^2 and 35.5 mJ/m^2, respectively for unmodified PMMA. Lower polar component with respect to dispersive component indicated the hydrophobic nature of PMMA. The polar component of all PMMA samples increased significantly after all RF oxygen plasma treatments. Harmonic Mean approach results pointed out that polar component reached three times higher value (31.4 mJ/m^2) of its initial value (10.2 mJ/m^2) after 100W 30min plasma application. Generally polar component of SFE increased gradually with increasing power at fixed application duration.

Mainly RF oxygen plasma treated PMMA surfaces possessed higher SFE values than untreated ones according to each approach. This was explained by the increase in the polar character of the plasma modified surfaces. Since polar component originates from the orientation of permanent electric dipoles featuring hydrogen bonding, dipole-dipole interactions, dipole-induced dipole interactions, charge transfer interactions, etc, hydrogen bonding capability of the surface with water molecules increases after plasma surface modification [Kitova et al., 2005]. So contact angle results support and can explain the improvement in the surface free energy as well as polar component of the SFE.

According to the Harmonic Mean approach total SFE increased from 45.2 mJ/m^2(for the sample C-0/0) to 69.6 mJ/m^2 for the sample O-100/30 which corresponding to maximum input energy (3000 Watt x Min). Total surface free energy increased with increasing plasma power at fixed application time. Additionally, for 50W treatment, extension of the application time was not effective in the enhancement of the polar component of SFE and it was found in the range of 29.2- 27 mJ/m^2.

At the low plasma power applications, (like 10W, for 5 min and also also 15 min treatments) there was no significant change in the polar, and dispersive components as well as total free energy according to Geometric Mean and Harmonic Mean approaches. Whereas for the sample O-10/30, increase in the polar component and decrease in the dispersive components were detected. Increase in the polar component of SFE was expected because of the newly created polar groups such as free carbonyl, carbonate, and the higher amount of previous polar groups created by the oxidation effect of the oxygen plasma treatment. Depending on that result it can

be said that total SFE increased with increasing polar component according to the all approaches on account of the presence of polar functional groups on the surface. Besides, oxygen plasma treatment affected the polar component rather than nonpolar component. XPS results supported that fact and also will be discussed in detail in section 5.3. Differently from 10W 5min treatment, carbonate groups are newly formed after 10W 30 min plasma application, and also an increase in the amount of free carbonyl groups were detected. These changes in the surface chemistry could be the reason of the dramatic increase in the polar component of the surface free energy as well as the total SFE. For 50W power applied samples, an increase in the polar component and a decrease in the dispersive component with increasing plasma exposure time was observed. Highest values of dispersive component was obtained for 100W plasma treated PMMA surfaces. According to Acid Base approach the highest values for polar and dispersive components such as 5.6 mJ/m^2 and 50.2 mJ/m^2 were obtained where total SFE was 55.8 mJ/m^2 for O-100/15 samples. In the literature, the dispersive component of PMMA is documented in the range of 28.8 to 118.1 mJ/m^2 according to Acid Base approach, and our results are found in this limit [Ozcan et al., 2008 (a)]. The effect of newly created carbonate group on the polar component of SFE could be explained by looking at the XPS results for 10W-100W 30 min oxygen plasma treated samples. The polar component of SFE remained constant around at 31 where at the same time the percentage of carbonate group was fixed at 4% for these mentioned conditions.

5.3 X-Ray Photoelectron Spectroscopy (XPS) Results of Oxygen Plasma Treated PMMA Films

The chemical structure of the monomer unit of PMMA addressing the C1s peaks is given in Figure 42. Representation of components of C1s envelope as a result of peak fitted XPS analysis for untreated PMMA was given in Table 17.

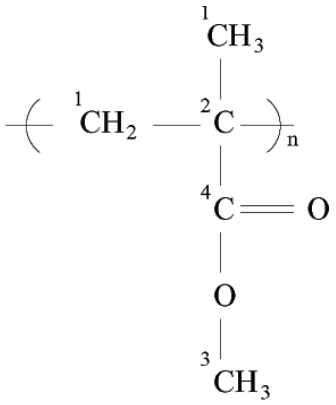

Figure 42: Chemical structure of monomer unit of PMMA

XPS analysis detected that untreated PMMA consisting of four different types of C atom because of the different chemical environment. However in the previous literature Fakes et al elucidated the C1s peaks of untreated PMMA as three main component giving the intensity ratio of 1:1:3 [Fakes et al, 1987]. According to our XPS results, C1s (1) peak located at 284.6 eV was attributed to C-C, C-H bonds (hydrocarbon) having a good agreement with literature results [Brinen et al., 1999, Chai et al., 2004 and Liu et al., 2010]. 285.6 eV positioning C1s (2) peak is assigned to quaternary carbon atom in α position to ester group and C1s (3) at 286.7 eV corresponded to methoxy group carbon which are similar to obtained by Tsougeni et al. [Tsougeni et al., 2009]. C1s (4) locating at 289.0 eV is assigned to the carbon in the ester group.

Table 17: The result of C1s peaks for untreated PMMA

Peak No	B.E (eV)	Relative Peak Areas (%)	Bond Type	Chemical Structure
1	284.6 ±0.2	47	Hydrocarbon	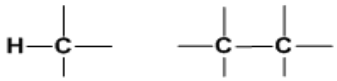
2	285.6 ±0.2	22	**C** atom in α position	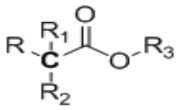
3	286.7 ±0.1	17	Methoxy group **C**	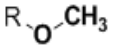
4	289.0 ±0.3	14	**C** in the ester group	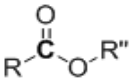
5	287.5 ±0.1	0	Free Carbonyl group	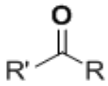
6	290.1 ±0.1	0	Carbonate group	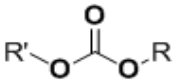

After oxygen plasma treatment two new functional groups are created. One of these two new functional groups was located at 287.5 eV was assigned to the free carbonyl groups and the other was positioned 290.1 eV corresponding carbonate groups. Table 17 represented the relative area ratios of C1s peaks for pristine and oxygen plasma treated PMMA samples. The XPS results of C1s spectra are given in Figures 43-52.

Table 18: Relative area ratios (%) of C1s peaks for oxygen plasma treated PMMA

Sample Name	C1s (1)	C1s (2)	C1s (3)	C1s (4)	C1s (5)	C1s (6)
C-0/0	47	17	22	14	0	0
O-10/5	41	17	17	9	16	0
O-10/15	28	20	33	2	17	0
O-10/30	22	14	17	16	27	4
O-50/5	34	15	19	15	12	5
O-50/15	26	21	22	8	20	3
O-50/30	31	14	18	17	16	4
O-100/5	26	25	32	2	15	0
O-100/15	44	11	22	16	7	0
O-100/30	28	18	23	14	13	4

It is obvious that oxygen plasma treatment reduced the ratio of C-C, C-H (hydrocarbon) bonds. This reduction was affected by plasma power and treatment time and mainly resulted in formation of free carbonyl and carbonate groups. For 10W 5min treatment, C1s (1) peak was reduced to 41% from 47% and this reduction went down to 22% for 10W 30 min treatment. Increasing treatment time caused more reduction in the ratio of C-C, C-H bonds for 10W application. As for 50W treatment there was a decrease in the relative ratio of hydrocarbon peak according to untreated sample but this time there was no uniform reduction. C1s (1) peak ratio decreased with increasing application time up to 15 min, but for 30 min treatment it increased to 31% still being lower than the untreated control sample. C1s (2) peak, which corresponding β shifted carbon because of its juxtaposition to O-C=O group, has the relative ratio 17% at the (control group). There was no change after 10W 5 min oxygen plasma treatment, but it was converted to 14% after 10W 30 min plasma application. The reduction of the ratio of C1s (2) peak was nearly the same as ~15% for the O-50/5 and O-50/30 samples but had interestingly higher value for the sample of O-50/15 as ~21%. The reduction ratio of C1s (3) peak which was assigned to methoxy group carbon, was also decreased from 22% to 17% for the samples treated

with 10W, for 5 min and 30 min. 50W oxygen plasma application did not cause significant change in the ratio of methoxy C1s (3) groups. It was almost the same as 22% for the samples of C-0/0 and O-50/15. The relative ratio of the carbon in the ester C1s (4) group significantly decreased from 14% to 9% with 10W application 100W 30 min plasma application did not cause any change in the ratio of C1s (4) peak according to the control group. For 10W and 50W plasma treatments C1s (4) peak,which showing carbon in the ester group, reduced significantly but then its amount increased for further application duration due to the combination of depleted bonds with oxygen in the plasma chamber. This could be understood from the reduction of the amount of methoxy group carbon. The reduction in the methoxy group carbon compensated for the increase of carbon in the ester group. According to the XPS results of C1s peaks, tremendously decreasing in the ester group, hydrocarbon C1s (1) peak and also methoxy group C1s (3) peak proved the formation of free carbonyl group because of the oxidation effect of oxygen plasma treatment. The relative ratio of newly formed free carbonyl group decreased continuously with increasing plasma power value for 5 min and 30 min oxygen plasma treatment. This having a good agreement with the previous literature such that Chai et al determined the C1s (5) ratio 4.85 % for 10s treatment and 1.46 % for 50s treatment. [Chai et al., 2004] 10W 5 min and 10W 15 min plasma treatment did not create any carbonate group on the surface of PMMA whereas carbonate group began to appear at 10W 30 min oxygen plasma treatment. So plasma treatment time is the key parameter for the formation of carbonate group on the surface of PMMA at the low power plasma process such as 10W. At this point there was a discrepancy between the results obtained by Tsougeni et al and ours. According to Tsougeni et al., carbonate groups appeared at the first instants during the application of RF helicon type oxygen plasma and then disappeared [Tsougeni et al., 2009]. But the results of present study proposed that carbonate groups appeared at longer plasma treatments such that 30 min. Moreover the change in power did not affect the ratio percentage of carbonate groups for 30 min exposure. This result demonstrate that for the formation of carbonate group lower powers can be applied. On the other hand, it was obvious that the main effect dominating the creation of carbonate groups was the treatment time. For 50W application, the C1s (6) peak ratio remained constant at around 4%.

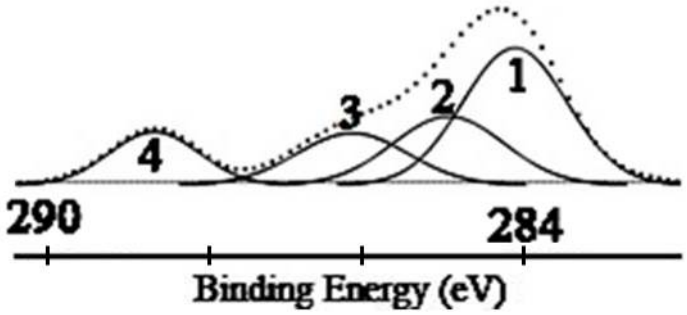

Figure 43: XPS C1s spectrum of C-0/0 sample

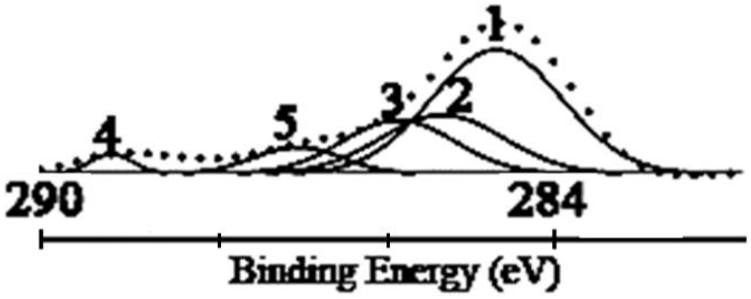

Figure 44: XPS C1s spectrum of O-10/5 sample

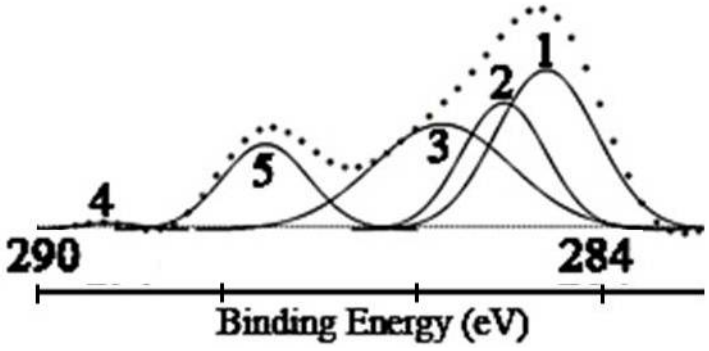

Figure 45: XPS C1s spectrum of O-10/15 sample

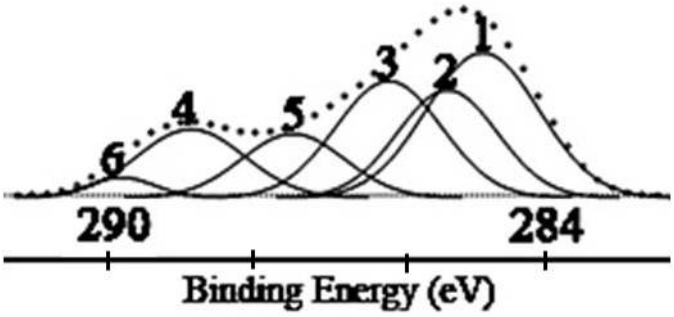

Figure 46: XPS C1s spectrum of O-10/30 sample

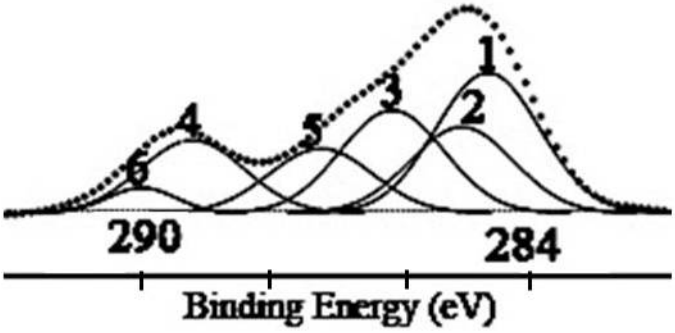

Figure 47: XPS C1s spectrum of O-50/5 sample

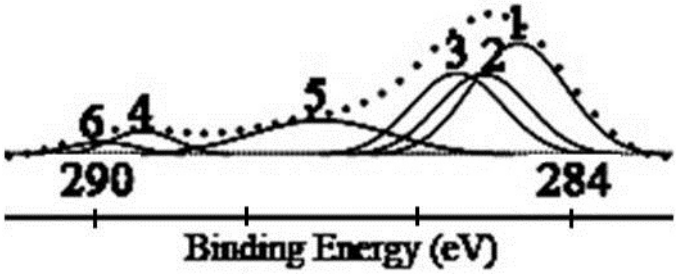

Figure 48: XPS C1s spectrum of O-50/15 sample

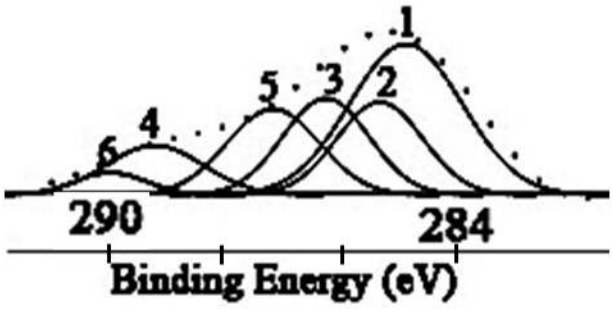

Figure 49: XPS C1s spectrum of O-50/30 sample

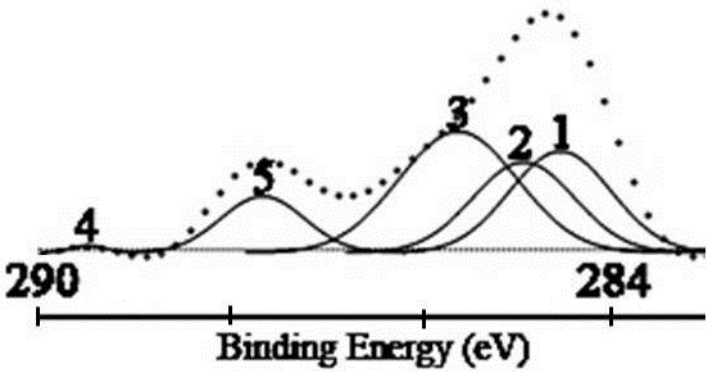

Figure 50: XPS C1s spectrum of O-100/5 sample

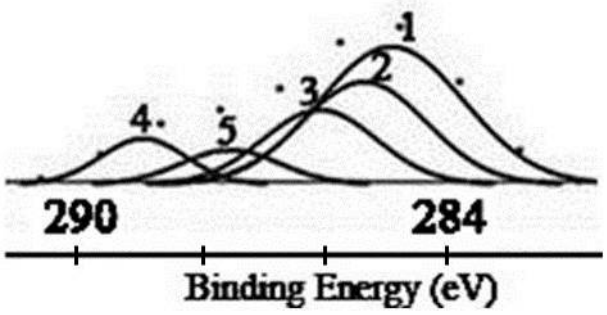

Figure 51: XPS C1s spectrum of O-100/15 sample

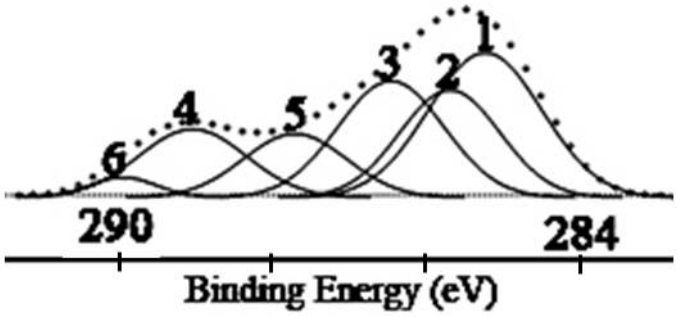

Figure 52: XPS C1s spectrum of O-100/30 sample

Relative area ratios of O1s peaks of PMMA films for control group and also oxygen plasma treated samples are given in Table 19.

Table 19: Relative area ratios (%) of O1s peaks of oxygen plasma treated PMMA

Sample Name	O1s (**1**) →O=C	O1s (**2**) → O-C
C-0/0	49	51
O-10/5	74	26
O-10/15	62	38
O-10/30	59	41
O-50/5	51	49
O-50/15	65	35
O-50/30	56	44
O-100/5	63	37
O-100/15	70	30
O-100/30	66	34

As can be seen from the table; the control group has almost equal amounts of C=O (1) and O-C (2) oxygen groups. XPS spectra of the control PMMA is given in Figure 52 the O1s spectrum of untreated PMMA consisted of O=C group (number 1) at binding energy of 532.3 eV and the other was O-C group (number 2) at binding energy of 533.8 eV. These were consistent with the reported values of Tsougeni et al.

[Tsougeni et al., 2009]. The concentration ratio of O=C/ O-C was found as 49/51 and also this ratio was found as 48/52 by Guruvenket et al. [Guruvenket et al., 2008]. As a result of oxygen plasma treatment, the amount of O-C bonds decreased gradually where at the same time the percentage of O=C bonds increased enormously. The highest amount of O=C bonds (74%) detected on the sample of O-10/5. 50W 5min oxygen plasma treatment created such a PMMA surface that having 51% O=C peak and 49% O-C peak. For 50W and 100W treatments the highest relative peak ratio of O=C bonds obtained at 15 min treatment which were 65% and 70% respectively.

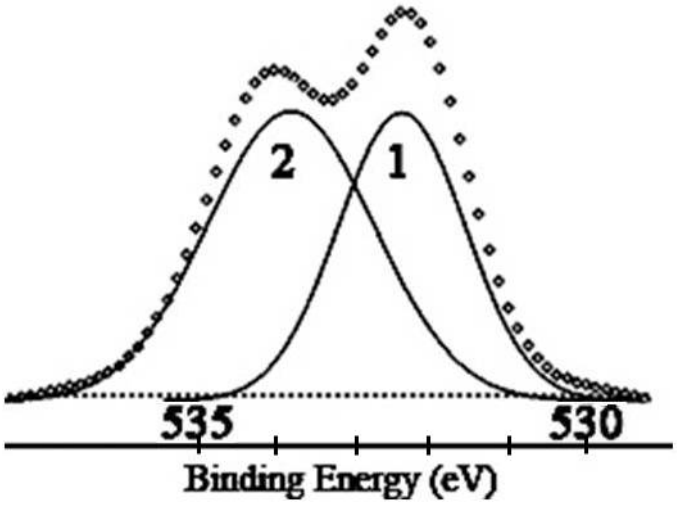

Figure 53: XPS O1s spectrum of C-0/0 sample

RF oxygen plasma treatment resulted in the depletion of O-C bonds and the formation of O=C bonds because of the lower bond dissociation energy of C-O linkage (360 kJ/mole). Plasma treatment caused preferential breaking of O-C bonds rather than O=C bonds which are having higher bond dissociation energy (799 kJ/mole). For low power value such as 10W, shorter exposure time was more effective to obtain high power value like 50W, depletion of O-C bonds increased with increasing treatment time up to 15 min. For longer time duration such as 30 min, depletion of bonds decreased but it was higher than the control group. It can be concluded that longer exposure times might be resulted in formation of cross linking (Figures 53-61).

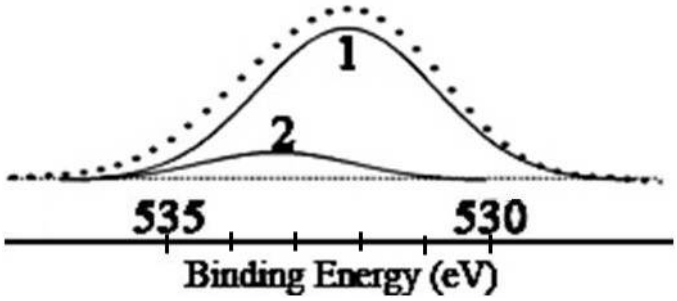

Figure 54: XPS O1s spectrum of O-10/5 sample

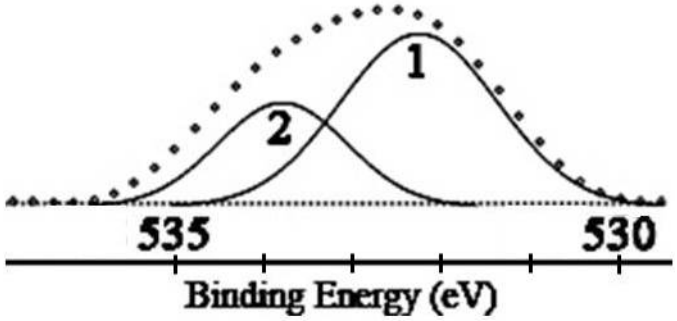

Figure 55: XPS O1s spectrum of O-10/15 sample

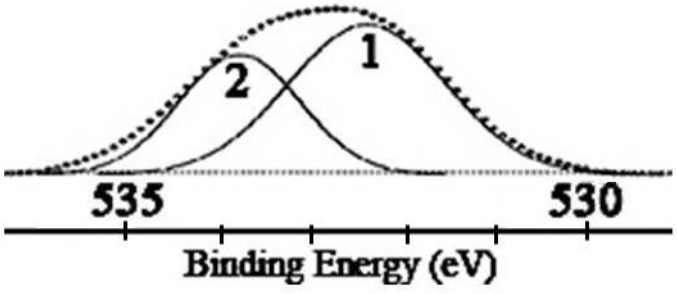

Figure 56: XPS O1s spectrum of O-10/30 sample

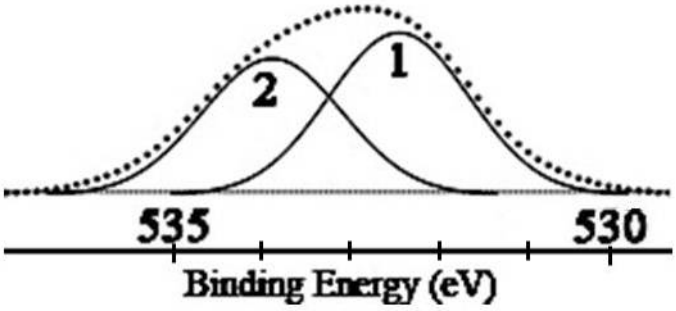

Figure 57: XPS O1s spectrum of O-50/5 sample

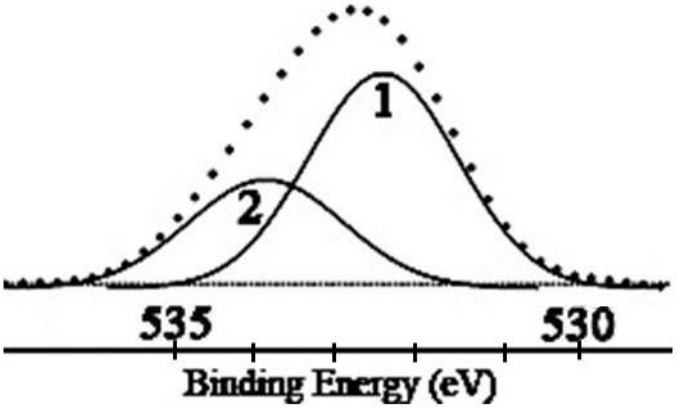

Figure 58: XPS O1s spectrum of O-50/15 sample

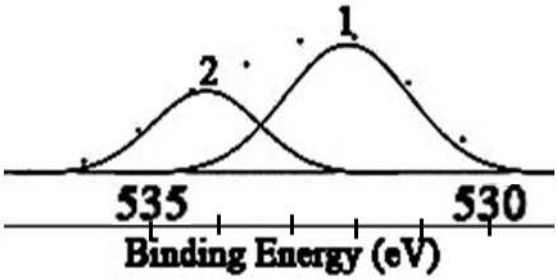

Figure 59: XPS O1s spectrum of O-50/30 sample

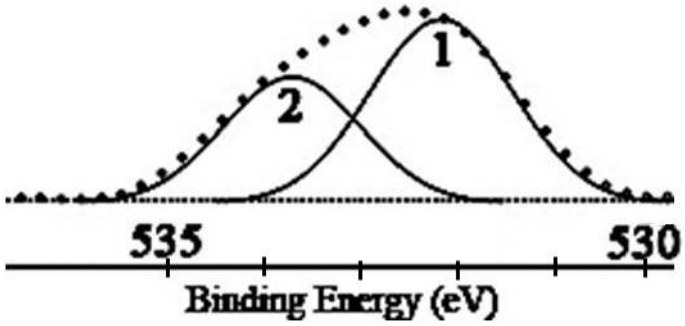

Figure 60: XPS O1s spectrum of O-100/5 sample

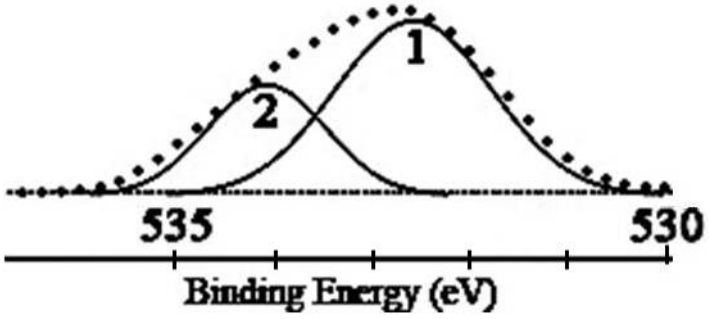

Figure 61: XPS O1s spectrum of O-100/15 sample

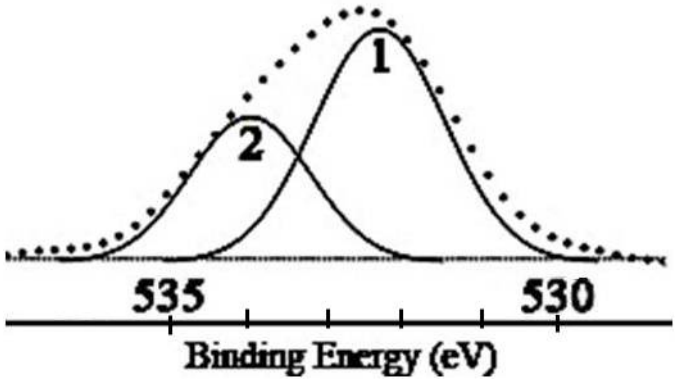

Figure 62: XPS O1s spectrum of O-100/30 sample

3.4 Atomic Force Microscopy (AFM) Analysis

Surface topography of prepared films of control PMMA is given in Figure 63. The surface of C-0/0 acted as a real flat surface having 0.5 nm roughness value. As it is seen in the AFM images, surface roughness increased gradually after oxygen plasma treatment. Root mean square (rms) roughness of sample O-100/5 was 6.48 nm. At the same power value (100W), increasing plasma treatment time to 30 min involved enormous increase in the roughness value up to 74 nm (Figure 65). This dramatic change in the surface roughness can be explained by the etching effect of oxygen plasma treatment. Also the height of the asperities increased with increasing plasma treatment time for 100W. Similar results indicating increase in surface roughness with high power and longer duration of plasma application are also indicated in literature [Tsougeni et al., 2009].

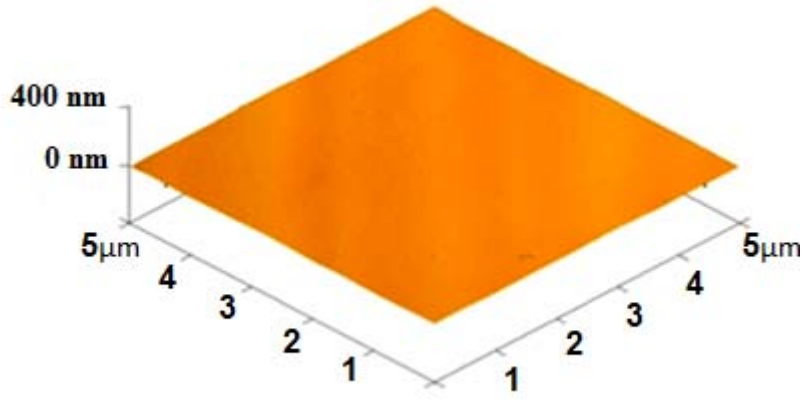

Figure 63: AFM image of C-0/0 sample

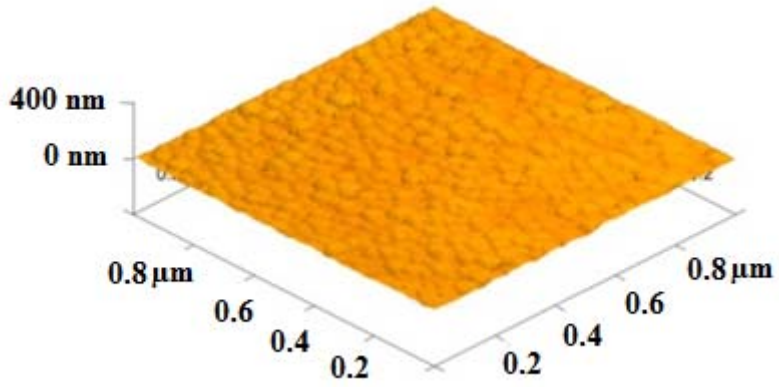

Figure 64: AFM image of O-100/5 sample

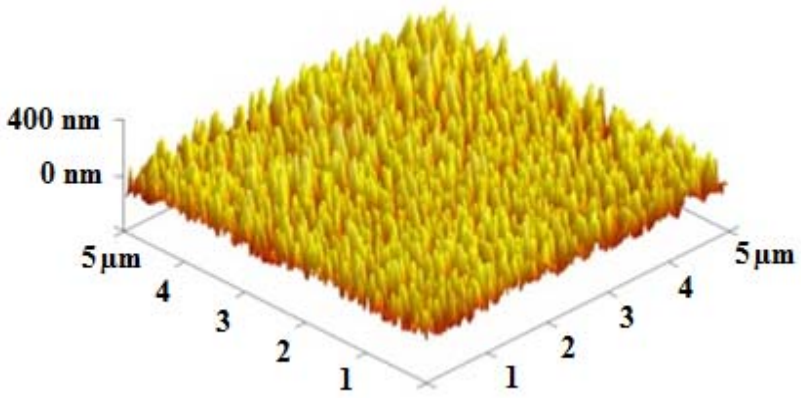

Figure 65: AFM image of O-100/30 sample

3.5 Electron Spin Resonance Spectroscopy (ESR) Analysis

Free radicals are chemical species that possess an unpaired electron in the outer shell of the molecule. Under normal conditions free radicals are usually unstable because of an unpaired electron, which leads to their high reactivity. The fact that in free radicals, the unpaired electron is involved, these species are paramagnetic, thus the most used method for detecting free radicals is electron paramagnetic resonance spectroscopy When an unpaired electron in a magnetic field interacts with a nuclear spin, the spectrum splits into two or more lines, which produce a hyperfine structure

in the spectrum. The splitting of the spectrum is expressed in terms of a hyperfine coupling constant (A value in G or mT units) and the relative position of the spectrum is expresses by the spectroscopic splitting factor (g value). The g value is determined from the resonance magnetic field and the resonance frequency observed as ESR signals [Damian et al., 2005].

ESR results indicated that oxygen plasma treatment leaded to the creation of free radicals on PMMA films. These newly created free radicals were most probably peroxides. According to literature peroxides were likely to be arosen on the surface of PMMA after plasma treatment [Baytekin et al., 2010]. Also the degradation of the PMMA concerning with the reduction in the methyl carbon and the increase in the oxygenated carbon species reported in the literature [Fakes et al., 1987]. These previous results were highly consistent with our ESR results. ESR spectra of oxygen plasma treated PMMA films, can be seen from Figure 66 and Figure 67, composing of three main sharp lines with a splitting constant of 23 G and 20 G and two subsidiary lines with a splitting constant of 11.5 G. There is a triplet at the centre of the spectrum, marked by black arrows, with a hyperfine coupling constant (hfcc) of 11.5 G and intensity ratio of 1:2:1. The lines of hfcc of are almost same for 5 min and 15 min plasma treatment for each input plasma power. So it can be concluded that type of the free radicals were independent from plasma power and time. The amount of the free radicals are related with the area under the curve and it decreased with increasing input power up to 50W. The amount of the free radicals increased at 100W plasma power application. This may be because of following coupling of created free radicals with reactive species in the environment of oxygen plasma. Increase in the plasma power could cause following coupling of created free radicals as previously mentioned. According to the literature, the most probable major radicals which can be created from PMMA are $\cdot COOCH_3$, $\cdot CH_3$ and $\cdot OCH_3$ [Ichikawa et. al., 1990]. Among these most probably created one with oxygen plasma treatment is reported as $\cdot COOCH_3$ [Ormerod et al., 1964].

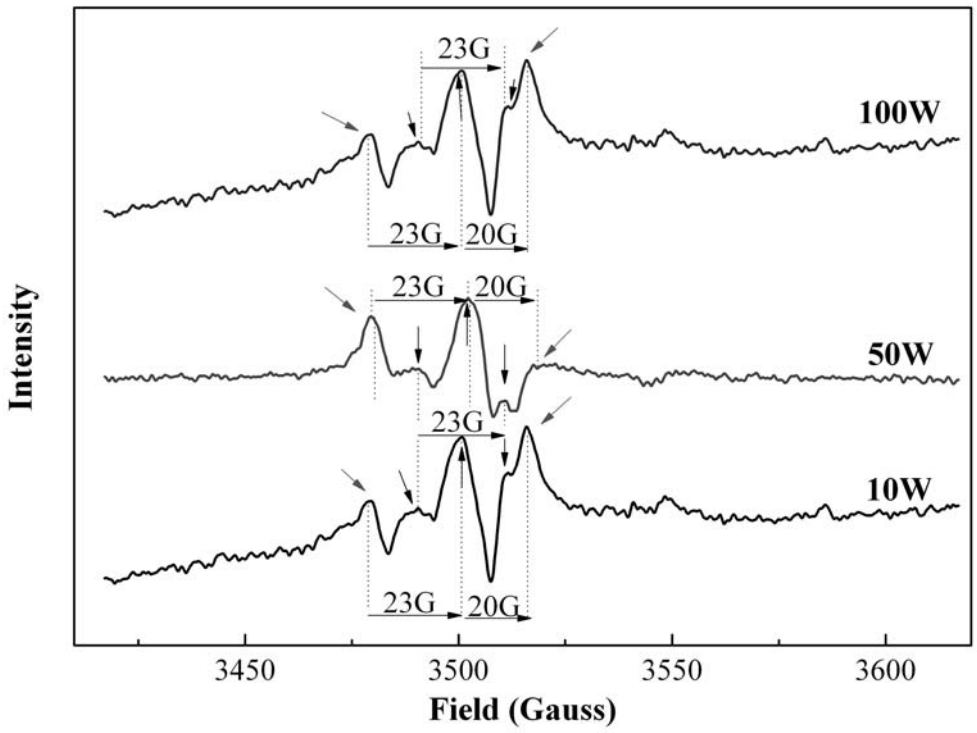

Figure 66: ESR spectra of 5 min oxygen plasma treated PMMA samples

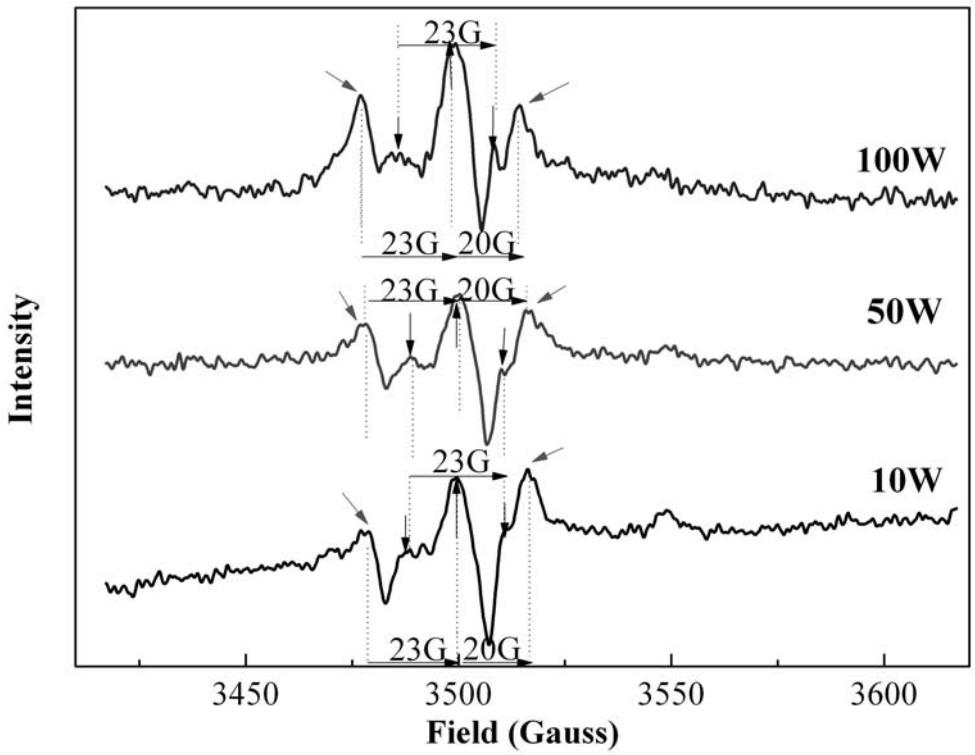

Figure 67: ESR Spectra of 15 min oxygen plasma treated PMMA samples

After plasma application, opening the reactor to the atmospheric pressure and letting the created radicals atmosphere, may be resulted in further reactions, or the radicals may be decayed leading a decrease in the concentration of the free radicals. Decay studies of radicals are very important for the further processes such as immobilization of molecules on the plasma modified surfaces. The knowledge about the activity time of free radicals can ensure some critical points and also extra time before going further processes such as binding any molecule.

ESR radical decay studies, as can be seen from the Figure 68, 69 and 70, were done and living radicals were examined up to 1 month at ambient air conditions. Our results demonstrated that the amount of the free radicals decreased incessantly at higher plasma input values. In other words, increasing plasma power caused faster decay of the free radicals. This can be examined as; higher power values brought about much more unstable modification environment causing free radicals with lower lifetime. The decay of the created radicals was investigated in order to adjust the time for immobilization of any molecule or cell attachment. So this present study

offers a unique route for determining the optimum plasma condition to the intended application.

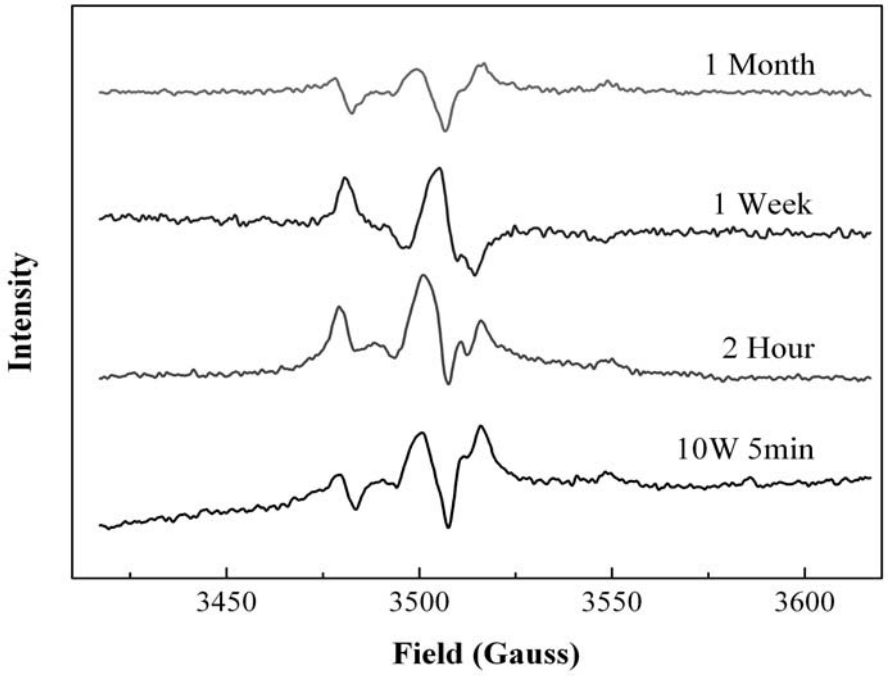

Figure 68: Radical Decay of sample O-10/5 at air

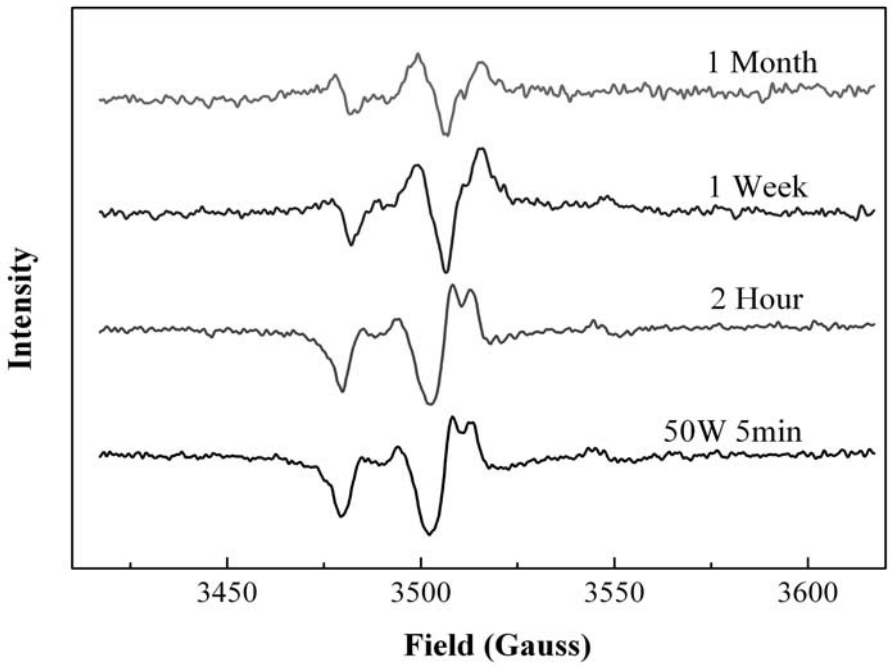

Figure 69: Radical Decay of sample O-50/5 at air

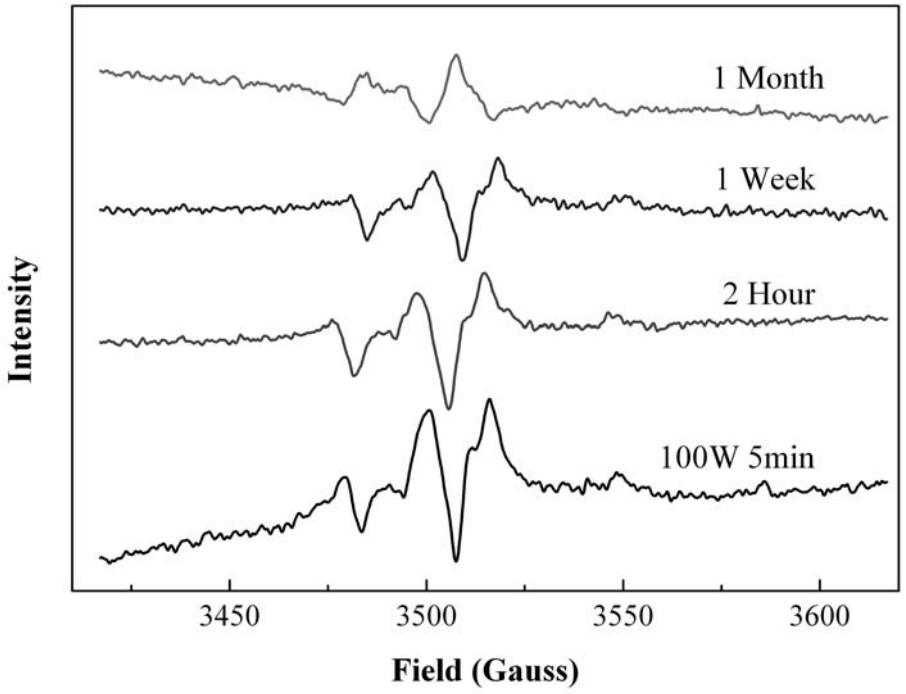

Figure 70: Radical Decay of Sample O-100/5 at air

CHAPTER 6

CONCLUSION

Control of the surface properties plays an essential role for many applications such as the performance of the adhesion process, paintability, colorability of materials and biosensor applications, etc. Although the bulk properties of some materials meet the desired properties, the surface may need to be modified. The techniques used for surface modification are various, such as chemisorptions, ozone treatment, gamma or UV irradiation, use of laser, ion beam, electron beam, flame, plasma treatment. Among these, plasma treatment is one generally preferred because of high probability of creating several surfaces expeditiously from a single sample retaining original bulk properties unchanged by changing the applied plasma parameters such as power, exposure time, gas type, flow rate, etc. So optimization of plasma parameters is critical for most of the applications to obtain the surface possessing the intended properties such like immobilization of various molecules on the surface. The immobilization of some specific molecules like DNA, proteins, biosensors depends on the specific chemical functional groups present on the surface. For instance oxygen containing functional groups such that carbonyl, hydroxyl, and carbonate leading good support for cell adhesion; on the other hand nitrogen based functional groups are highly prefered for carboxyl containing molecules. For this purpose, solvent casted polymethylmetacrylate (PMMA) films were firstly modified by nitrogen RF plasma with various powers (10W, 50W, 100W) for different periods (5min, 15min and 30min).

The effects of these plasma parameters on hydrophilicity and surface free energy were investigated. Surface free energy measurements were carried out according to Geometric Mean, Harmonic Mean, and Acid-Base approach and an increase in hydrophilicity with power and time was obtained. Surface chemistry investigation of revealed that nitrogen plasma treatment decomposed the ester groups creating

nitrogen functional groups such as imine, primary amine, amide and nitrozo which could be used to immobilize carboxyl containing molecules. Argon plasma treatment was also carried out with various powers (10W, 50W and 100W) for different periods (5min, 15min and 30min) in order to see the effects of an inert gas. Superhydrophilic surfaces were obtained especially when the power and the time were increased. The most hydrophilic surface was obtained for the sample A-100/30 with the water contact angle of 11° that was almost superhydrophilic property.

XPS analysis results indicated that carboxylic acid, free carbonyl and hydroxyl groups formed after argon plasma treatment. Since it was tought that these functional groups are causing superhydrophilicity; the idea of performing oxygen plasma treatment to produce higher amount of oxygen based functional groups came up to investigate their role on superhydrophilicity. Oxygen RF plasma surface modification of PMMA films with various powers (10W, 50W, 100W) for different periods (5min, 15min and 30min) were carried out in order to investigate the effects of these plasma parameters on hydrophilicity, surface free energy, surface chemistry and surface topography.

Also, the types of surface free radicals created with oxygen plasma treatment were analysed and the decay of these radicals were examined by electron spin resonance spectroscopy (ESR). Oxygen plasma treatment reduced the contact angle of PMMA films, especially the lowest contact angle values obtained for higher plasma powers and durations and it was found that plasma treatment increased the surface free energy for all samples by increasing the polar components introducing functional groups such as free carbonyl and carbonate groups on the surface.

Atomic force microscopy (AFM) analysis revealed that the roughness of the surface increased considerably from ~0.5 nm to ~75 nm for the sample O-100/30. ESR analysis indicated the presence of peroxy radicals on the surface of the oxygen plasma treated PMMA and the intensity of these radicals increased with increasing plasma power. Decay study of the newly created radicals demonstrated that after 1 month under the atmospheric conditions there were still peroxy radicals on the surface of PMMA and it was also observed increasing plasma power caused faster decay of the free radicals. This may be important for the immobilization time of some molecules after altering the surface. In some cases there may be no need for

waiting or it may be useful to know that surface radicals are still active after 1 year so having knowledge about the life time of created radicals offers a route for binding process.

This study gives a detailed characterization of PMMA surfaces after plasma modification with three different gases such as nitrogen, argon and oxygen.

After optimization of plasma operation conditions for binding any specific molecules, it is worth trying to immobilize a bioactive molecule such that a protein or enzyme which could be helpful to built a biosensor. Besides, obtaining superhydrophobic PMMA surface by introducing fluorine containing chemical functional groups might be interesting and useful for self cleaning material applications. Binding molecules to the active groups created by plasma can lead numerous path in industrial applications.

REFERENCES

Amor S. B., Baud G., Jacquet M., Nanse G., Fioux P., Nardin M., 'XPS characterization of plasma-treated and alumina-coated PMMA', Appl. Surf. Sci., 153: 172-183, 2000.

Barhai P. K., Sharma R., Yadav A. K., Singh A. K., Gaur H., Buck V., 'Surface modification of PMMA with DLC using RF-PECVD', ECS Transactions, 25: 829-836, 2009.

Baytekin H. T., Wirth T., Gross T., Sahre M., Unger W. E. S., Theisen J., Schmidt M., 'Surface analytical characterization of micro-fluidic devices hot embossed in polymer wafers: Surface chemistry and wettability', Surface Interface Analysis, 42: 1417-1431, 2010.

Becker H., Locascio L. E., 'Polymer Microfluidic Devices, Talanta, 56: 267-287 , 2002.

Bhowmik S., Chaki T. K., Ray S., Hoffman F., Dorn L., 'Effect of surface modification of high density Polyethylene by direct current and radio frequency glow discharge on wetting and adhesion characteristics', Metallurgical and Materials Transactions A , 35: 865-877 , 2004.

Bogaerts A., 'The glow discharge: An exciting plasma', Journal of Analytical Atomic Spectrometry, 14: 1375-1384 , 1999.

Boozer A. H., 'Physics of magnetically confined plasmas', Reviews of Modern Physics, 76: 1071-1142, 2004.

Brinen J. S., Greenhouse S., Pinatti L., 'ESCA and SIMS studies of plasma treatments of intraocular lenses', Surface and Interface Analysis, 17: 63-70, 1991.

Burton Z., Bhushan B., 'Hydrophobicity, adhesion, and friction properties of nanopatterned polymers and scale dependence for micro and nanoelectromechanical systems', Nanoletters, 5: 1607-1613, 2005.

Cantin, S., Bouteau, M., Benhabib, F., Perrot, F. 'Surface free energy evaluation of well-ordered Langmuir–Blodgett surfaces comparison of different approaches', Colloid. Surface. A., 276: 107–115, 2006.

Castner D. G., Ratner B. D., 'Biomedical surface science: foundations to frontiers', Surf. Sci., 500: 28-60 , 2002.

Chai J., Lu F., Li B., Kwok D. Y., 'Wettability interpretation of oxygen plasma modified Poly (methyl methacrylate)', Langmuir, 20: 10919-10927, 2004.

Charles C., Matlakowski G. G., Boswell R. W., Goullet A., Turban G., Cardinaud C., 'Characterization of silicon dioxide films deposited at low pressure and temperature in a helicon diffusion reactor' J. Vac. Sci. Technol. A, 11: 2954-2965, 1993.

Chehade M., Fraco., Elder M. J., Fracs M., 'Intraocular lens materials and styles: A Review', Australian and New Zealand Journal of Ophthalmology, 25: 255-263, 1997.

Chen T. H., Liu C. H., Teng J. F., Su C. H., Sheu H. L., Lin S., 'Atmospheric-pressure spin plasma jets processing of polymethylmethacrylate surface using experimental design methodology', Surface Interface Analysis, 41: 886- 892, 2009.

Chu P. K., Chen J. Y., Wang L. P., Huang N., 'Plasma surface modification of biomaterials', Materials Science and Engineering, 36: 143-206, 2002.

Combe C. E., Owen B. A., Hodges J. S.,'A protocol for determining the surface free energy of dental materials', Dental Materials, 20: 262-268 , 2004.

D'Sa R. A., Burke G. A., Meenan B. J., 'Protein adhesion and cell response on atmospheric pressure dielectric barrier discharge-modified polymer surfaces', Acta Biomaterialia, 6: 2609-2620, 2010.

Dabhade R. V., Bodas D. S., Gangal S. A., 'Plasma treated polymer as humidity sensing material- A feasibility study', Sensors and Actuators B, 98: 37-40, 2004.

Damian G., 'Study of free radicals in gamma irradiated metoclopramid using spin trapping ESR spectroscopy', Romanian J. Biophys, 15: 121-126, 2005.

Denes F. S., Manolache S., ‘ Macromolecular plasma chemistry: An emerging field of polymer science’, Progress in Polymer Science, 29: 815-885, 2004.

Deshmukh R. R., Shetty A. R., ‘Comparison of surface energies using various approaches and their suitability’, J Appl. Polym. Sci., 107: 3708-3717, 2008.

Dorranian D., Abedini Z., Hojabri A., Ghoranneviss M., ‘Structural and optical characterization of PMMA surface treated in low power nitrogen and oxygen RF plasmas’, Journal of Non-Oxide Glasses, 1: 217-229, 2009.

Fakes D. W., Newton J. M., Watts J. F., Edgell M. J., ‘Surface modification of a contact lens co-polymer by plasma-discharge treatments’, Surface Interface Analysis, 10: 416-423, 1987.

Fowkes F. M., ‘Attractive forces at interfaces’, Industial and Engineering Chemistry, 56: 40-52, 1964.

Fox H. W., Zisman W. A., ‘The spreading of liquids on low energy surfaces. II. Modified Tetrafluoroethylene polymers’, J Colloid Sci., 7: 109-121, 1952.

Gao L., McCarthy T. J., ‘Wetting and superhydrophobicity’, Langmuir, 25: 14100-14104, 2009.

Gomathi N., Sureshkumar A., Neogi S., ‘RF Plasma treated polymers for biomedical applications’, Current Science, 94: 1478-1486, 2008.

Gozum N., Unal E. S., Yaycioglu R. A., Gucukoglu A., Ozgun C., ‘Visual performance of acrylic and PMMA intraocular lenses’, Eye, 17: 238-242, 2003.

Gröning P., Küttel O. M., Coen M. C., Dietler G., Schlapbach L., ‘ Interaction of low energy ions (< 10 eV) with Polymethylmetacrylate during plasma treatment’, Appl. Surf. Sci., 89: 83-91, 1995.

Guruvenket S., Iyer G. R. S., Shestakova L., Morgen P., Larsen N B., Rao G. M., ‘ Fluorination of Polymethylmethaacylate with Tetrafluoroethane using DC glow discharge plasma’, Appl. Surf. Sci., 254: 5722-5726, 2008.

Hasirci V., Tezcaner A., Hasirci N., Süzer Ş., ‘ Oxygen plasma modification of Poly(3- hydroxybutyrate-co-3-hydroxyvalerate) film surfaces for tissue engineering’, J Appl. Polym. Sci., 87: 1285-1289, 2003.

He B., Patankar N. A., Lee J., ‘Multiple equilibrium droplet shapes and design criterion for rough hydrophobic surfaces’, Langmuir, 19: 4999-5003, 2003.

Hegemann D., Brunner H., Oehr C., ‘ Plasma treatment of polymers for surface and adhesion improvement’, Nuclear Instruments and Methods in Physics Research B, 208: 281-286, 2003.

Horbett T. A., Schway M. B., Ratner B. D., ‘Hydrophilic-hydrophobic copolymers as cell substrates-effect on 3T3 cell-growth rates’, J Colloid Interface Sci., 104: 28-39, 1985.

Ichikawa T., Yoshida H., ‘Mechanism of radiation-induced degredation of Polymethylmetacrylate as studied by ESR and electron spin echo methods’, J Polym. Sci.: Part A, 28: 1185-1196, 1990.

Johansson B. L., Larsson A., Ocklind A., Öhrlund A., ‘Characterization of air plasma-treated polymer surfaces by ESCA and contact angle measurements for optimization of surface stability and cell growth’, Journal of Applied Polymer Science, 86: 2618- 2625, 2002.

Junkar I., Vesel A., Cvelbar U., Mozetic M., Strnad S., ‘Influence of oxygen and nitrogen plasma treatmant on PET polymers’, Vacuum, 84: 83-85, 2010.

Kayırhan N., Denizli A., Hasirci N., ‘Adsorption of blood proteins on glow discharge modified polyurethane membranes’, J Appl. Polym. Sci., 81: 1322-1332, 2001.

Kennedy K. C., Chen T., Kusy R. P., ‘Behaviour of photopolymerized silicate-glass-fiber-reinforced Dimethacrylate composites subjected to hydrothermal ageing’, J Materials Science: Materials in Medicine, 9: 243-248, 1998.

Kim C., Ryu C., Kim B.W., Sim S. J., Chae H., Yoon H. C., Yang S. S., ‘Microfluidic dialysis device fabrication for protein solution enrichment and its

enrichment by plasma surface treatment of a membrane', J Korean Physical Society, 51: 993-999, 2007.

Kitova S., Minchev M., Danev G., ' Soft plasma treatment of polymer surfaces', J Optoelectronics and Advanced Materials, 7: 249-252, 2005.

Kodjikian L., Beby F., Rabilloud M., Bruslea D., Halphen I., Fleury J., Grange J. D., Garweg J. G., 'Influence of intraocular lens material on the development of acute endophthalmitis after cataract surgery?', Eye, 22: 184-193, 2008.

Kokubu E., Yoshinari M., Matsuzaka K., Inoue T., 'Behaviour of rat periodontal ligament cells on fibroblast growth factor-2-immobilized titanium surfaces treated by plasma modification', Journal of Biomedical Materials Research Part A, volume??: 70-75, 2008.

Lai J., Sunderland B., Xue J., Yan S., Zhao W., Folkard M., Michael B. D., Wang Y., 'Study on hydrophilicity of polymer surfaces improved by plasma treatment', Appl. Surf. Sci., 252: 3375-3379, 2006.

Landgraf R., Kaiser M. K., Posseckardt J., Adolphi B., Fischer W. J., 'Functionalization of polymer surfaces by oxygen plasma treatment', Procedia Chemistry , 1015-1018, 2009.

Li Y., Huang X. J., Heo S. H., Li C. C., Choi Y. K., Cai W. P., Cho S. O., 'Superhydrophobic bionic surfaces with hierarchical microsphere/ SWCNT composite arrays', Langmuir, 23: 2169-2174, 2007.

Lin Y., Wang L. L., Zhang P. B., Wang X., Chen X. S., Jing X.B., Su Z. H., 'Surface modification of Poly(L-lactic acid) to improve its cytocompatibility via assembly of polyelectrolytes and gelatin', Acta Biomaterialia, 2: 155-164, 2006.

Liu J., Pan T., Woolley A. T., Lee M. L., 'Surface-modified Poly(methyl methacrylate) capillary electrophoresis microchips for protein and peptide analysis', Anal. Chem., 76: 6948-6955, 2004.

Liu X., Tang S., Choi H. K., Choi H. S., 'Effect of plasma treated polymer substrates on fabricating surface microsystems through LBL coating', Macromolecular Research, 18: 413-420, 2010.

Mandracci P., Mussano F., Ricciardi C., Ceruti P., Pirri F., Carossa S., 'Low temperature growth of thin film coatings for the surface modification of dental prostheses', Surface & Coating Technology, 202: 2477-2481, 2008.

Mangipudi V., Tirrell M., 'Direct measurements of the surface energy of corona-treated Polyethylene using the surface forces apparatus', Langmuir, 11: 19-23, 1995.

Messina G. M. L., Satriano C., Marletta G., ' A multitechnique study of preferential protein adsorption on hydrophobic and hydrophilic plasma modified polymer surfaces', Colloids and Surfaces B, 70: 76-83, 2009.

Miettinen V. M., Vallittu P. K., 'Release of residual Methylmethacrylate into water from glass fiber Poly(methylmethacrylate) composite used in dentures', Biomaterials, 18: 181-185, 1997.

Miura T., Hayakawa T., Okumori N., Iohara K., Yoshinari M., 'Antifungal activity against candida albicans on PMMA coated with Protamine derivatives', J Oral Tissue Engineering, 8: 30-38, 2010.

Morent R., Geyter N. D., Desmet T., Dubruel P., Leys C., 'Plasma surface modification of biodegradable polymers: A Review, Plasma Processes and Polymers, 8: 171-190, 2011.

Moroni L., Wijn D. J. R., Blitterswijk V.,' C. A. Integrating novel technologies to fabricate smart scaffolds', J Biomater. Sci., Polym. Ed., 19, 543-572, 2008.

Mukhopadhyay S., Roy S. S., D'Sa R. A., Mathur A., Holmes R. J., McLaughlin J. A., 'Nanoscale surface modifications to control capillary flow characteristics in PMMA microfluidic devices', Nanoscale Research Letters, 6:411-423, 2011.

Hasirci N., Endogan T., Vardar E., Kiziltay A., Hasirci V., 'Effect of oxygen plasma on surface properties and biocompatibility of PLGA films' Surf. Interface Anal., 42: 486-491, 2010.

Onda T., Shibuichi S., Satoh N., Tsujii K., 'Super water repellent fractal surfaces', Langmuir, 12: 2125-2127, 1996.

Ormerod M. G., Charlesby A., 'The radiation chemistry of polymethacrylic acid, polyacrylic acid and their esters: An electron spin resonance study', J. Polymer, 5: 67-87, 1964.

Oss V. C. J., Good R. J., Chaudhury M. K., 'Additive and nonadditive surface tension components and the interpretation of contact angles', Langmuir, 4: 884-891, 1988.

Oss V. C. J., Good R. J., Chaudhury M.K., 'The role of van der Waals forces and hydrogen bonds in hydrophobic interactions between biopolymers and low energy surfaces', Journal of Colloid and Interface Science, 111: 378-390, 1986.

Ozcan C., Hasirci N., 'Evaluation of surface free energy for PMMA films', J. Appl. Polym. Sci., 108: 438-446, 2008 (a).

Ozcan C., Zorlutuna P., Hasirci V., Hasirci N., 'Influence of oxygen plasma modification on surface free energy of PMMA films and cell attachment', Macromol. Symp., 269: 128-137, 2008 (b).

Ozdemir Y., Hasirci N., Serbetci K., 'Oxygen plasma modification of Polyurethane membranes' , J Mater. Sci.: Materials in Medicine, 13: 1147-1152, 2002.

Ozden N., Akaltan F., Suzer S., Akovali G., ' Time related wettability characteristic of acrylic resin surfaces treated by glow discharge', The Journal of Prosthetic Dentistry, 82: 680- 684, 1999.

P. Favia, R. d'Agostino, 'Plasma treatments and plasma deposition of polymers for biomedical applications', Surface Coatings and Technology, 98: 1102-1116, 1998.

Panditaraj K. N., Selvarajen V., Deshmukh R. R., Gao C., 'Modification of surface properties of PP film using DC glow discharge air plasma', Appl. Surf. Sci., 255: 3965-3971, 2009.

Papakonstantinou D., Amanatides E., Mataras D., Ioannidis V., Nikolopoulos P., 'Improved surface energy analysis for plasma treated PET films', Plasma Process. Polym. , 4: 1057-1062, 2007.

Ramakrishna S., Mayer J., Wintermantel E., Leong K. W., 'Biomedical applications of polymer-composite materials: A review', Composites Science and Technology, 61: 1189-1224, 2001.

Roucoules V., Gaillard F., Mathia T., Lanteri P., 'Hydrophobic mechanochemical treatment of metallic surfaces. Wettability measurements as means of assessing homogenity', Adv. Colloids Interface Sci., 97: 177-201, 2002.

Schulz U., Munzert P., Kaiser N., ' Surface modification of PMMA by DC glow discharge and microwave plasma treatment for the improvement of coating adhesion', Surface and Coating Technology, 142-144: 507-511, 2001.

Sun T., Feng L., Gao X., Jiang L., ' Bioinspired surfaces with special wettability', Acc. Chem. Res., 38: 644-652, 2005.

Tang S., Choi H. S., 'Comparison of low and atmospheric pressure radio frequency plasma treatments on the surface modification of Poly (methyl methacrylate) plates', J Phys. Chem. C., 112: 4712-4718, 2008.

Tennico Y. H., Koesdjojo M. T., Kondo S., Mandrell D. T., Remcho V. T., 'Surface modification-assisted bonding of polymer-based microfluidic devices', Sensors and Actuators B: Chemical, 143: 799-804, 2010.

Thevenot P., Hu W. J., Tang L. P., 'Surface chemistry influences implant biocompatibility, current topics in medicinal chemistry, 8: 270-280, 2008.

Tsao C. W., Hromada L., Liu J., Kumar P., DeVoe D. L., ' Low temperature bonding of PMMA and COC microfluidic substrates using UV/Ozone surface treatment', Lab Chip, 7: 499-505, 2007.

Tsougeni K., Vourdas N., Tserepi A., Gogolides E., 'Mechanisms of oxygen plasma nanotexturing of organic polymer surfaces: From stable superhydrophilic to superhydrophobic surfaces', Langmuir, 25: 11748-11759, 2009.

Tziampazis E., Kohn J., Moghe P. V., 'PEG-variant biomaterials as selectively adhesive protein templates: model surfaces for controlled cell adhesion and migration, Biomaterials, 21: 511-520, 2000.

Wei Y., Wang X., Gao J., Chen Y., 'Plasma-induced graft polymerization of Poly(ethylene glycol) on Poly (methyl methacrylate) surfaces for improving antistatic property', Journal of Applied Polymer Science, 118: 943-949, 2010.

Wen C. H., Chuang M. J., Hsiue G.-H., 'Asymmetric surface modification of polyethyleneterephthalate film by CF_4 plasma immersion', Appl. Surf. Sci., 252: 3799-3805, 2006.

Wu Z., Xanthopoulos N., Reymond F., Rossier J. S., Girault H. H., 'Polymer microcips bonded by O_2 plasma activation', Electrophoresis, 23: 782-790, 2002.

Yildirim M. S., Kesimer M., Hasirci N., Kilic N., Hasanreisoğlu U., 'Adsorption of human salivary mucin MGI onto glow discharge plasma treated acrylic resin surfaces', Journal of Oral Rehabilitation, 33: 775-783, 2006.

Yoshinari M., Kato T., Matsuzaka K., Hayakawa T., Inoue T., Oda Y., Okuda K., Shimono M., 'Adsorption behaviour of antimicrobial peptide histatin 5 on PMMA', Inc. J. Biomed Mater Res Part B: Appl. Biomater. B, 77: 47-54, 2006.

Zenkiewicz M., 'Methods for the calculation of surface free energy of solids', Journal of Achievements in Materials and Manufacturing Engineering, 24: 137-145, 2007.

Zhang L., Wu D., Chen Y., Wang X., Zhao G., Wan H., Huang C., 'Surface modification of polymethyl methacrylate intraocular lenses by plasma for improvement of antithrombogenicity and transmittance', Applied Surface Science, 255: 6840-6845, 2009.

APPENDIX A

SFE VERSUS POWER GRAPHS

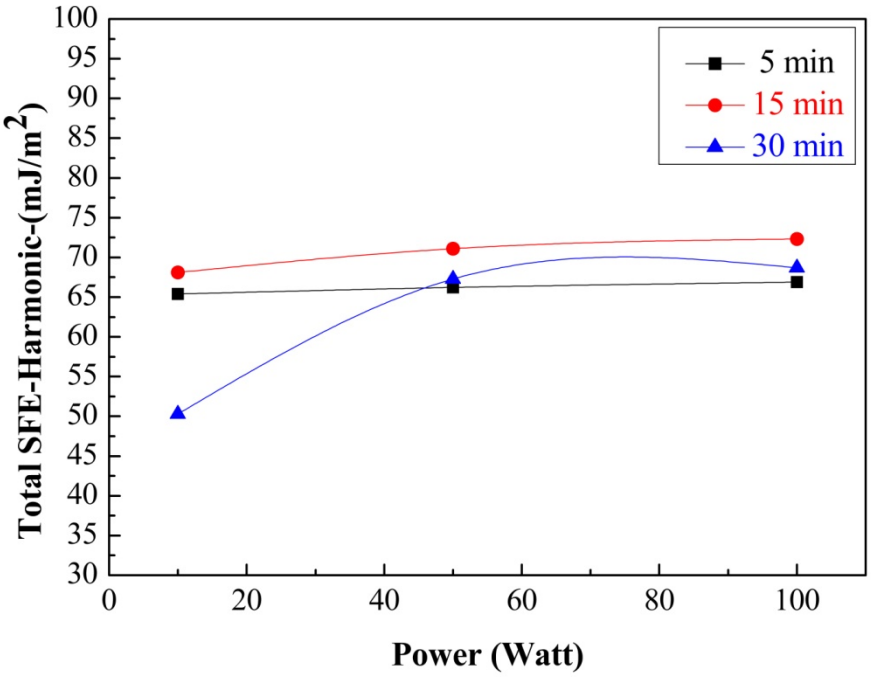

Figure A 1:Total SFE (Harmonic Mean) versus power graph for 5-15-30 min nitrogen plasma treated PMMA films

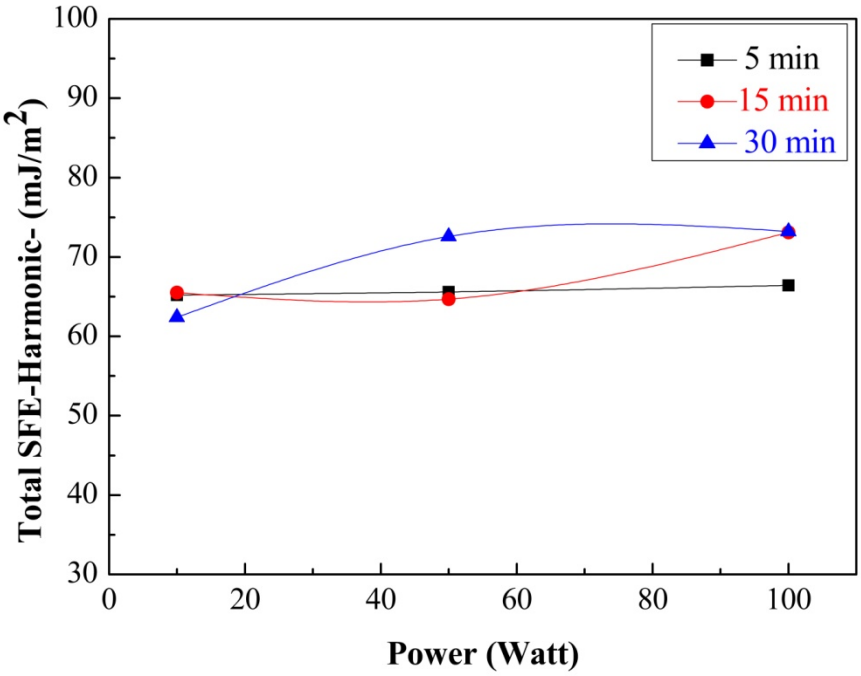

Figure A 2: Total SFE (Harmonic Mean) versus power graph for 5-15-30 min argon plasma treated PMMA films

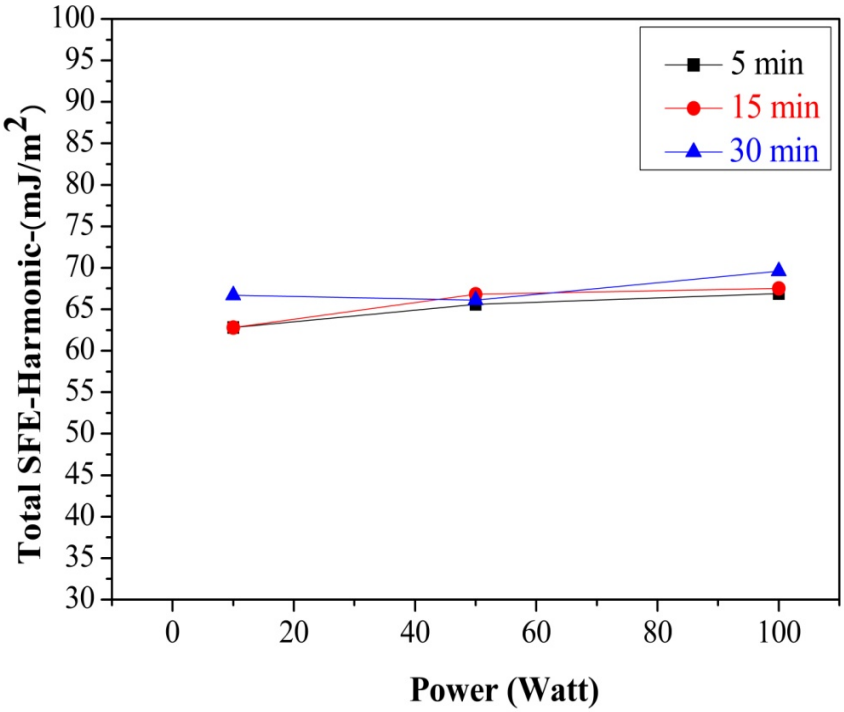

Figure A 3: Total SFE (Harmonic Mean) versus power graph for 5-15-30 min oxygen plasma treated PMMA films

APPENDIX B

SFE CALCULATION OF CONTROL GROUP

Calculation of SFE for control group according to Harmonic Mean Approach;

$$\gamma_L (1+\cos\theta) = 4\left(\frac{\gamma_L^{d} \cdot \gamma_S^{d}}{\gamma_L^{d} + \gamma_S^{d}} + \frac{\gamma_L^{p} \cdot \gamma_S^{p}}{\gamma_L^{p} + \gamma_S^{p}}\right)$$

γ_L=72.8 for distilled water so;

72.8 (1+Cos 71.3)= 4[21.8 γ_S^d/ 21.8+ γ_S^d] + 4[51 γ_S^p/51+ γ_S^p]

γ_L=50.8 for diiodomethane so;

50.8 (1+Cos 71.3)= 4[50.8 γ_S^d/ 50.8+ γ_S^d] + 4[0 γ_S^p/ 0+ γ_S^p]

γ_L=58 for formamide so;

58 (1+Cos 71.3)= 4[39 γ_S^d/ 39+ γ_S^d] + 4[19 γ_S^p/ 19+ γ_S^p]

γ_L= 44 for dimethylsulfoxide so;

44 (1+Cos 71.3)= 4[36 γ_S^d/ 36+ γ_S^d] + 4[8 γ_S^p/ 8+ γ_S^p]

Solving these equations for the two test liquid couples;

γ^p and γ^d becomes γ^p=10.2, γ^d=35.5.